E. Blackburn
fiche.

DETERMINATION OF GLASS CONTENT IN FLY ASHES AND BLAST-FURNACE SLAGS

E. DOUGLAS, P. MAINWARING, M. VAN ROODE, and R.T. HEMMINGS

MINERALS RESEARCH PROGRAM
MINERAL SCIENCES LABORATORIES

CANMET REPORT 85-6E

OCTOBER 1985

Available in Canada through

Authorized Bookstore Agents
and other bookstores

or by mail from

Canadian Government Publishing Centre
Supply and Services Canada
Ottawa, Canada K1A 0S9

Catalogue No. M38-13/85-6E Canada: $7.25
ISBN 0-660-12155-7 Other Countries: $8.70

Price subject to change without notice

DETERMINATION OF GLASS CONTENT IN FLY ASHES AND BLAST-FURNACE SLAGS

E. Douglas[1], P. Mainwaring[2], M. van Roode[3], and R.T. Hemmings[4]

SYNOPSIS

In North America, there is an increased interest in the pozzolanic and cementitious properties of mineral wastes and in the potential for using these wastes as partial portland-cement replacement in concrete, either in the form of blended cement or as mineral admixtures at the mixer.

Most waste materials are reactive when in a glassy state. A general theory, common to all these by-products, should explain the behaviour of glassy materials incorporated in portland cement in concrete.

The purpose of this study was to find an accurate procedure to measure glass content in mineral wastes in order to predict their behaviour in concrete for offshore construction. A number of methods were used for measuring glass content in nine fly ashes and two blast furnace slags. The methodologies for two X-ray diffraction techniques were developed in this study. These two techniques are applicable to all classes of glassy waste materials. On the other hand, the quantitative X-ray diffraction method to evaluate the glass content of a material with a number of uncommon crystalline phases may be a very time-consuming technique. The non-crystalline X-ray diffraction approach cannot be used for materials which cannot be vitrified through rapid quenching.

---

[1]Research Scientist, Construction Materials Section and [2]Head, Process Mineralogy Section, Mineral Sciences Laboratories, CANMET, Energy, Mines and Resources Canada, Ottawa, K1A 0G1.

[3]Research Scientist, Ontario Research Foundation, Present address: Solar Turbines Inc., San Diego, California.

[4]Project Manager, Ontario Research Foundation, Mississauga, Ontario, L5K 1B3.

DÉTERMINATION DU CONTENU EN VERRE
DES CENDRES VOLANTES ET DES LAITIERS DE HAUTS FOURNEAUX

E. Douglas[1], P. Mainwaring[2], M. van Roode[3], et R.T. Hemmings[4]

RÉSUMÉ

En Amérique du Nord, on s'intéresse de plus en plus aux propriétés pouzzolaniques et au pouvoir agglutinant de certains déchets minéraux ainsi qu'à leur utilisation possible comme produit de remplacement partiel du ciment portland dans le béton, soit sous forme de constituants dans les ciments mélangés ou comme adjuvants minéraux au béton.

La plupart des déchets minéraux sont réactifs lorsqu'ils sont dans un état vitreux. Il semble donc possible de formuler une théorie générale, applicable à tous ces sous-produits, pour expliquer le comportement des matières vitreuses quand elles sont incorporées au ciment portland.

Le but de cette étude était de trouver un procédé précis pour mesurer le contenu en verre des déchets minéraux afin d'expliquer leur comportement dans les bétons conçus pour des constructions marines. Diverses méthodes ont été utilisées pour mesurer le contenu en verre de neuf cendres volantes et de deux laitiers de hauts fourneaux. La marche à suivre pour l'utilisation de deux techniques de diffraction des rayons X a été mise au point au cours de cette étude et est applicable à tous les déchets minéraux vitreux. D'autre part, la méthode quantitative par diffraction des rayons X pour évaluer le contenu en verre d'un matériau contenant certaines phases cristalinnes peu communes peut demander beaucoup de temps. Une méthode non cristalline de diffraction des rayons ne peut être utilisée dans le cas de matériaux qui ne peuvent être vitrifiés par trempe rapide.

---

[1]Chercheur scientifique, Section des matériaux de construction et [2]Chef, Section de la minéralogie appliquée, Laboratoires des sciences minérales, CANMET, Énergie, Mines et Ressources Canada, Ottawa, K1A 0G1.

[3]Chercheur scientifique, Fondation de recherche de l'Ontario Adresse actuelle: Solar Turbines Inc., San Diego (Californie).

[4]Chef de projet, Fondation de recherche de l'Ontario, Mississauga (Ontario) L5K 1B3.

ACKNOWLEDGEMENTS

Work on this project was conducted by the Ontario Research Foundation under the auspices of CANMET, contract number 155Q23440-3-9193. The authors wish to thank the members of the Steering Committee for this program, Dr. P.K. Mehta, professor, University of California, Berkeley, Dr. D.M. Roy, professor, The Pennsylvania State University, Dr. V.S. Ramachandran, Section Head, Building Materials Section, National Research Council of Canada, and Dr. V.M. Malhotra, Section Head, Construction Materials Section, CANMET, for their direction and helpful suggestions given during the program review meetings.

The principal investigators at ORF were Dr. M. van Roode and Dr. R.T. Hemmings. Dr. V.M. Malhotra and Dr. E. Douglas acted as scientific authorities for this project.

CONTENTS

SYNOPSIS i

RÉSUMÉ iii

ACKNOWLEDGEMENTS v

INTRODUCTION 1

ORIGIN AND PRODUCTION OF CEMENTITIOUS AND POZZOLANIC BY-PRODUCTS 1

- Slags 1
- Fly Ash 2
- Silica Fume 2

GLASS CONTENT MEASUREMENTS: BACKGROUND INFORMATION 2

- Methodology for Glass Content Determination 2
  - X-Ray Techniques 3
    - Quantitative X-ray determination (QXRD method) 3
    - Non-crystalline scattering methods 3
    - Amorphous intensity method 3
    - Amorphous hump method 4
    - Amorphous-crystalline scattering method 4
    - Differential intensity method 4
  - Optical Techniques 4
    - McMaster individual particle analysis 4
    - South African optical procedure 4
    - Parker and Nurse optical method 5
    - Rheinhausen optical method 5
  - Spectroscopic Techniques 5
    - Automated ultraviolet reflectance method 5
    - Rheinhausen ultraviolet method 5
    - Infrared techniques 5
    - Nuclear magnetic resonance 5
  - Electron-Optical Techniques 5
  - Solution Techniques 6
  - Density Method 6
  - Differential Thermal Analysis (DTA) 6

Selection of Glass Content Methodology 6
XRD techniques 7
Optical techniques 7
Spectroscopic techniques 7
Electron-optical techniques 7
Solution method 7
Density method 7
DTA method 7
EXPERIMENTAL METHODS 7
Materials 7
Density Determinations 7
Particle Size Analysis - Wet Sieving 7
Surface Area Analysis - Blaine 8
Surface Area Analysis - B.E.T. 8
X-Ray Powder Diffraction Measurements 8
Fourier Transform Infrared Spectroscopy (FTIR) 8
Optical Examination - McMaster Technique 8
Optical Examination - Image Analysis 8
Electron Optical Investigation 8
EXPERIMENTAL RESULTS 9
Chemical Analysis 9
Specific Gravity Determinations 9
Particle Size Analysis - Wet Sieving 9
Surface Area Analysis - Blaine 9
Surface Area Analysis - B.E.T. 9
Glass Content Methodology (1): Optical Examination by Image Analysis 9
Glass Content Methodology (2): Electron Optical Investigation 9
Glass Content Methodology (3): McMaster Technique 10
Glass Content Methodology (4): Quantitative X-Ray Diffraction Method (QXRD) 10
Feasibility of Approach - Model Study on the Cordierite System 10
Preliminary Evaluation 11
The QXRD Method Applied to Fly Ashes - Rapid Scans 11

Identification of Major Crystalline Phases in the Fly Ashes 11
Selection of Standard 11
Quantitative Determination of Crystalline Phases and Glass Content 11
Improvements to the QXRD Method 12
Selection of CaF_2 Standard 12
Reduction of Particle Size 12
Preparation of Standard Curves 13
Crystalline and Glass Content of Fly Ashes 13
Thunder Bay Fly Ash 14
The QXRD Method Applied to Blast-Furnace Slags 14
Preparation of Standard Curves 14
Crystalline and Glass Content of Slags 14
Glass Content Methodology (5): Non-Crystalline Scattering Method (NCXRD) 14
Feasibility of Approach - Model Study on the Cordierite System 14
Preliminary Evaluation 14
The NCXRD Method Applied to Fly Ashes - Rapid Scans 15
Improvements to the NCXRD Method 15
Cordierite System 15
Fly Ashes and Slags 15
Glass Content Methodology (6): Differential Intensity Method (DIXRD) 16
Feasibility of Approach - Model Study on the Cordierite System 16
The DIXRD Method Applied to Wabamun Fly Ash 16
Glass Content Methodology (7): The Amorphous Hump Method (AHXRD) 17
Glass Content Methodology (8): Density Approach 17
Structural Evaluation Using X-Ray Diffraction 17
Fourier Transform Infrared (FTIR) Spectroscopy 17
DISCUSSION 18
Chemical Analysis 18
Specific Gravity 18
Particle Size and Surface Area 18

Glass Content Methodologies 19
Comparison of the QXRD and NCXRD Methods 19
QXRD method 19
NCXRD method 20
Electron Optical Investigation 21
X-Ray Diffraction Studies of Glass Structure 21
Na_2O-SiO_2 and SiO_2 Glasses 22
Na_2O-CaO-SiO_2, CaO-SiO_2, CaO-Al_2O_3, and CaO-Al_2O_3-SiO_2 Glasses 22
Fly Ashes, Slags, and Vitreous Analogues 22
Conclusions from the XRD Study 24
Fourier Transform Infrared (FTIR) Spectroscopy 24
Overall Composition 24
Composition of the Individual Particles 24
FTIR Spectra of Fly Ashes and Slags 24
Conclusions from the FTIR Study 26
SUMMARY AND CONCLUDING REMARKS 27
RECOMMENDATIONS 28
REFERENCES 30
APPENDIX A - MODEL GLASSES FOR X-RAY DIFFRACTION 79

TABLES

1. Annual production of glassy waste materials in Canada 35
2. Sources and quantities of iron blast furnace slags in Canada 35
3. Sources and quantities of steel slags in Canada 36
4. Sources and quantities of copper, nickel, and lead smelting slags in Canada 36
5. Production/utilization statistics for coal ash: Major ash uses in the world (1977) 37
6. Techniques for glass content determination 38
7. Methods of glass content determination that are potentially applicable 38

8. Composition of fly ashes and blast furnace slags 39

9. Specific gravities of the source materials 40

10. Densities, particle sizes, and surface areas of the source materials 40

11. Comparison of concentrations of selected oxides from SEM/EDXA analysis and chemical analysis 41

12. EDXA oxide analysis of Wabamun fly ash in cross-section 41

13. Results of modified McMaster individual particle analysis on Standard and Atlantic slags 42

14. Mineralogy of Canadian fly ashes and slags 43

15. Intensity ratios for four phases and NaCl 43

16. Contents of crystalline phases and glass in seven Canadian fly ashes 44

17. Settling parameters 44

18. Composition of mixtures prepared for the standard curves (in grams) 45

19. Peaks scanned for the standard curves..... 45

20. Crystalline and glass content of eight Canadian fly ashes (wt %) 46

21. Composition of the mixtures prepared for standard curves for melilite and merwinite 46

22. Peaks scanned for the standard curves for melilite and merwinite 47

23. Crystalline and glass contents of two blast furnace slags 47

24. Glass contents determined with the differential intensity method 48

25. Specific gravities of three fly ashes and analogues determined by pycnometry 48

26. XRD $2\theta_{I_{max}}$ for nine fly ashes, two slags, and their glassy analogues 49

27. Glass content values (wt %) determined by various methods 49

A1. Nucleation/crystallization parameters 83

FIGURES

1. Optical micrograph of Wabamun fly ash in an Elvacite medium (magnification 137x) 53

2. SEM micrograph of Wabamun fly ash in an Elvacite medium (magnification 20 μ) 54

3. Cross section of Wabamun fly ash after ion etching 55

4. Another view of cross section of Wabamun fly ash after ion etching 56

5. SEM micrograph of location 3 in Fig. 4 at higher magnification 57

6. SEM micrograph of a plerosphere 58

7. SEM micrograph of location 4 in Fig. 4 at higher magnification 59

8. XRD patterns for Cordierite glass/α-Cordierite mixtures for glass content determination (QXRD method) 60

9. Intensity ratios for Cordierite glass/α-Cordierite mixtures versus glass content (QXRD Method) 61

10. Standard curve for α-Quartz 2θ = 20.8, $2\theta'$ = 28.3 62

11. Standard curve for Mullite 2θ = 60.6, $2\theta'$ = 28.3 63

12. Standard curve for Magnetite 2θ = 30.1, $2\theta'$ = 28.3 64

13. Standard curve for Hematite 2θ = 24.1, $2\theta'$ = 28.3 65

14. Standard curve for Melilite: 2θ = 31.20, $2\theta'$ = 46.97 66

15. Standard curve for Merwinite: 2θ = 31.30, $2\theta'$ = 28.40 67

16. Intensity ratio of glassy halo at 24° 2θ versus glass content for Cordierite glass/α-Cordierite mixtures 68

17. XRD patterns of mixtures of vitrified and redevitrified Forestburg fly ash 69

18. Intensity ratio of glassy halo at 25° 2θ versus glass content for Forestburg glass and redevitrified glass mixtures 70

19. Scattering intensity $\bar{I}_X - \bar{I}_O$ at 2θ-24° versus glass content for Cordierite glass/α-Cordierite mixtures 71

20. Scattering intensity $\bar{I}_X$-$\bar{I}_0$ at 2θ-25° versus glass content for Wabamun fly ash 72

21. Reconstituted XRD scans of Wabamun fly ash 73

22. Intensity ratio of amorphous hump versus NaCl standard (2θ-31.7°) for Cordierite glass/α-Cordierite mixtures 74

23. X-ray diffraction patterns of glasses in Na_2O-SiO_2 system 75

24. X-ray diffraction patterns of glasses in Na_2O-CaO-SiO_2 and other systems 76

25. FTIR spectra of fly ashes and slags 77

26. FTIR spectrum of Sundance fly ash in the 4000-400 cm^{-1} range 78

INTRODUCTION

Mineral waste materials (such as blast furnace slag, copper, nickel and lead slags, fly ash, and silica fume) are by-products of metallurgical furnaces and power plants. Most of these products are disposed of in waste dumps, or are used as landfills, railroad ballast, or in other low-value applications. In North America, there is an increased interest in the pozzolanic and cementitious properties of mineral wastes and in the potential to use these wastes as partial portland-cement replacement in concrete, either in the form of blended portland cement or as mineral admixtures at the mixer. This use of mineral wastes would result in reduced costs in concrete manufacture and in better utilization of available resources. It would also produce materials with longer-term strength and greater resistance to weathering and to aggressive chemical action (1).

Neither the origin nor the chemical composition but, rather, the mineralogical composition and particle characteristics determine the pozzolanic and cementitious properties of these materials (2).

Basically, the chemical composition indicates the presence of the same elements, although their properties can vary widely. Most waste materials are reactive when in a glassy state. Therefore, it is logical to assume that a general theory - common to all these by-products - should be outlined to explain the behaviour of glassy materials incorporated in portland cement in concrete.

The purpose of this study is to find an accurate procedure to measure glass content in mineral wastes with a view to the prediction of their behaviour in portland-cement concrete in offshore construction.

In this report, a brief description of the mineral wastes is given, followed by a discussion of the different methods available for glass-content measurements. The study centers on the experimental work mainly in blast furnace slags and fly ashes, and an exhaustive discussion is presented. All the mineral wastes tested are from Canadian sources, except one blast furnace slag which is from the U.S.A.

ORIGIN AND PRODUCTION OF CEMENTITIOUS AND POZZOLANIC BY-PRODUCTS

The annual production of glassy waste materials such as slags, fly ashes, and silica fumes in Canada is about 12.5×10^6 tonnes. A breakdown of the various categories is shown in Table I (3,4,5).

SLAGS

Slags can be classified into three categories, depending upon their origin:

- iron blast furnace slag
- steel plant slags
- non-ferrous slags.

Iron blast furnace slag is a by-product of pig iron production. It results from the fusion of fluxing stone, gangue, and fuel ash during the pyroprocessing of metallic ores. The first report on the utilization of ferrous slags appeared in 1862 when Langens discovered that iron blast furnace slag, granulated from the molten state by quenching in water, possessed good cementing properties (6). Since then slags have been used in Europe to reduce the energy consumed in making concrete. A list of sources and quantities of blast furnace slags produced in Canada is given in Table 2.

Four general classes of blast furnace slag may be distinguished:

- air-cooled, largely crystalline slag, used as aggregate or granular base material;
- foamed or expanded slag, used as lightweight aggregate (this type is no longer produced in Canada because of the air pollution problems caused by H_2S during foaming);
- granulated slag, formed when molten slag is rapidly quenched with excess water (this is the primary source of slags used for hydraulic cements in Europe, Japan, and the U.S.A.);

- pelletized slag, produced by expanding molten blast furnace slag under water sprays and passing the resulting pyroplastic material over a spinning drum.

Granulated and pelletized slags contain most of the lime, magnesia, silica, and alumina in a glassy state. Finely ground to between 400 to 600 m^2/kg (Blaine method), the slags develop cementitious properties that render them suitable for partial portland-cement replacement.

Steel plant slags are produced during the conversion of pig iron to steel. Cooled slowly in air, steel slags are practically inert but rapid quenching in excess water produces a highly glassy material with cementitious properties. Sources and quantities of steel slags produced in Canada are listed in Table 3.

The composition of steel-making slags varies widely (7), and therefore they are not utilized for their hydraulic activity. They are either returned to the blast furnace for recovery of iron, or are used for highway base or granular fill.

Non-ferrous slags are produced in smelting operations as a by-product in the production of copper, nickel, and lead. They contain a high percentage of iron and a low percentage of lime. It is not clear whether granulation increases their pozzolanic properties (8,9). Table 4 lists the sources and quantities produced in Canada (10,11).

FLY ASH

Fly ash is a by-product from the combustion of pulverized coal in thermal power plants. Mechanical collectors or electrostatic precipitators separate the ash as a fine particulate residue prior to discharge to the atmosphere. The chemical composition of fly ash is determined by the types and relative amounts of mineral matter in the coal used. More than 85% of most fly ashes comprise compounds and glasses formed from SiO_2, Al_2O_3, CaO, and MgO. Fly ash used as a pozzolan to replace some of the portland cement in concrete impacts improved specific engineering properties to the binders.

Fly ashes can be divided into two categories:

- Low-calcium, Class F, fly ash, which is a product of the combustion of anthracite and bituminous coals, usually contains less than 5% CaO and consists mainly of aluminosilicate glass with probably a core of crystallized non-reactive aluminosilicates (2).

- High-calcium, Class C, fly ash, composed mostly of silicate glass containing a total of 15 to 35% CaO, MgO, Al_2O_3, and alkali oxides is the product of the combustion of lignite and subbituminous coals, and has cementitious and pozzolanic properties.

Table 5 lists the production and utilization figures for coal ash on a worldwide basis (4). It can be seen that of the 2.6×10^6 tonnes of coal ash produced in Canada in 1977 only 27.1% was utilized. In 1981, a total of 21 coal-fired thermal generating stations produced about 3.7×10^6 tonnes of ash, including 2.5×10^6 tonnes of fly ash (4).

SILICA FUME

The present study deals with the characterization and glass content measurements only in fly ashes and in blast furnace slags. The objective is to develop a general theory for the role of glassy waste products in concrete for offshore construction. The term "slag" will be used to name blast furnace slags.

GLASS CONTENT MEASUREMENTS: BACKGROUND INFORMATION

METHODOLOGY FOR GLASS CONTENT DETERMINATION

A number of studies have addressed the importance of glass content of slags for the strength of slag-concrete. Schwiete and Dolbor (12) modified quenching conditions for each of 30 slags and found that the predominant factor affecting strength was glass content. Slags with 30 to 40% could still be employed, however. Smolczyk (13)

did not find a linear relationship between glass content and strength, and Demoulian et al. (14) reported that the strengths of slags with glass contents in excess of 95% were reduced.

The degree to which glass content can be measured with precision is doubtful, however, and the results between various techniques are not always in agreement. The various methods of glass content determination in slags have been reviewed by Hooton (15).

Table 6 lists the various methods of glass content determination reported for glass-ceramics, polymers, slags, and other waste materials.

X-Ray Techniques

X-ray diffraction (XRD) techniques have been used to determine the glassy or crystalline contents of such diverse materials as slags (15), mineral dusts (16), portland cement (17), coal ashes (18), glass-ceramics (19), and polymers (20). All methods are essentially based on the assumption that the crystalline and non-crystalline components of a material make distinguishable contributions to the scattering intensity of its XRD pattern.

Broadly speaking, two approaches have been used. In the first one, the percentages of each of the crystalline phases is determined from the crystalline scattering and the glass content is computed by difference. The second approach involves the calculation of the glass content directly from the non-crystalline scattering. Both approaches can be used, in principle, for the determination of the glass content of glassy waste materials.

Quantitative X-ray determination (QXRD method)

In a sample containing glassy and crystalline phases, the mass fraction of each crystalline phase can be determined by measuring peak intensities at selected 2Θ-values as ratios to the peak intensity of an added internal standard. This technique has been used extensively for the quantitative determination of the crystalline phases in slags (15), mineral dusts (16), portland cement (17), coal ashes (18), and glass-ceramics (19). The method, which can give an accuracy of ±5%, has been described in detail by Klug and Alexander (21).

Crucial to the success of the method are the following factors:

- a chemically stable internal standard with several strong diffraction lines in the XRD pattern, free of interference from the crystalline phases to be identified;
- a particle size less than 5 μm;
- the preparation of standard curves to improve accuracy;
- sufficient counting time and/or repeated scanning to improve accuracy.

Provided the major crystalline phases can be identified, this technique is particularly useful since it enables the calculation of glass content by difference and the quantitative estimation of the composition of the glassy phase by subtraction of the elemental content of the crystalline phases from the overall composition.

Simons and Jefferey (18) used the QXRD technique to determine the crystalline and glass content of a number of pulverized fuel ashes from U.K. and U.S. sources. Glass contents calculated varied from 52 to 87%.

Hooton and Emery reported glass contents between 10 and 100% for a number of commercial slags from various sources using the QXRD technique (22).

Mehta has used the QXRD technique to indicate the magnitude of the content of various crystalline phases in U.S. fly ashes (23).

Non-crystalline scattering methods

A number of variants exist in this approach in which the non-crystalline scattering is determined either in conjunction with, or without, an added internal standard. The crystalline scattering may be considered as well.

Amorphous intensity method

In this approach the glass content is calculated by comparing the intensity of the amorphous halo at a suitable 2Θ-value between samples to be ana-

lyzed and a standard which is fully vitreous. The technique in this form has been used for the dedermination of the glass and crystalline content of single-phase glass-ceramics (24). The accuracy claimed was ±5% or better. The method requires the preparation of fully vitreous and crystalline analogues with the same overall composition as the waste material.

Amorphous hump method

In another variant, the glass content is estimated by comparing the area of the amorphous halo with the area of a selected peak of an added internal standard. This approach, referred to as the "amorphous hump method," has been used to determine the glass content of pozzolans (15).

Since the position and area of the hump depend on the composition of the glass, a series of standard glasses of a range of compositions is required. Also, as pointed out by Mather (25), the use of copper radiation on iron causes a halo due to secondary iron X-ray emission. No calibration curves are required for this method.

Amorphous-crystalline scattering method

This technique, which can be used if a 100% amorphous standard is not available, has been reported for polymers. For the method to be applicable (a) samples with a considerable range of crystallinity must be available, and (b) it must be possible to draw an acceptable demarcation line between the crystalline and amorphous scattering over some angular interval that encompasses the principal amorphous halo.

In general, good agreement has been found among the methods listed above. The advantage of the amorphous-crystalline scattering method is that there is no need for vitreous and crystalline analogues of the glassy waste material under consideration.

Differential intensity method

The method devised by Wakelin et al. (26) for polymers is based on the calculation of an integral or correlation crystallinity index:

$$\text{Integral index: } C_i = \frac{\sum_{2\theta_o}^{2\theta_m} (I_u - I_a)}{\sum_{2\theta_o}^{2\theta_m} (I_c - I_a)}$$

$$\text{Correlation index: } (I_u - I_a) = C_c\,(I_c - I_a + B)$$

where: I_u = intensity of sample at designated 2θ-values

I_a = intensity of the amorphous polymorph over the 2θ-values

I_c = intensity of the crystalline polymorph over the 2θ-values.

The intensity values are measured over small 2θ-increments (e.g., 0.05°).

Optical Techniques

Techniques using optical microscopy are based on statistical counting of glassy and crystalline particles. A number of variants have been developed for slags.

McMaster individual particle analysis

This procedure, originally developed by Emery et al. (27), was modified by Hooton and Emery (22) to distinguish between clear glassy particles, birefringent crystalline particles, and opaque milky particles. Well-washed, -65 μm/+45 μm grains, immersed in ethylene glycol, are observed under cross-polarized light at 400 x magnification. The glass particles do not transmit cross-polarized light (whereas most crystalline materials do) and tend to glow due to birefringence. This method was found to correlate well with the QXRD method for slags.

South African optical procedure

This cross-polarized light procedure has been adopted in Canada by Standard Slag Cement Company (28). This method uses the -65 μm/+45 μm fraction of ground slag immersed in camphor oil. The opaque particles are assumed to be glass; orange

translucent particles are crystalline. At least four or five counting areas need to be scanned. This method was found to be highly insensitive to changes in glass content.

Parker and Nurse optical method

The original method published in 1949 (29) is currently employed in a modified form by Frodingham Cement Company in Britain. Grains -90 µm/+53 µm, of slag immersed in bromoform are examined by transmitted light at 200 x magnification using an eyepiece with a graticula. The percentage of opaque particles is subtracted from 100 to obtain the percentage of glass.

Rheinhausen optical method

This method was developed at the Rheinhausen Institute for Blast Furnace Slags, Rheinhausen, West Germany. A polished section is made of -60 µm/+40 µm ground slag, bedded into a plastic material polished in plastic. The polished sample is etched with 1% of HNO_3 and HF vapour. An integration occular is used to count the vitreous and crystalline components. This method has been described by Schroder (30).

Spectroscopic Techniques

Several techniques have been developed to determine the glass content of slags, polymers, etc., using ultraviolet and vibrational spectroscopy.

Automated ultraviolet reflectance method

This method, described by Foster (31), employs an ultraviolet (UV) spectrophotometer fitted with a solid sample chamber. The technique measures the percentage of emission at 590 nm compared to a standard, arbitrarily assigned value of 100% glass. Since the standard may actually contain less than 100% glass, glass contents in excess of 100% are sometimes observed by this method (31).

Hooton and Emery reported that this technique, although able to identify slags of low glass content, may give erroneous results for slags with higher glass contents (28). Another drawback may be the interference with the UV radiation due to minor oxide contents (32).

Rheinhausen ultraviolet method

This method was described by Schroder (30). A preliminary study of this technique, using a portable UV light source, showed this procedure to be more qualitative in nature. The technique also poses a hazard to the eyes of the operator. As with the Automated UV Reflectance Method, minor oxide staining may cause interference (32).

Infrared techniques

Although infrared absorption is not a good measure of long-range order of crystallinity, certain infrared bands of polymers can be specifically related to the configuration states of molecular chains. Various workers have been able to relate the intensities of specific infrared bands to the amorphous fraction of polymers (20, 33-35).

Dougherty (36) reported the use of an infrared technique in conjunction with an internal standard to calculate the glass content of slags and fly ashes. The method was reported to give good correlation with other techniques for slags but poor correlation for fly ashes.

Nuclear magnetic resonance

This technique, which gave results for organic polymers in good agreement with XRD data, may not be useful for inorganic glasses because of the measuring temperature requirement which has been found to be in excess of the glass transition temperature for organic polymers (20).

Electron-Optical Techniques

Electron-microscopy for determining the per cent crystallinity of glass-ceramics is well known. Carrier (37) described an SEM technique in which the glassy phase of a partially devitrified glass-ceramic is selectively etched leaving the crystalline phase in relief. The volume per cent of the crystalline material can be determined by areal analysis, lineal analysis, or point counting on electromicrographs. The technique is more complex for glass-ceramics with more than one crystalline phase. Several solvents may be required to preferentially etch the various phases, leaving an often complex relief. The method is applicable

if the crystal size is in excess of 0.1 μm. The glass content is obtained by difference.

Doherty and Leombruno (38) describe a TEM technique for the determination of the crystalline phases in a glass-ceramic using a selected area diffraction technique and dark-field micrography. Amorphous material can be photographed by placing an aperture in the amorphous halo and taking a photograph of the area underneath it.

TEM can also be used to study the glassy and crystalline phases in even the smallest (submicron) fly ash particle (39). However, a substantial amount of development work will be required to adapt these methods to routine glass content determinations of materials as complex as fly ashes.

Solution Techniques

Hulett et al. (40,41) have described a technique by which the fly ash can be quantitatively separated into three matrices:

- glass
- mullite-quartz
- magnetic spinel.

The method involves size-fractioning and magnetic separation. The iron containing spinels and oxides is removed from the aluminosilicate residue by treatment with concentrated HCl. The glass phase is removed from the non-magnetic phases by etching with 1% HF, leaving behind a mullite-quartz rich residue. The method is potentially useful since it will enable a calculation of the glass content and the composition of the glassy phase.

Density Method

Crystallization in a system is accompanied by an increase in density. The glass content by volume can be represented by:

$$x_{a,v} = \frac{\ell_c - \ell}{\ell_c - \ell_a}$$

where: ℓ_c = crystalline density
ℓ_a = amorphous density
ℓ = density of the unknown sample.

The glass content by mass is given by:

$$x_{a,m} = \frac{\ell_e}{C} \frac{(\ell_c - \ell)}{(\ell_c - \ell_a)}$$

This method, which has been used for polymers (20), requires that the densities of a fully vitreous sample, a fully re-devitrified sample, and the unknown sample can be determined. The results agree well with those determined by XRD techniques (34).

It is implicit in this method that:

- The density of the amorphous phase is the same in the fully vitreous and unknown sample.

- No pores exist in the fully vitreous and unknown specimens.

It is unlikely that these conditions will apply rigorously for glassy waste materials. This is particularly true for fly ashes which contain substantial proportions of hollow spherical particles (cenospheres).

Differential Thermal Analysis (DTA)

This method has been used in Germany and South Africa in relationship to hydraulic properties, but with little success (32,42). The method is based on measuring the area of the slag devitrification exotherm (800-900°C) for a known weight of sample. Unfortunately, each mineral has its own exotherm (43) and the results change with the chemical composition of the slag.

Selection of Glass Content Methodology

For the purposes of determining the glass content of the different types of glassy waste materials the following criteria have been used:

- The technique must be applicable to slags, fly ashes, and glassy waste materials.

- The technique must be accessible and inexpensive.

- The technique should not require elaborate preparation and handling.

Applying these selection criteria to the techniques described in the previous sections, the following conclusions have been reached:

XRD techniques

All five XRD techniques listed in Table 6 are potentially applicable for the determination of the glass content in glassy waste materials. The QXRD technique has the added advantage that it provides a route by which the glass composition can be calculated as well.

Optical techniques

The optical techniques have limited value only, since they are based on the ability to separate glassy and crystalline particles. This condition is invalid for fly ashes where the crystalline phases are embedded in the glassy matrix.

Spectroscopic techniques

The UV methods are unlikely to be useful because of the interference of colouring oxides. The NMR method is probably not useful because of the requirement to perform measurements close to the softening point of the glass. The latter technique also requires access to expensive NMR equipment. The infrared technique may prove to be useful, provided that vibrational frequencies common to all components of a complex system such as a fly ash, can be found.

Electron-optical techniques

SEM is probably not very useful because of the small crystalline size in fly ashes. TEM may be useful if a way can be found to examine a representative sample of the glassy waste material.

Solution method

This method ranks with the QXRD technique as one of the potentially more useful methods since it has been applied to fly ashes and it can give glass composition as well as glass content.

Density method

The density method is worthwhile investigating because of its simplicity. The requirement is, however, that a fully vitreous and devitrified analogue of the glassy waste material can be prepared. The density technique resembles in this respect the non-crystalline scattering techniques.

DTA method

This method appears to have limited applicability to homogeneous materials, such as slags. The techniques worthy of consideration are listed in Table 7.

EXPERIMENTAL METHODS

MATERIALS

Nine Canadian fly ashes, one Canadian slag, and one American slag were analyzed as follows:

- by X-ray fluorescence (XRD) Na_2O, MgO, Al_2O_3, SiO_2, P_2O_5, K_2O, CaO, TiO_2, Fe_2O_3, Ca_2O_3, and MnO_2;
- by Direct Current Plasma (DCP) B_2O_3, PbO, and ZnO;
- by a wet technique SO_2.

The loss on ignition (LOI) was also determined, as well as total carbon content (Table 8).

DENSITY DETERMINATIONS

Specific gravities of the source materials were determined by pycnometry and by the Le Chatelier method. The specific gravities were determined on as-received samples and on samples ground for 30 min in an automatic grinder.

PARTICLE SIZE ANALYSIS - WET SIEVING

Particle size analysis by wet sieving was carried out as follows. The source materials were rehomogenized prior to testing. A mass of 10 g of each sample was washed with distilled water until

no more fines were passed through a 45 µm sieve. The percentage by mass retained on the 45 µm sieve was calculated.

SURFACE AREA ANALYSIS - BLAINE

Blaine surface area analysis was carried out for Wabamun and Dalhousie fly ashes. Specific gravities were co-determined using the Le Chatelier method with ethanol displacement.

SURFACE AREA ANALYSIS - B.E.T.

Samples of Reynolds Al_2O_3 (known surface area: 8.0 $m^2.g^{-1}$) and the source materials were characterized by specific surface area analysis (B.E.T. triple point method). The samples were outgassed overnight at room temperature. Two of the samples (Reynolds Al_2O_3 and Wabamun fly ash) were subsequently analyzed using nitrogen as the adsorbing gas. Since the results for Reynolds Al_2O_3 were lower than expected, measurements were also carried out using krypton as the adsorbing gas. Outgassing was carried out for 60 h at room temperature. The result for Reynolds Al_2O_3 showed better agreement with the expected value. Krypton was subsequently used for all other samples.

X-RAY POWDER DIFFRACTION MEASUREMENTS

X-ray powder spectra were recorded using a diffractometer equipped with goniometer, using a nickel-filtered CuK_α radiation at 40 kV and 30 mA. The range of measurements was 20-6° to 71° and the scan speed for rapid scans was 2°/min. Peak intensities for glass content determinations were also determined using slow scanning and stationary (point) counting.

FOURIER TRANSFORM INFRARED SPECTROSCOPY (FTIR)

Infrared spectra of the as-received source materials were measured using a Fourier Transform Infrared spectrometer. The samples were run as KBr pellets. The Thunder Bay fly ash was also run using photo-acoustic spectroscopy. It was found that the FTIR reflectance spectrum measured with the latter technique was similar to the FTIR absorbance spectrum using KBr pellets. Since adsorption spectra are easier to prepare, it was decided to use this technique for the samples.

OPTICAL EXAMINATION-McMASTER TECHNIQUE

The modified McMaster Individual Particle Analysis Method (CSA A363-MI983) was used to determine glass contents of the two blast-furnace slag samples of this study. The granulated as-received slags were wet-sieved to provide a fraction -63/+45 µm sieve. Immediately before examination, a small amount of sample is placed on a glass slide and a drop of ethylene glycol or camphorated oil is applied. A cover plate is placed on top and sheared to spread the fluid and to obtain a uniform, single layer of particles.

OPTICAL EXAMINATION - IMAGE ANALYSIS

Slurries of homogenized fly ash samples were prepared using a 10% solution of Elvacite in isopropanol. The slurries were pressed in a tablet, 2.5 cm in diameter using a specimen mount press (Buehler) at 9000 psi. The tablets were left to dry for a 24-h period prior to optical examination. Image analysis was carried out using an Image Analyzer.

ELECTRON OPTICAL INVESTIGATION

An extensive electron optical investigation was carried out on a selected (Wabamun) fly ash. The sample, in an Elvacite medium without any further application of a coating, was subjected to scanning electron microscopic examination (SEM) in conjunction with energy dispersive X-ray analysis (EDXA).

A more extensive electron optical investigation was carried out using Wabamun fly ash in epoxy. Initial examination was carried out on cut discs, 2.5 cm in diameter. To obtain information on the interior of the fly ash particles, the samples were cut to 1-mm-thick slices. The specimens were subsequently subjected to argon ion-milling for approximately eight hours. The etched samples were carbon-coated prior to SEM examination.

EXPERIMENTAL RESULTS

CHEMICAL ANALYSIS

Table 8 shows the results of chemical analysis for the nine fly ashes and two blast-furnace slags investigated in this study. The composition has been expressed for the common oxides of the major elements. Loss on ignition values and carbon contents are also shown. For fly ashes, the CaO content varied from 1.29 to 13.0%. The slags contained 35.1% and 40.1%, respectively.

SPECIFIC GRAVITY DETERMINATIONS

Table 9 shows specific gravities of the source materials. Both pycnometry and the Le Chatelier technique were used for seven Canadian fly ashes. Since pycnometry was found to be more reliable, this technique was the only one used for the remaining samples. Specific gravities for the first set of samples were shown for the as-received samples as well as for samples ground for 30 min in an automatic grinder. The Dalhousie fly ash showed an as-received specific gravity of 3.10 and 3.05 after grinding, as compared with 2.00 to 2.67 for other fly ashes.

PARTICLE SIZE ANALYSIS - WET SIEVING

The results of wet sieving of the source materials are shown in Table 10. The data give the percentage by mass retained on a 325 mesh (45 µm) sieve. The Thunder Bay fly ash seems to be the coarsest fly ash.

SURFACE AREA ANALYSIS - BLAINE

Blaine surface areas in $m^2.g^{-1}$ for Wabamun and Dalhousie fly ashes are listed in Table 10.

SURFACE AREA ANALYSIS - B.E.T.

Table 10 lists the surface areas determined for the eleven source materials of this study using the B.E.T. (triple point) technique with krypton as the adsorbing gas. B.E.T. measurements using nitrogen gave values of:

7.3 $m^2.g^{-1}$ for Reynolds Al_2O_3 and
1.4 $m^2.g^{-1}$ for Wabamun fly ash.

The results are in some cases up to tenfold greater than those obtained by the Blaine method, probably due to the nature of the hollowed cenospheres.

GLASS CONTENT METHODOLOGY (1):
OPTICAL EXAMINATION BY IMAGE ANALYSIS

Figure 1 shows an optical micrograph (magnification 137x) of a Wabamun fly ash in an Elvacite medium prior to image analysis. The sample showed predominantly spherical beads - some white opaque and some transparent - in the darker medium. Several spherical fly ash beads were identified as being hollow (cenospheres). Several crushed beads could also be observed.

Image analysis was carried out using an Image Analyzer. Assuming that the opaque white areas in Figure 1 represented devitrified material, the content of crystalline matter was determined as 6.6%. The glass content was computed as 93.4% by difference.

GLASS CONTENT METHODOLOGY (2):
ELECTRON OPTICAL INVESTIGATION

An electron optical investigation was carried out for Wabamun fly ash. The first step was an examination of a cut disc prepared for optical examination and image analysis. Figures 2a and 2b show SEM micrographs at different magnifications. Several spherical fly ash particles can be distinguished as well as some crushed material.

Table 11 lists the concentration range observed for selected oxides as well as the concentration of these oxides in the fly ash overall.

Subsequently, the SEM study was continued on a Wabamun sample mounted in epoxy and polished by ion-etching. Figure 3 shows a view of the sample cross-section in secondary electron (a) and backscatter modes (b).

Figure 4 shows another view of the sample after etching.

Figure 5 shows a close up of location 3 in Figure 4 at higher magnification.

Figure 6 is a SEM micrograph of a cross-section through a spherical fly ash particle at location 3 showing smaller particles in the interior (plerosphere).

Figure 7 is a SEM micrograph of a non-spherical particle at location 4 on Figure 4. EDXA analysis was carried out at several points in the particles. The results have been summarized in Table 12.

The SEM investigation was conducted with the primary objective to establish whether an electron optical approach could be used to establish the glass content of fly ashes and slags. It was hoped that enough contrast in the sample cross-sections would be available to discern the crystalline phases from the glassy phase in the particle quantitatively by image analysis. An examination of the cross-sections showed no clear demarcation between the glassy phase and the remainder. The SEM approach was therefore abandoned for glass content methodology development.

GLASS CONTENT METHODOLOGY (3): McMASTER TECHNIQUE

The two blast-furnace slags, Standard and Atlantic, were analyzed by the modified McMaster Individual Particle technique (CSA A363-M1983). This method, developed by Emery and coworkers at McMaster University, distinguishes between clear glassy particles, birefringent crystalline particles, and opaque milky particles. Particles that glow milky white but not with definite birefringence under crossed polars should be considered crystalline (generally opaque in plane light).

The problems that arise with the McMaster method is the interpretation of what to count as glass or crystalline, and the estimation of their relative percentages in a given particle. The percentage estimations should not vary appreciably among observers, but the actual assigning of glass or crystalline to particles or sections of particles does, in some cases, depend on the operator. Particles or sections of particles which either stay dark under crossed polars or exhibit definite birefringent colour changes on stage rotation under crossed polars pose no problem and can be estimated fairly accurately for glass content.

The problem arises with two other types of particles. The first are those that appear opaque or stained under plane polarized light and exhibit a milky, translucent glow under crossed polars. According to the instructions for the McMaster method these should be considered as crystalline. The second group are those which are centrally dark with a fringe of either milky or translucent brightness around their edges.

The various determinations of glass content have been compiled in Table 13. There is a great deal of variation among the results obtained by different operators. In the data sets collected by operator A, particles that looked opaque under plane light but black under crossed polars were not included for the calculation of the glass content. Operators B and C included these same particles as 100% crystalline. Both these operators used the gypsum plate for their glass content estimations. It appears, then, that operator A will tend to observe higher glass contents than either operator B or operator C. Table 13 shows this to be the case.

GLASS CONTENT METHODOLOGY (4):
QUANTITATIVE X-RAY DIFFRACTION METHOD (QXRD)

The literature assessment of glass content methodology showed this technique to be one of the potentially more useful methods.

The method is a direct route to a quantitative determination of the content of a particular crystalline phase. The combined amounts of the crystalline phases enable, indirectly, calculation of the glassy content by difference. The mass present for each crystalline phase is computed from the characteristic peak intensity of this crystalline phase as a ratio to the peak intensity of an added internal standard. The mass fraction of each phase is then determined by comparison of the intensity ratio in the sample to the intensity ratio for pure synthetically produced phases.

FEASIBILITY OF APPROACH -
MODEL STUDY ON THE CORDIERITE SYSTEM

To demonstrate the feasibility of using the QXRD method a glass/glass-ceramic system based on

cordierite was chosen. This substance has the formula:

$$2MgO.2Al_2O_3.5SiO_2$$

and its composition by mass

$$(MgO: 13.78\%,\ Al_2O_3: 34.86\%,\ SiO_2: 51.36\%)$$

bears some resemblance to the glassy waste materials of this study if one substitutes MgO for CaO.

Cordierite, which occurs as a mineral and as the substrate for low expansion ceramics, has been extensively characterized. Mixtures of glassy cordierite and the α-cordierite crystalline polymorph were prepared to demonstrate the feasibility of the QXRD technique.

Preliminary Evaluation

A preliminary evaluation of the QXRD method involved the determination of selected peak intensities in the XRD patterns of cordierite glass/α-cordierite mixtures, to which NaCl was added as an internal standard. Mixtures were prepared containing 100%, 75%, 50%, 25%, and 0% glassy cordierite, respectively. XRD spectra for the mixtures are shown in Figure 8.

The following peaks were selected for the calculations:

(NaCl: 31.7°, 2.821; 45.5°, 1.994
α-cordierite: 21.7°, 4.09;
26.3°, 3.39; 28.5°, 3.13; 29.6°, 3.02).

The relative peak intensities versus α-cordierite content are graphically depicted in Figure 9. It can be seen that the intensity ratio:

$$\frac{(I_{Cor,2\theta}/I_{NaCl,2\theta'})}{(I_{Cor,2\theta}/I_{NaCl,2\theta'})_{100}} \times 100\%$$

versus α-cordierite content is a straight line.

Linear regression gives:

$$y = 0.9961x + 2.3 \quad (r = 0.9981).$$

Thus, the correlation is highly significant.

THE QXRD METHOD APPLIED TO FLY ASHES - RAPID SCANS

Having demonstrated the feasibility of the QXRD method for the cordierite system, the method was used to calculate the crystalline and glassy content of the first set of fly ashes as follows.

Identification of Major Crystalline Phases in the Fly Ashes

Table 14 lists the source materials of this study and the major crystalline phases identified from their XRD patterns. All fly ashes have quartz as one of their crystalline components, most contain mullite and a few contain magnetite or hematite. This preliminary investigation did not attempt to characterize trace phases.

Selection of Standard

NaCl was chosen as a standard since it was found that this compound had two strong peaks (d-spacings 2.821 and 1.994), at least one of which did not interfere with the major peaks of each of the above four phases.

Quantitative Determination of Crystalline Phases and Glass Content

A preliminary quantitative determination of each of the four phases identified in the seven Canadian fly ashes was carried out as follows:

- XRD patterns were recorded for each of the four phases (α-quartz, mullite, magnetite, hematite) with NaCl. The amount of NaCl reference added was 10% by mass. From the XRD spectra the intensity ratios of each of the lines selected for the phases (two or three) with each of two lines of NaCl was computed. The intensity ratio:

$$\frac{I_{phase\ X,2\theta}}{I_{NaCl,2\theta'}}$$

corresponds to a mass ratio of 9 g phase X/g NaCl. The intensity ratios for the four phases are listed in Table 15.

- As for the pure phases, the intensity ratios for the various line combinations for a specific phase have been calculated for the seven Canadian fly ashes. The mass of each phase is then calculated as an average over the various line combinations.

- The percentages by mass of the four crystalline phases and the glass content for the seven Canadian fly ashes have been compiled in Table 16.

Glass Content = 100% - Σcrystalline phases - LOI

IMPROVEMENTS TO THE QXRD METHOD

Based on these findings, it is considered that the QXRD technique can be further improved as follows:

- Choice of internal standards. Important considerations are that the standard:

  - be readily obtainable in high purity;

  - give sharp diffraction lines;

  - provide strong diffraction lines near the phases of interest to be determined;

  - not be superimposed by the phases of interest or by other materials (commonly found within the glassy waste material).

- Since NaCl is somewhat hygroscopic, standards other than this compound should be considered.

- More accurate measurements can be performed by reducing the crystallite size to <5 μm by extended grinding.

- The accuracy can be increased by carrying out multiple scans for each composition.

- The accuracy can also be increased by increasing the scanning time per peak.

- Instead of using only two points (intensity ratio at 9 g phase/g NaCl and 0,0), a larger number of intensity ratios corresponding to a series of crystalline phase/standard compositions could be measured. This would give a more accurate standard curve.

Selection of CaF_2 Standard

CaF_2 was selected as an internal standard since it is less hygroscopic and it has at least one line which does not interfere with the lines of the four crystalline phases found in the fly ashes.

Reduction of Particle Size

Klug and Alexander (21) discussed the effect of crystalline size on the reproducibility of intensity data. It was found that the mean deviation intensity over ten values for 15-50 μm powder was 18.2%; whereas for a <5 μm powder it was only 1.2%. Care was therefore taken to use crystalline powders with a particle size <5 μm. Particles of this size range were prepared by settling trials.

According to Stokes' Law:

$$V_f = \frac{d^2 g\ (\rho s - \rho L)}{18\ \mu}$$

where: V_f = velocity (cm s^{-1})
g = gravitational constant: 980 cm s^{-2}
ρ_s = density solid (g cm^{-3})
ρ_L = density liquid (g cm^{-3})
d = diameter particle (cm)
μ = viscosity of the liquid (p).

On the basis of the velocity, V_f, the average time can be calculated for a 5 μm particle to settle over a specified distance. Particles <5 μm will require more time. The procedure is to suspend the crystalline powders in a suitable solvent in a graduated cylinder and leave the suspension for the calculated time. The relevant parameters for selected materials for this study are listed in Table 17. The top 20 cm of the suspension were siphoned off and dried at 60°C for 16 h. Some error is expected to be introduced into this technique as a result of the presence of particles of varying specific gravity in fly ash.

Preparation of Standard Curves

Standard Curves were prepared for α-quartz, mullite, hematite, and magnetite with CaF_2 as an internal standard and a glass composition (CaO, 15.62%; MgO, 2.55%; SiO_2, 65.98%; Al_2O_3, 15.84%) as diluent. The compositions of the mixtures used for the standard curves are listed in Table 18. A number of lines were selected for each phase as well as for CaF_2 for intensity determinations. Table 19 lists the peaks and ranges scanned for the various crystalline phases.

The α-quartz-glass-CaF_2 system was used to establish basic methodological parameters. Initially, a series of ten slow scans was carried out on a mixture of α-quartz, diluent, and CaF_2, to determine the number of duplicate scans required to obtain acceptable intensity values. It should be noted that the preparation of the standard curves is extremely time consuming and this investigation was aimed at achieving a reasonable trade off between accuracy of the intensity values obtained and the number of duplicate scans required to achieve a certain precision.

Statistical treatment showed that three consecutive scans were sufficient to produce results generally within 2% of the average value. Standard curves were subsequently produced by determining the intensities of selected characteristic peaks and calculating the ratio of characteristic peaks of α-quartz and CaF_2 for each scan:

$$IR\ (Intensity\ Ratio) = \frac{I_{Q,2\theta}}{I_{F,2\theta'}}$$

where: $I_{Q,2\theta}$ = intensity of a characteristic peak of α-quartz at 2θ.

$I_{F,2\theta'}$ = intensity of a characteristic peak of CaF_2 at $2\theta'$.

The procedure followed in computing the intensity ratios was as follows:

- For a freshly packed sample specimen, all peaks were scanned sequentially. Each peak intensity determination involved three measurements (area under the peak, starting intensity, and end intensity). The peak area was scanned for 100 s; the starting and end intensities were scanned for 40 s each. The peak intensity was calculated as:

  Peak intensity = Peak area intensity (Starting background + End background) x 1.25.

- The slow scanning was repeated twice with a freshly packed sample. The average peak intensity was then calculated over three consecutive scans. The calculation gave:

  $I_{Q,2\theta}$ and $I_{F,2\theta'}$.

- The intensity ratios were then calculated using:

$$IR = \frac{I_{Q,2\theta}}{I_{F,2\theta'}}$$

- For each composition, the intensity ratios were plotted against the concentration in terms of g α-quartz per g CaF_2. One standard curve was prepared for each combination of α-quartz and CaF_2 peaks. Similar curves were prepared for the other three minerals.

Typical standard curves are shown in Figures 10 to 13.

Crystalline and Glass Content of Fly Ashes

The QXRD technique was used to determine the content of the four crystalline phases, α-quartz, mullite, magnetite, and hematite of eight Canadian fly ashes (Thunder Bay was not investigated in view of the different mineralogy found for this fly ash compared to that of the other fly ashes as discussed below).

Table 20 summarizes the crystalline and glass contents for the eight Canadian fly ashes.

Thunder Bay Fly Ash

Thunder Bay fly ash showed an XRD pattern which was substantially different from that of the other fly ashes. Peaks attributable to sulphur-bearing phases could be identified. This finding is not unexpected since chemical analysis showed a S content of 6.84%, much higher than that of any of the other fly ashes. The sulphur-bearing phases are $CaSO_4$ (anhydrite) and, possibly $Na_3Al(SO_4)_3$, and CaS.

THE QXRD METHOD APPLIED TO BLAST-FURNACE SLAGS

The QXRD method in its improved form was also used to determine the glass content of two granulated blast-furnace slags. Rapid XRD scans showed that Standard slag, produced by National Slag Ltd., Hamilton, Ontario, had melilite as the only crystalline phase. The Atlantic slag produced by Atlantic Cement Company, Inc., Stamford, Conn., was found to contain merwinite as its only crystalline phase.

The preparation of the melilite and merwinite crystalline phases is described in Appendix A. The fine powders (<6 μm) of these materials were used together with vitrified Standard slag glass and Atlantic slag glass powders (<5 μm) for the standard curves.

Preparation of Standard Curves

Standard curves were prepared for melilite and merwinite using CaF_2 as the internal standard and Standard slag glass and Atlantic slag glass as the diluent. The compositions prepared are listed in Table 21. Peaks scanned for the various mixtures are given in Table 22. Standard curves are shown in Figure 14 (Melilite) and 15 (Merwinite). The intensity ratios were calculated somewhat differently from the procedure described above. Intensity ratios were computed by first calculating $I_{M,2\theta}/I_{M,2\theta}$, values for each individually packed sample and then averaging over the three $I_{M,2\theta}/I_{M,2\theta}$, values for three consecutively packed samples.

Crystalline and Glass Content of Slags

Following the preparation of the standard curves, mixtures of each of the two slags were prepared with an appropriate amount of CaF_2. Table 23 demonstrates the calculation of the crystalline and glass contents of each sample.

GLASS CONTENT METHODOLOGY (5):
NON-CRYSTALLINE SCATTERING METHOD (NCXRD)

This potentially useful X-ray diffraction approach to glass content determination uses the non-crystalline XRD technique described by Ohlberg and Strickler (24). The glassy content is determined by measuring the intensity of the amorphous halo in the XRD pattern of the substance of interest at a suitable 2θ-value and comparing it with the intensity of the amorphous halo of the vitreous analog of this substance. Unlike the QXRD method this approach leads to a direct measurement of glass content and is, therefore, potentially more accurate.

Feasibility of Approach -
Model Study on the Cordierite System

To demonstrate the feasibility of the NCXRD approach, mixtures of cordierite glass and α-cordierite were examined. Cordierite ($2MgO.2Al_2O_3.5SiO_2$) was also used to do a preliminary evaluation of the QXRD technique.

Preliminary Evaluation

The preparation of cordierite glass and α-cordierite is described in Appendix A. Mixtures of cordierite glass and α-cordierite containing 0, 25, 50, 75, or 100% glassy material were prepared for XRD analysis.

Using the mixtures of cordierite glass and α-cordierite, the non-crystalline scattering at 2θ-24° was determined. The non-crystalline scattering is a measure of the glass content as follows:

$$\% \text{ Glass} = \frac{I_X - I_B}{I_g - I_B} \times 100$$

where: I_X = intensity of the amorphous halo at 2θ = 24° for the cordierite glass/α-cordierite mixtures;

I_g = intensity of the amorphous halo at 2θ = 24° for cordierite glass;

I_B = intensity of the amorphous halo of the fully crystalline α-cordierite.

A plot of the relative intensity versus glass content is shown in Figure 16. The regression data are:

$$y = 1.006x + 0.00280 \quad (r = 0.9997).$$

The correlation of glass content and intensity ratio for this model system is excellent.

THE NCXRD METHOD APPLIED TO FLY ASHES - RAPID SCANS

Following the demonstration of feasibility of the NCXRD method to the cordierite system the method was subsequently applied to a fly ash. The fly ash chosen was Forestburg and the XRD patterns are shown in Figure 17. The relationship between relative intensity and glass content is shown in Figure 18.

At this preliminary stage, no fully redevitrified analogue could be obtained. In later experiments, fully crystalline redevitrified Forestburg fly ash glass was used. The glass content of the mixtures in the rapid scan experiments described here has been corrected for the residual glass content (38.5%) of the redevitrified fly ash.

The relationship between relative intensity and glass content of the mixtures can be represented by:

$$y = 1.03x + 5.026 \quad (r = 0.993).$$

Again, the correlation is good. Using the data of Figure 18, the glass content of Forestburg fly ash was found to be 85.0%.

Improvements to the NCXRD Method

As with the QXRD technique, the NCXRD method can be improved in several ways:

- The number of data points can be increased by measuring the non-crystalline scattering of an increased number of mixtures of the glassy and crystalline phases.
- The intensities can be more accurately determined with stationary counting than from rapid scans.
- Intensity data for each mixture should be collected for several freshly packed samples.
- A standard should be run at regular intervals to check the reproducibility of the scattering observed.

These aspects have all been taken into account in the glass content determinations described in this section.

Cordierite System

The suggestions in the preceding section were implemented when intensity of a series of cordierite glass/α-cordierite mixtures was redetermined.

Mixtures were prepared containing 0, 10, 20, ... 100% cordierite glass by mass; the balance being α-cordierite. The scattering intensity of each mixture was prepared by counting for 100 s at $2\theta = 24°$. Each mixture was scanned three times using freshly packed samples for each determination. A soda-lime glass reference was run between mixtures as a standard. Figure 19 shows a plot of $I_x - I_o$ versus glass content where:

I_x = scattering intensity of a mixture containing x% glass

I_o = scattering intensity of a mixture containing 0% glass.

The mixture can be represented by the linear relationship

$$I_x - I_o = 3.44 \times 10^{-2} \% \text{ glass} - 1.29 \times 10^{3}.$$

The correlation coefficient was found to be 0.9969. Thus, the correlation is highly significant.

Fly Ashes and Slags

In order to use the NCXRD method, it is required that a fully vitreous analogue of the glassy

waste material can be prepared. A fully crystalline analogue is, strictly speaking, also required, but this condition is somewhat less severe since the percentage of residual glass can be estimated from the residual scattering intensity at the selected 2θ value and a suitable base line in the rapid XRD scan. The preparation of glassy and crystalline analogues is described in Appendix A.

Mixtures containing 0, 10, ..., 100% fly ash or slag glass, with the balance being the redevitrified analogue, were then prepared as for cordierite. Intensity ratios were determined for the standard curves. As an example, a standard curve is shown in Figure 20.

GLASS CONTENT METHODOLOGY (6):
DIFFERENTIAL INTENSITY METHOD (DIXRD)

The Differential Intensity X-Ray technique (DIXRD) described by Wakelin et al. (26) for polymers involves the calculation of the percentage crystallinity from an integral or correlation index. These indices are defined as:

$$\text{integral index: } C = \frac{\sum_{2\theta_o}^{2\theta_m} (I_u - I_a)}{\sum_{2\theta_o}^{2\theta_m} (I_c - I_a)} \qquad (1)$$

Correlation index:

$$(I_u - I_a) = C_c(I_c - I_a) + B \qquad (2)$$

where: I_u = intensity of the (partly crystalline) sample at designated 2θ-values.

I_a = intensity of the amorphous polymorph at these 2θ-values.

I_c = intensity of the crystalline polymorph at these 2θ-values.

The intensity values are measured over small 2θ-increments (at the most 0.5°).

In essence, this technique estimates the proportion of crystalline matter by observing how closely the diffraction pattern of an unknown substance resembles that of its fully crystalline analogue. The indices give the percentage crystallinity directly, and the glass content, indirectly, by difference. The DIXRD approach differs from the QXRD method in that the total amount of crystalline matter, and not the amounts of the individual phases, is computed.

Feasibility of Approach -
Model Study on the Cordierite System

A preliminary investigation was carried out to determine the feasibility of glass content determinations for fly ashes and slags using the differential intensity XRD method. As for the non-crystalline XRD technique, the technique was first used to measure the glass content of systems with a known glass content. Again, the system used was cordierite ($2MgO,2Al_2O_3.5SiO_2$).

From a rapid XRD scan of the glassy polymorph, it was determined that the amorphous halo was in the 2θ range of 10.0-40.0°.

Percentages of the crystallinity and glass contents of the two cordierite mixtures (A and B) are given in Table 24. It can be seen that the agreement between the known and the calculated values is good when the correlation index is used but rather poor when using the integral index.

The DIXRD Method Applied to Wabamun Fly Ash

Given the encouraging results for the cordierite system, the two differential intensity techniques have been applied to Wabamun fly ash - for which fully vitreous and redevitrified analogues had been prepared. Table 24 gives crystallinity indices and glass contents. It can be seen that the correlation index (which is believed to be the more reliable measure of crystallinity) is unreasonable, giving a crystalline content of -1.0%. The correlation coefficient ($r = -0.0508$) shows that $I_u - I_a$ and $I_c - I_a$ are not correlated.

The reconstituted XRD scans (Fig. 21) illustrates the origin of the poor correlation. The crystalline phases in the as-received fly ash and its redevitrified analogue clearly show significant differences.

The correlation index, C_c, was therefore recalculated leaving out the strongly scattering 2Θ values of the fly ash and its redevitrified analogue. The recalculated glass content (83.6%) is close to the value found using the integral index (82.0%). This value is closer to the glass content calculated with the QXRD technique (76.1%) than the value calculated using the Non-Crystalline Scattering Method (62.1%). Clearly, it would be interesting to use the DIXRD method in this modified form to establish glass content values for comparison with alternate techniques.

GLASS CONTENT METHODOLOGY (7):
THE AMORPHOUS HUMP METHOD (AHXRD)

A particular variant of the Non-Crystalline XRD method is the "Amorphous Hump" technique. The technique has been used to determine the glass content of pozzolans.

The glass content is determined by measuring the ratio of the area under the amorphous halo, A_H, and a prominent peak of a suitable standard, A_S. The area ratios were estimated from the counting of squares. The ratio:

$$GAH = \frac{A_H}{A_S}$$

plotted against the glass content should obey a linear relationship. Figure 22 shows the relationship of GAH vs glass content for the cordierite mixtures. The internal standard was NaCl. Linear regression gives:

$$y = 0.948x + 0.1296 \quad (r = 0.958)$$

Although acceptable, the correlation coefficient is not nearly as good as is generally found for the NCXRD method. The theoretical curve predicts a $GAH/GA_{100} = 0.75$. Using the experimentally observed relation of Figure 16, we find 74.3%, close to the actual value of 75.0%.

GLASS CONTENT METHODOLOGY (8): DENSITY APPROACH

Since most of the Canadian fly ashes surveyed in this study could be fully vitrified and the quenched glass could be redevitrified, the use of density determinations for glass content measurements was investigated. This technique has been used to determine the degree of crystallinity of polymers (22).

The glassy fraction can be computed as:

$$x_a = \frac{\rho a\ (\rho c - \rho)}{(\rho c - \rho a)}$$

where: ρ = density fly ash
ρa = density glass
ρc = density crystalline material.

A preliminary evaluation of this approach was carried out for three fly ashes (Wabamun, Sundance, and Forestburg) and their vitreous and redevitrified analogues. The results are listed in Table 25. The specific gravities of the fly ashes are pycnometric values measured after grinding. The values for the glassy and crystalline polymorph were measured for -45 µm powders.

It can be seen that the specific gravities of the glassy and crystalline analogues are not very different and that both of these are greater than that of the fly ash itself. It appears that the use of the density method has little potential for glass content determinations of fly ashes.

STRUCTURAL EVALUATION USING X-RAY DIFFRACTION

Table 26 gives the diffraction maxima of the nine fly ashes and two slags investigated in this study. Also listed in Table 26 are the diffraction maxima of the fully vitreous analogues of the glassy waste materials. Representative XRD patterns are shown in Figure 23.

FOURIER TRANSFORM INFRARED (FTIR) SPECTROSCOPY

Figure 24 shows FTIR spectra in the 1800-400 cm^{-1} range for the eleven source materials. Figure 25 gives FTIR spectra over the 4000-400 cm^{-1} range for Sundance fly ash.

DISCUSSION

CHEMICAL ANALYSIS

Table 8 shows the results of chemical analysis for the eleven source materials of this study. The major components for the fly ashes are:

- SiO_2 (37.1 - 58.6%)
- Al_2O_3 (12.3 - 23.2%)
- Fe_2O_3 (3.33 - 38.9%)
- CaO (1.29 - 13.0%).

Some of the fly ashes contain significant quantities of other oxides. Thus, Thunder Bay has 6.84% SO_3. Both Estevan and Thunder Bay have ~3% MgO and ~7 - ~8.5% Na_2O, respectively. Nanticoke and Lakeview have relatively high carbon contents and LOI values.

On the basis of the analytical results the fly ashes can be classified as follows:

- Bituminous coal fly ashes (Class F): Nanticoke, Lakeview, Lingan.

- Subbituminous and lignitic coal fly ashes (Class C): Wabamun, Sundance, Forestburg, Estevan, Thunder Bay.

- Dalhousie does not quite fit any of the above categories. If SiO2 and Al_2O_3 content are lower than commonly associated with a bituminous coal fly ash, its CaO content is too low for the subbituminous/lignitic type. This fly ash has an unusually high Fe_2O_3 content (~39%), which accounts for its unusual composition.

Using the other major classification, all fly ashes except Estevan and Thunder Bay have in excess of 70% of ($\Sigma SiO_2 + Al_2O_3 + Fe_2O_3$) and can thus be classified as class F fly ashes.

Estevan and Thunder Bay have somewhat less than 70%, but still in excess of 50% of the major network formers, and can be classified as class C fly ashes. In fact, this classification is not very useful here, since the high CaO content - normally associated with the C type - (15-35%) is not observed for Estevan and Thunder Bay; whereas some of the class F fly ashes have a much higher CaO content often attributed to this group (<5%).

The compositions of the two granulated blast-furnace slags are quite different from the chemical make-up of the fly ashes. SiO_2 and Al_2O_3 contents are much lower, while CaO and MgO contents are much higher. The compositions are typical of those anticipated for these materials from North American sources.

SPECIFIC GRAVITY

The specific gravities of the as-received source materials (Table 10) vary considerably. There is definitely a correlation with the Fe_2O_3 content for the fly ashes ($r = 0.78$ for the pycnometric values of the as-received samples).

As expected the pycnometric specific gravities increase after grinding; presumably because of the lowering of the amount of voids in the source materials.

Specific gravities determined by the Le Chatelier bottle technique are somewhat erratic with an exceptionally high value found for Lakeview and much larger differences for the as-received and ground materials. In some instances (e.g., Wabamun, Lakeview) the as-received densities were found to be higher than those of the ground materials (due to the presence of lightweight floating particles reducing the apparent volume). Pycnometric values which appear somewhat more reliable have, therefore, been used throughout the remainder of this discussion.

PARTICLE SIZE AND SURFACE AREA

Pycnometric specific gravities and surface areas for the eleven source materials of this study are listed in Table 10. The following observations were made:

- X-ray sedimentation indicates a much greater fraction of particles (<45 µm) than measured by wet sieving (325 mesh, 45 µm).

- B.E.T. (Krypton) analysis gives substantially greater surface areas compared with X-ray sedimentation. This phenomenon was also observed by Mehta (23) for American fly ashes. Since B.E.T. takes pores and crevices of the particulate materials measured into account, it is believed that this technique more adequately represents the accessible surface area during the hydration of these waste materials than the Blaine or the X-ray sedimentation technique.

GLASS CONTENT METHODOLOGIES

Table 27 lists the glass content values for the eleven source materials of this study. Two methods, the QXRD and NCXRD techniques, gave almost complete data sets. No value was obtained for Thunder Bay using the QXRD technique, since its mineralogical composition was significantly different from the other materials. Since the preparation of the standard curves was the most time-consuming task for the development of the QXRD technique, no attempt was made to evaluate the glass content of Thunder Bay fly ash using this method.

The NCXRD technique could not be applied to Dalhousie fly ash, since a fully vitreous analogue of this material could not be prepared - presumably because of its high iron oxide content.

The McMaster Individual Particle technique was used to determine the glass contents of the two slag compositions. This technique, which appears to be subject to considerable operator variation, could not be extended to fly ashes since the crystallites in the latter cannot be distinguished under the optical microscope and the presence of a number of phases complicates the observations.

The DIXRD technique was only applied to one fly ash. This method deserves a more extensive evaluation.

Image Analysis in conjunction with optical or electron microscopy appears to be troublesome for the same reasons given for the McMaster technique. The distinction between glassy and crystalline phases is not very clear.

The density approach to glass content determinations was found not to be very useful.

Comparison of the QXRD and NCXRD Methods

A comparison between QXRD and NCXRD techniques shows a rather poor correlation ($r = -0.60$) between the two data sets (Dalhousie and Thunder Bay excluded). The large discrepancies between the two techniques are noticeable, for Nanticoke and Lakeview and for Atlantic slag, as well as for the substantially lower glass content obtained for Wabamun using the NCXRD technique. Replicate glass content determinations by NCXRD for Wabamun and Atlantic slag gave essentially the same glass contents, indicating good precision and suggesting that the differences are attributable to systematic factors.

At this stage, it is difficult to judge which of the two approaches to glass content determination using X-ray diffraction gives the more accurate values. Both the QXRD and NCXRD approaches have potential sources of error which are summarized below.

QXRD method

- The glass content is essentially computed indirectly by subtracting the sum of the masses of the crystalline phases and LOI from 100%. Errors in each of the crystalline contents and in LOI will propagate and affect the final result.

- The accuracy of the standard curves is an important factor in the determination of the content of the crystalline phases. Care was taken during the preparation of the standard mixtures to control crystallite size and to optimize the counting of the scattering intensity. An examination of the standard curves show that linearity is closely observed. However, improvements can be made in the composition range chosen. Ideally, the curve should be centered about an intensity of 1 for the peaks corresponding to the crystalline phase and to the standard. Some of the standard curves prepared are outside this optimum range, specifically some of the α-quartz and mullite curves.

- Having prepared the standard curves, an amount of the internal standard should be added to the glassy waste material to give an intensity peak ratio of about 1. The amount of CaF_2 added to the fly ashes was generally in excess of what was required for the optimum intensity ratio for a particular peak combination, and the intensity ratio values, therefore, are often less than 1. This is particularly the case for the iron oxide phases, hematite and magnetite, which for most fly ashes were only present in amounts of a few percent or less. An adjustment of the mass of CaF_2 to give the optimum intensity ratio for a specific peak combination for each crystalline phase can be expected to improve accuracy as well as the precision of the computed crystalline contents.

- Finally, the use of the QXRD approach for glass content determinations depends on the initial identification of the crystalline phases present. The preparation of the standard curves, preferably several for each crystalline phase, is a time-consuming operation. It follows, therefore, that the QXRD method will be most useful for the routine determination of glass contents of fly ashes, slags, and other waste material from specific sources which are not subject to the variations in chemical and mineralogical compositions observed among samples from different sources.

NCXRD method

- The NCXRD approach provides a direct method for glass content determination based on the intensity of the X-ray scattering of the glassy phase in the source material itself. The accuracy of the NCXRD method is, therefore, to a large extent dependent on its inherent ability to estimate the glass content of the source material. The 2θ-value selected for the glass content determination should be selected in such a way as to minimize interference of the crystalline scattering component of the XRD pattern. Care was taken in this study to select 2θ values located between peaks, both for the glassy waste material as well as for the compositions used to determine the standard curve. At the same time, the intensity of the non-crystalline scattering should be close to the intensity maximum of the amorphous component; i.e., the 2θ value selected for intensity measurements should be close to the 2^{θ} value with maximum non-crystalline scattering. In all cases, except for the cordierite preliminary evaluation, it was found that a 2θ value of 25° was satisfactory. This value was close to the $2\theta_{Imax}$ value of the source materials for this study.

- A second factor affecting the accuracy of this technique stems from a consideration of the structure of the glassy phase. We will discuss in subsequent sections XRD and spectroscopic evidence which can be used in the interpretation of the structures of the glassy waste materials. The shape and the $2\theta_{Imax}$ value of the amorphous component of the XRD pattern reflect the structure of the glassy phase. The NCXRD approach is based on a comparison of a selected scattering intensity of the glassy component of the source material and the glassy component of the mixtures used for the preparation of the standard curves. Ideally, these two glassy components should be identical in composition and structure. In fact, they are not exactly the same. The vitrified glass is 100% glassy and its composition (corrected for carbon content) should be that of the source material overall. The composition of the glassy component of the source material will normally not be identical to the overall composition since the precipitation of the crystalline phases will alter the composition of the glassy phase. A comparison of the $2\theta_{Imax}$ values of the source materials and that of their vitrified analogues (Table 27) is reassuring since their proximity suggests that the shapes of the amorphous components of the XRD patterns are probably similar. The potential error will likely be minor if the glass content of the source material is high since the composition will be close to that of its vitrified analogue.

Apart from the potential sources of error listed here, there are no a priori reasons which suggest that the QXRD method is superior to the NCXRD approach, or vice versa. Both techniques give results which appear to be reasonable in view of results reported on slags in the literature. The aforementioned low glass contents found for Nanti-

coke and Lakeview (QXRD) and for Atlantic slag (NCXRD) are somewhat puzzling, however, particularly since the alternate approach gives values which are in the range expected. It is noteworthy that the low QXRD values were observed for fly ashes with high LOI and carbon contents. In the absence of clear preferences for one of the two approaches, the average glass content from the QXRD and NCXRD data (Table 27) will, therefore, be used in the remainder of the discussion.

Electron Optical Investigation

The results obtained using a combination of scanning electron microscopy (SEM) and energy dispersive analysis (EDXA) for the characterization of Wabamun fly ash has been mentioned above. Although, SEM/EDXA does not appear to be a route for glass content evaluation, much useful information was obtained from the micrographs and EDXA analyses.

A cursory examination of the surface of a cut disc in which Wabamun fly ash particles were embedded in an Elvacite medium shows spherical particles as well as some crushed material (Fig. 4a and b). Chemical analysis by EDXA carried out at eight different locations, showed that within one fly ash sample particles are found with vastly different compositions (Table II, Fig. 2). For example, a large spherical particle (A in Fig. 2a) was found to have SiO_2, Al_2O_3, and CaO contents close to those found for the overall fly ash composition. On the other hand, particles were also observed where the TiO_2 (B in Fig. 2a), CaO (D in Fig. 2a) or FeO (H in Fig. 2a) contents were far in excess of those of the average composition. SEM/EDXA shows a picture of the fly ash which is a very heterogenous material as far as composition is concerned. Table II also lists side-by-side the average of the oxide contents over the location sampled by SEM/EDXA and the overall composition determined by chemical analysis. The wide range of concentrations actually observed is certainly not evident from EDXA average values.

Another in-depth look at Wabamun fly ash by SEM/EDXA is given in Figures 1 to 7 and in Table 12. These polished cross-sectional views show a variety of particle shapes and a range of compositions. The following particle types could be discerned:

- Solid spheres containing gas bubbles that are relatively small compared to the diameter. Analysis of one sphere (A in Fig. 3) showed it to be high in CaO and FeO. These spherical particles are probably predominantly glassy.

- Cenospheres - empty spheres in which the wall thickness is relatively small compared to the particle diameter. The wall may contain small bubbles as well. Figure 4 shows a grouping of cenospheres (location 3 and a few neighbouring particles). A closeup is shown in Figure 5. EDXA analysis at location 3 shows this particle to be mostly an alumino-silicate (Table 13).

- Plerospheres - spherical particles containing smaller spherical particles inside. For example, Figure 6 shows a plerosphere containing smaller solid spheres and cenospheres.

- Irregularly shaped particles (Figure 4, location 4). A close up and EDXA analysis at four different spots in this particle indicates a predominantly alumino-silicate composition with some variation in the content of the other oxides, notably CaO.

In conclusion, SEM/EDXA analysis shows a great deal of variation both in particle shapes and sizes. The composition varies a great deal between individual particles - and to a somewhat lesser extent - within a particle. These observations suggest that the chemical composition of a glassy waste material, such as a fly ash, is complex and probably not an easily accessible indicator for performance in concrete formation and related processes.

X-Ray Diffraction Studies of Glass Structure

The collection of data from an extensive X-ray diffraction study on model glasses, commercial glasses, the eleven source materials of this study and their glassy analogues were described above. This study was sparked by a recent study on the glassy nature of fly ashes by Diamond (47).

While studying the glassy nature of fly ashes, Diamond (44) observed that U.S. fly ashes with low (<20 wt %) CaO content show an amorphous diffraction halo with an intensity maximum centered between 23° and 27° 2θ. Within that composition range, the angular position of the maximum was found to increase linearly with CaO content. The position of the intensity maximum for fly ashes with higher (>20 wt %) CaO content was found at a 2θ value of about 32°. Diamond attributed the latter maximum to a calcium aluminate structural type.

To elucidate the origin of the intensity maximum of the amorphous halo in the X-ray powder diffraction pattern of fly ashes, the X-ray powder patterns of a number of synthetic glasses in the Na_2O-SiO_2, CaO-SiO_2, Na_2O-CaO-SiO_2, and CaO-Al_2O_3-SiO_2 systems were studied together with X-ray powder patterns of some commercial glasses, and the source materials of this study.

Na_2O-SiO_2 and SiO_2 Glasses

Fused silica, SiO_2, has a diffraction maximum at 2θ = 21.3°. Figure 23 shows that the amorphous halo in the X-ray diffraction patterns of Na_2O-SiO_2 glasses contains at least two components centres at 2θ values of about 24.5° and 30.4-22.5°, respectively.

Valenkov and Poral-Koshits (45) have shown that the XRD patterns of Na_2O-SiO_2 glasses could be constructed by adding together the glassy diagrams of $Na_2O.SiO_2$ (sodium metasilicate) and SiO_2; each diagram being given a weight factor proportional to its relative concentration. It has been suggested by these authors that Na_2O-SiO_2 glasses are not homogeneous but that the two structures exist side by side.

It is likely that the two diffraction maxima observed in the X-ray patterns of the Na_2O-SiO_2 glasses result from scattering contributions of distinct structural units. The lower diffraction maximum could arise from a siliceous unit, while the higher diffraction maximum could be attributed to a lower polymerized silicate grouping - possibly a metasilicate.

Na_2O-CaO-SiO_2, CaO-SiO_2, CaO-Al_2O_3, and CaO-Al_2O_3-SiO_2 Glasses

An examination of the X-ray patterns of the glasses of these series, some of which are shown in Figure 24, reveal that glasses of widely differing compositions have similar X-ray patterns and similar diffraction maxima. For example, glasses ($CaO.SiO_2$), ($CaO.0.3Al_2O_3.0.4\ SiO_2$), and ($C_{12}A_7$) have $2\theta_{Imax}$ values between 30.0 and 31.0°.

On the basis of the similarity in the diffraction maxima of high-calcium fly ashes (CaO > 20%) and $C_{12}A_7$, Diamond (44) proposed that a calcium aluminate glass was probably responsible for the diffraction maxima of fly ashes with CaO contents in excess of 20%. The diffraction data presented in this study show that, in fact, a number of glass compositions based on the major oxides likely to be present in fly ashes could be responsible for the diffraction maximum at a 2θ value of about 32° observed by Diamond.

FLY ASHES, SLAGS, AND VITREOUS ANALOGUES

Table 26 shows $2\theta_{Imax}$ values for the eleven source materials of this study and their vitreous analogues. The $2\theta_{Imax}$ values were found to range from 23.0 to 30.8°. For the glassy analogues, values between 24.0 and 29.5° were observed.

Considering the nine fly ashes only, the relationship between analytical CaO content and $2\theta_{Imax}$ may be represented by:

$$y = 23.2 + 0.17x.$$

However, the correlation is poor (r = 0.42). Including the two slags gives:

$$y = 23.0 + 0.20x.$$

Now the correlation is vastly improved (r = 0.86). For the vitreous analogues (10 samples) the relationship becomes:

$$y = 24.1 + 0.12x$$

and the correlation further improves (r = 0.89).

Better correlations are obtained by considering $2\theta_{imax}$ versus total modifier content (i.e., the major oxides: CaO + MgO + Na_2O + K_2O). Considering fly ash glasses only, we find r = 0.70. For all eleven source materials, r = 0.92. And for ten glassy analogues r = 0.94. We conclude that:

- A better correlation is obtained when source materials of all available concentrations (up to ~40% CaO) are considered.
- The correlation is better when the glassy analogues are considered, presumably because there exists a better correlation with the overall composition.
- A better correlation still is obtained when the total modifier content is considered.

The data reported in this study suggest that the amorphous halo is the result of the scattering of distinct structural units in the glass. Each of these units could be responsible for the distinct diffraction maximum. Structural inferences based on the position of the dominant diffraction maxima could be simplistic since they may exclude additional information available from the amorphous component of the diffraction patterns.

Secondly, it should be noted that fly ashes are complex substances, both chemically and mineralogically. The chemical composition indicates the presence of a number of major elements represented conventionally as the oxides, SiO_2, Al_2O_3, CaO, Fe_2O_3, as well as small amounts of minor elements, such as TiO_2, MnO_2, etc. The major mineral phases are α-quartz, mullite, and iron-containing spinel-type phases (19). Even if fly ashes were homogeneous substances, the composition of the glassy phase would be complete and unambiguous assignments difficult.

Thirdly, it is unlikely that the glassy component of the fly ashes has a composition identical to that of the overall composition. The presence of SiO_2-, Al_2O_3-, and Fe-oxide rich crystalline phases will tend to give a glassy component depleted in these oxides and enriched in CaO. It would be more appropriate to correlate the CaO content of the glassy phase with the diffraction maximum rather than the CaO content of the fly ash overall.

Finally, it has been shown by Lauf (39) and confirmed by this study, that individual fly ash particles may have a very different chemical and mineralogical make-up. The amorphous halo in the diffraction pattern, therefore, represents the average of the scattering contributions of the individual fly ash particles.

Taking into account the complicating factors referred to above, we will now comment on Diamond's findings (44) against the background of the diffraction data on synthetic and commercial glasses of this study.

Diamond concluded that the diffraction maxima between 23° and 27° observed for the low-calcium fly ashes (<20 wt % CaO) were indicative of a siliceous glass structure. The data reported here appear to support this conclusion since the Na_2O-SiO glasses with the higher silica contents and the commercial glasses all have primary intensity maxima in this range. Fused silica was found to have a diffraction maximum slightly below this range.

The sudden jump in the diffraction maximum to a $2\theta_{Imax}$ value of about 32°, observed by Diamond (44) for high calcium (>20 wt % CaO) fly ashes, also becomes clear from the data in Figure 25. For most compositions in the Na_2O-SiO_2 series, two diffraction maxima are present with the maximum at the higher $2\theta_{Imax}$ value becoming pre-eminent for glass (32% Na_2O). We surmise that a similar phenomenon is responsible for the sudden emergence of the high diffraction maximum for the high calcium fly ashes reported by Diamond (44).

Presumably, both maxima are present in most fly ashes but it requires a CaO content of about 20% in the fly ash overall before the higher maximum becomes predominant. In view of our third comment made above, it is likely that the effective CaO content in the glassy phase may, in effect, have to exceed 20% before the higher maximum emerges.

It is interesting to note again the remarkable similarity in the X-ray patterns and the diffraction maxima for the $CaO-Al_2O_3-SiO_2$ glasses. There is no evidence for a secondary maximum at lower 2θ values suggesting a structure which is highly depolymerized.

CONCLUSIONS FROM THE XRD STUDY

The major conclusions of the X-ray powder diffraction study carried out on model and commercial glasses, fly ashes, and slags are:

1. The amorphous halo may contain several diffraction maxima attributable to different structural units in the glassy component of the source material.

2. The sudden jump observed in the diffraction maxima of U.S. fly ashes with CaO contents in excess of 20%, observed by Diamond (44), is probably attributable to a different 2θ maximum being pre-eminent in these fly ashes.

3. It has been shown in this study that a number of different glass compositions may give similar $2\theta_{imax}$ value close to the value observed for $C_{12}A_7$.

4. Better correlations are found for various glassy waste materials if the $2\theta_{imax}$ values are considered versus the total modifier content.

FOURIER TRANSFORM INFRARED (FTIR) SPECTROSCOPY

There are a number of factors that ought to be considered when interpreting the FTIR spectra of the fly ashes and slags of these studies.

Overall Composition

Since composition and structure are related the content of the major network formers SiO_2, Al_2O_3, Fe_2O_3, and of the major modifiers, CaO, MgO, and Na_2O is of importance. Once the oxide content is known, the structural features can be deduced by comparing the vibrational spectra of the waste materials studied here with data from the literature on minerals and glasses of similar compositions.

Composition of the Individual Particles

SEM work carried out during this project has shown that there is a great deal of variation in the composition of individual particles. Thus, the composition, deduced from the vibrational spectra, is an average over the entire sample examined. This factor is more important for fly ashes than for slags since the latter category of glassy waste materials is expected to be more homogeneous in the elemental make-up of its individual particles.

FTIR SPECTRA OF FLY ASHES AND SLAGS

The FTIR spectra of the nine Canadian fly ashes and two blast furnace slags (Fig. 25) are similar in several respects. They all show a strong dominant broad band centered between 1085 and 928 cm^{-1}, at ~1430 cm^{-1} and ~1630 cm^{-1}. Finally, these spectra also show a broad asymmetric band located between 3426 and 3462 cm^{-1}. These features and their relevance to the structure of the glassy waste materials will now be discussed in turn.

~3400 cm^{-1}, ~1630 cm^{-1}

The vibrational spectrum of weakly absorbed water is characterized by broad bands at ~3400 cm^{-1} and ~1600 cm^{-1}. These features were invariably found in the FTIR spectra of the materials studied here. Figure 26 shows the spectrum of the Sundance fly ash between 4400 and 400 cm^{-1}. The two H_2O peaks are clearly distinguishable.

The broad band at ~3400 cm^{-1} can be attributed to the symmetric and asymmetric stretching vibrations of adsorbed water. The ~1630 cm^{-1} band is the deformation vibration (ν_2) of adsorbed water.

The presence of the two water bands is evidence that some H_2O is always found in these fly ashes and glasses. The peak positions indicate that the water is weakly adsorbed rather than chemically bound. The adsorption presumably takes place through the formation of moderately strong hydrogen bonds (18).

~1430 cm^{-1}

A band at approximately this position was clearly found for the two blast furnace slags but was absent in the FTIR spectra of the fly ashes. This band may be attributable to nitrates, carbonates, or borates. Chemical analysis showed that the C-content was quite low (0.76% for Standard slag and 0.04% for Atlantic slag). The position of the band, however, clearly indicates the presence of carbonate (20). It is likely that the band arises because of the presence of $CaCO_3$ formed by the reaction of Ca^{2+} in the slag with atmospheric CO_2. The ~1430 cm^{-1} band is absent for the fly ashes which have a substantially lower Ca^{2+} content.

1300-750 cm^{-1}

The strongest feature in the FTIR spectra is a broad band centered between 1085 and 928 cm^{-1} in this range. The position of the band is indicative of a strong silicate component, presumably with a contribution of aluminate and alumino-silicate groupings. It was mentioned in the previous section that isolated SiO_4 polyhedra have stretching frequencies in the 100-800 cm^{-1} range, whereas condensed SiO_4 polyhedra adsorb between 1200 and 900 cm^{-1}.

With each of these categories, there are a great number of structures possible, each giving rise to several strong bands. A great deal of information is available from the structures of minerals. Isolated SiO_4 tetrahedra are found for the orthosilicate mineral, $ZrSiO_4$ (zircon), and the olivines (M'_2SiO_4; M' = Ca, Mn, Fe, Co, Ni). These minerals give a strong band in the 100-850 cm^{-1} range which may be split into several sub-bands.

Condensed silicates usually have two sets of bands, one of which is observed at higher frequency than those of the isolated SiO_4 polyhedra attributable to the asymmetric stretching vibrations of Si-O-Si and O-Si-O groupings. For example, bands are found between 1200 and 950 cm^{-1} for chain-type silicates (SiO_3), which make up the network structures of Li_2SiO_3 and Na_2SiO_3. The ring-type silicate found in an α-$CaSiO_3$ (pseudowollastonite) and $Cu_6Si_4O_{18}$ (dioptase) also adsorb in this range.

The second set of bands associated with the symmetric stretching vibrations of Si-O-Si and O-Si-O groupings can be found at the low end of the isolated SiO_4 range between 900 and 550 cm^{-1}.

Condensed silicates with higher degrees of polymerization, such as those found in talc and bentonitic clays, follow similar trends as for the chain-type silicates. But there usually is a good deal of overlap with the range associated with isolated SiO_4 polyhedra.

Silicate glasses have bands that are usually broadened compared to those of the crystalline compounds of identical composition but the positions of highest intensity are often similar. This suggests that the structures of the glasses are close to those of their crystalline polymorphs.

The presence of Al will not change this picture significantly, since Al can replace Si as a network former, and Si-O-Al stretching and bending vibrations often adsorb in the same range as Si-O-Si equivalents. The ratio of Si:Al in the fly ashes ranges from 3.5:2 to 5:2 for most of the compositions studied. A reasonable description of the main band in this range would be ν_{as} Si-O-Si or ν_{as} Si-O-Al (asymmetric stretch).

Although the FTIR spectra do not allow a detailed assignment of the structural features and, by necessity, give an overall or average picture, some interesting deductions can be made. First, the frequency at which the dominant band in this range reaches its maximum is an indication of the overall degree of polymerization of the network. In general, a lower frequency maximum will correspond to a lower degree of polymerization, i.e., a network with a lower degree of connectivity.

Thus, Estevan fly ash, Standard slag, and Atlantic slag, with band maxima between 957 and 928 cm^{-1}, will be much less polymerized than, for example, Lakeview fly ash which has a band maximum at 1085 cm^{-1}. It can be expected that a weaker network structure would be more easily broken down under chemical attack. The band maximum in this respect could be correlated with chemical reactivity; i.e., a lower maximum can be expected to correspond with a more reactive waste material.

The ratio of network formers to modifying cations affects the degree of polymerization. An increase in modifier content will tend to cause the rupture of Si-O and Al-O bonds in the network leading to a more depolymerized structure.

The correlation coefficients for ν_{Si-O} with CaO content and total modifier content were found to be -0.755 and -0.840, respectively. Thus, a higher modifier content and - to a lesser extent - a higher CaO content will give rise to a lower band maximum, also to a more depolymerized network and a more reactive material. It would be interesting to establish experimentally the extent to which the band maximum correlates with the reactivity of these waste materials.

One point of caution ought to be raised here. It is possible that Al may partially act as a modifier for these waste materials, particularly when the content of the other modifiers is low. It is beyond the scope of this investigation to establish to what extent this has occurred for this system.

There are some minor features in this range worth noting. First, we note the decrease in ν_{Si-O} for the three Alberta fly ashes - Wabamun, Sundance, and Forestburg. This decrease does not correspond to the change in the CaO content observed. However, it becomes understandable when considering the decrease in SiO_2 content and the increase in total modifier content.

The Thunder Bay fly ash shows the presence of two minor sharp peaks at 1142 and 1103 cm^{-1} within the main band at 1016 cm^{-1}. This fly ash was also found to have different crystalline phases compared with the other fly ashes (sulfates). The 1103 cm^{-1} band is possibly the ν_3 stretching frequency of the sulfate (SO_4) group. This is likely since the corresponding ν_4 bending vibration can also be discerned at 610 cm^{-1}. The bands at 1142 cm^{-1} (and at 638 cm^{-1} and 676 cm^{-1}) could also originate in sulfate vibrations. Anhydrite ($CaSO_4$) has bands at 1108, 1128, and 1160 (ν_3) and at 609, 628, and 674 (ν_4).

676-795 cm^{-1}

All FTIR spectra show a band in this region. A band in the 800-600 cm^{-1} region has been attributed to ν_3 Si-O-Si or ν_3 Si-O-Al (symmetric vibrations) (29). This band follows the same trend as the corresponding asymmetric stretch (ν_{as}), a decrease in frequency when the network is more depolymerized. The band at 684 cm^{-1}, observed in the FTIR spectrum of Dalhousie, can be attributed to ν_s Si-O-Fe, since the substitution of Fe for Al lowers the frequency of this band.

520-453 cm^{-1}

The band in this region is centered at ~463 cm^{-1} for most compositions. It can be assigned to the O-Si-O deformation mode of the silicate network. This band increases in frequency when the network is more depolymerized. This is indeed observed for the Standard and Atlantic slags but not for the Estevan fly ash.

550-571 cm^{-1}

The band at this position is found for Nanticoke, Lakeview, Lingan, and Dalhousie. It is possible that this band can be attributed to an Fe-O vibration since its presence is only noted in glassy waste materials with a high Fe-content.

CONCLUSIONS FROM THE FTIR STUDY

Fourier Transform infrared spectroscopy was found to be a useful technique for the correlation of compositional and structural parameters in fly ashes and slags. In particular, the position of the major silicate-aluminate stretching band can be correlated with the total modifier (CaO + MgO + Na_2O + K_2O) content and to a lesser extent with the CaO content of the glassy waste material. The technique is potentially applicable for the correlation of structure and reactivity of glassy waste materials.

SUMMARY AND CONCLUDING REMARKS

A substantial amount of data on nine Canadian fly ashes and two blast furnace slags have been collected under this program. The results are summarized below.

1. Chemical analysis data show that the fly ashes investigated contain low (<5%) or intermediate CaO (5-15%) levels. The SiO_2 content varies substantially (37.1-58.6%) while the Al_2O_3 content was usually about ~21%. One fly ash - Dalhousie - had an exceptionally high iron content (38.9% Fe_2O_3) and low aluminum (12.3% Al_2O_3) and silicon content (37.1% SiO_2). The two slags have a chemical composition common for North American blast-furnace slags.

2. B.E.T. (triple point) surface area determinations gave values between 0.4 and 4.4 $m^2.g^{-1}$. These values are often an order of magnitude greater than the Blaine surface areas. It was concluded that the B.E.T. technique is more appropriate than the Blaine method for the determination of a representative surface area for fly ash and slag.

3. Two methods for glass content determinations were used extensively for the source materials of this study. Quantitative X-Ray Diffraction (QXRD) was used to compute the mass percentages of α-quartz, mullite, magnetite, and hematite, and the glass content by difference. Non-Crystalline X-Ray Diffraction (NCXRD) used the intensity of the amorphous hump at specified 2θ-value of the glassy waste material of interest, relative to a series of standard mixtures. The methodologies for these two techniques developed under this program. Glass contents ranged from 53.5 to 94.5% using the QXRD method, and from 42.8 to 99.3% with the NCXRD approach. The correlation of glass contents determined by the two approaches was found to be poor ($r = -0.60$).

4. Several other approaches for glass content determination were addressed following input from the literature assessment. Differential Intensity X-Ray Diffraction (DIXRD) is an approach which could be a potentially useful technique. The McMaster Individual Particle Analysis can only be applied to slags. It was found that the glass contents determined with this approach varied considerably among operators, although the reproducibility of the results for each operator was found to be good. Optical or electron optical examination combined with image analysis shows little promise for glass content determination of fly ashes since the glassy and crystalline phases cannot be clearly discriminated with the equipment used in this study.

5. Electron optical examination (SEM) of Wabamun fly ash showed the presence of at least four types of particles: solid spheres, cenospheres, plerospheres, and irregularly shaped particles. Energy dispersive X-ray analysis (EDXA) showed a great deal of compositional variation among the individual particles and to a lesser extent within particles.

6. An extensive structural investigation was carried out using X-ray powder diffraction on model glasses, commercial glasses, and the eleven source materials of this study. The sudden jump observed by Diamond for the diffraction maxima of fly ashes containing in excess of 20% CaO was explained on the basis of the XRD results for model glasses. It was shown that generally more than two diffraction maxima can be observed. The jump observed can be attributed to the emergence of another maximum becoming the dominant feature in the amorphous halo. It was shown in this study that model glasses of widely varying compositions show similar 2θ-maxima close to the 2θ-maximum of $C_{12}A_7$ glass. Finally improved correlations were found if the diffraction maxima were compared with the total modifier content of the glassy waste materials.

7. FTIR spectra were collected for the source materials of this study as an additional means for structural characterization. The frequency maximum of the dominant silicate-aluminate stretching peak was observed to be inversely correlated with the total modifying oxide content.

8. As far as the major objectives of this program is concerned - the development of a general theory for predicting the behaviour of glassy waste materials (fly ashes, silica fumes, and slags) - some progress has been made towards the

establishment of methods for characterizing these materials and understanding their structure and their glassy phases. Specifically, the major achievements of this program have been in the following areas:

Surface area characterization

B.E.T. analysis using Krypton rather than nitrogen was shown to be an effective means of establishing the surface area of glassy waste materials.

Glassy content determination

Two approaches using X-ray diffraction were developed to determine the glass contents of glassy waste materials. These techniques (QXRD and NCXRD) have the advantage over optical approaches that, potentially, they can be applied to all classes of glassy waste materials since they are independent of the ability to visually distinguish between the phases.

Structure of the glassy waste materials

X-ray diffraction and FTIR spectroscopy were found to be useful techniques for the characterization of the glassy waste materials. New insights were obtained in the nature of the amorphous halo in the X-ray diffraction patterns. These insights are a refinement and improvement of the studies reported by other workers.

The results obtained to date under this program will be extremely useful for subsequent investigations aimed at an elucidation of the hydration kinetics and mechanisms of the glassy waste materials characterized in this study.

RECOMMENDATIONS

The following recommendations are made on the basis of the literature assessment and the results of the experimental investigations discussed in this final report.

1. Glass Content Methodology

Two methods (QXRD and NCXRD) have been developed under this program for glass content determination. These two techniques are, in principle, applicable to all classes of glassy waste materials, i.e., fly ashes, silica fumes, and the various types of slags. It has also become clear that each of these techniques has certain disadvantages for certain glassy waste materials.

The QXRD technique may be a very time-consuming way to evaluate the glass content of a sample which has a substantial number of uncommon crystalline phases. The NCXRD approach, on the other hand, cannot be used for a material which cannot be vitrified through rapid quenching.

An assessment ought to be made of the time and effort involved in developing each of these approaches to the point where they can be used routinely for the rapid determination of glass content. This point needs particular consideration when considering the incorporation of the techniques developed under this program in standards for use by industry.

Also, the procedures developed for the preparation of standard curves in the QXRD approach could be improved to obtain more representative crystalline phase/internal standard ranges.

The poor correlation between the QXRD and NCXRD methods for the nine source materials evaluated by both techniques is a matter of concern. A round-robin approach involving several laboratories, using the procedures described in this report, may be required. Also, it is recommended to extend the number of source materials greatly to obtain a statistically more meaningful estimate of the reliability of the two approaches.

A useful extension of the program could involve a comparative study using several optical techniques (FTIR, Raman), electron optical, as well as the QXRD and NCXRD approaches for glass content determinations of blast-furnace slags. These slags have a relatively simple mineralogical make-up, often containing only one crystalline phase, and the glassy phase is homogeneous.

The Differential Intensity X-Ray Diffraction (DIXRD) method subjected to a preliminary evaluation under this program deserves further study. An evaluation of this approach could easily be included in a subsequent phase of the program since the vitreous and redevitrified analogues of ten source materials have already been prepared.

2. Structural Characterization

X-ray diffraction, FTIR spectroscopy, and SEM/EDXA have been used successfully to characterize the eleven source materials of this study. Substantial progress was made in clarifying the nature of the diffraction maximum observed in the amorphous halo in the XRD pattern.

The observation of multiple diffraction maxima in model glasses and the dependence of the 2θ-values and the relative intensities of these maxima on composition were found to be important factors.

Further clarification could be obtained if a series of model glasses were prepared using the approach described in Appendix A. These glasses would have the average composition of the glassy phase of fly ashes. Diffraction patterns could be collected for these glasses and diffraction maxima could be observed without the interference of accompanying crystalline phases. By including a number of high-Ca fly ashes - if necessary from U.S. sources - XRD patterns could be collected of a series of fly ashes and analogues of their glassy phases covering a wide CaO content range. This investigation would be useful in establishing how compositional factors correlate with X-ray diffraction features.

FTIR and Raman spectroscopy could be used for future studies in clarifying structural features underlying the reactivity of the glassy waste materials. A lowering of the silicate-aluminate stretching frequency can be interpreted as evidence of a more depolymerized network which can be expected to be more reactive. FTIR data may, therefore, be supportive of reactivity data from hydration studies.

SEM/EDXA could be useful in classifying particle types and their average compositions. It would be worthwhile to determine whether certain oxides, notably CaO, Fe_2O_3 and TiO_2, show high concentrations in relatively few particles or whether they are distributed more or less evenly over all particles. The data collected for Wabamun fly ash suggest that the former description may be more representative than the latter.

A new technique for chemical characterization of particle types in fly ashes is being used in CANMET. This method uses the individual particle chemistry, as determined by EDXA, compared to a mineral composition file in order to identify and name the particles in a field in the electron microprobe. Quartz, mullite, and total Fe-oxides are identified, as are particles of different glass compositions. Several assumptions must be made regarding the total crystallinity of quartz and mullite. Results obtained to date suggest comparable results with X-ray diffraction techniques.

REFERENCES

1. Roy, D.M., and Idorn, G.M. "Hydration, structure and properties of blast furnace slag cements, mortars and concrete"; ACI Journal; November-December 1982.

2. Mehta, P.K. "Pozzolanic and cementitious by-products as mineral admixtures for concrete - A critical review"; Proceedings of the 1st International Conference on the use of Fly Ash, Silica Fume, Slag and Other Mineral By-products in Concrete; July 31 - August 5, Montebello; 1983.

3. Berry, E.E. "The cementitious properties of slags - A critical review"; Contract of Energy, Mines and Resources Canada (CANMET); March 1982.

4. Berry, E.E.; Hemmings, R.T; and Burns, J.S. "Coal ash in Canada: Ash as a potential resource"; Canadian Electrical Association; Report GI95; August 16, 1982.

5. Wolfsiefer, J. "Study for the U.S. and Canada"; Internal Norcem Report; March 1979.

6. Lea, F.M. The Chemistry of Cement and Concrete; Chemical Publishing Co.; New York; 1971.

7. Collings, R.K., and Wang, S.S.B. "Mineral waste resources of Canada, Report No. 7, Ferrous metallurgical wastes"; CANMET Report 80-19E; Energy, Mines and Resources Canada; May 1980.

8. Douglas, E., and Mainwaring, P.R. "Hydration and pozzolanic activity of non-ferrous slags"; Am. Ceram. Soc. Bull., Vol. 64(5), pp. 700-06; 1985.

9. Douglas, E.; Mainwaring, P.R.; and Hemmings. R.T. "Pozzolanic properties of Canadian non-ferrous slags"; 2nd International Conference on the use of fly ash, silica fume, slag and natural pozzolans in concrete; Madrid, Spain; April 1986.

10. Collings, R.K., and Wang, S.S.B. "Universal waste resources of Canada. Report No. 8 - Non-ferrous metallurgical wastes"; CANMET Report 81-17E; Energy, Mines and Resources Canada, Ottawa, 1981.

11. Douglas, E. "Canadian ferrous and non-ferrous slags for resource and energy conservation"; Division Report ERP/MSL 83-61(TR), CANMET, Energy, Mines and Resources Canada; Ottawa, 1983.

12. Schwiete, H.E. "The effect of cooling conditions and the chemical composition on the hydraulic properties of haematitic slags"; Forchungs-bericht des Lands Nordheim-Westfalen, No. 1186; 1983.

13. Smolczyk, H.G. "Glass structure and identification of slags"; Proceedings of the 7th Int. Congr. on the Chemistry of Cement, Paris, I(III), 3-17; 1980.

14. Demoulian, E.; Gourdin, P.; Hawthorn, F.; and Vernet, C. "Influence of slag chemical composition and texture on their hydraulicity"; Proceedings of the 7th Int. Congr. on the Chemistry of Cement, Paris, 2(III), 89-94; 1980.

15. Hooton, R.D. "Pelletized slag cement, hydraulic potential and autoclave reactivity"; Ph.D. thesis, Civil Engineering, McMaster University; Hamilton, Ontario.

16. Clark. G.L., and Reynolds, D.H. "Ind. Eng. Chem, Anal., Ed. Vol. 8, 36; 1936.

17. Sehlke, K.H.L. "X-ray diffraction as a method of determining the Portland cement content of mixtures of Portland cement and milled granulated blast furnace slag"; Cement & Lime Manufacturer, XL, 4, 57-62; 1967.

18. Simons, H.S., and Jeffery, J.W. "An X-ray study of pulverized fuel ash"; J. Appl. Chem. 10, 328-336; 1960.

19. Williams, J.P.; Carrier, G.B.; Holland, H.J.; and Farncomb, F.J. "The determination of the crystalline content of glass-ceramics", J. Materials Science, 2, 513-520; 1967.

20. Alexander, L.E. X-Ray Diffraction Methods in Polymer Science; Chapter 3, John Wiley & Sons Inc., New York; 1969.

21. Klug, H.P., and Alexander, L.E. "X-Ray Diffraction Procedures for Polycrystalline and Amorphous Materials"; John Wiley & Sons; 1954.

22. Hooton, R.D., and Emery, J.J. "Glass content determination and strength development predictions for blast furnace slag"; Proceedings of the CANMET/ACI First Int. Conf. on the use of fly ash, silica fume, slag and other mineral by-products in concrete; Montebello, Quebec, Canada; 1983. Paper SP 79-50, pp. 943-964.

23. Mehta, P.K. "Testing and correlation of fly ash properties with respect to pozzolanic behaviour"; Electric Power Research Institute Project 1260-26, Final Report, January 1984.

24. Ohlberg, S.M., and Strickler, D.W. "Determination of percent crystallinity of partly devitrified glass by X-ray diffraction"; J. Amer. Ceram. Soc., 45, 170-171; 1962.

25. Mather, K. Member of ASTM Committee C.1. Personal Communication (August 23, 1974) in ref. 4.

26. Wakelin, J.H.; Virgin, H.S.; and Crystal, E. J. Appl. Phys., 30, 1654; 1959.

27. Emery, J.J.; Kim, C.S.; and Cotsworth, R.P. "Base stabilization using pelletized blast furnace slag"; J. of Testing and Evaluation, 4(1), 94-100; 1976.

28. Hooton, R.D., and Emery, J.J. "Determining the glass content of the vitrified blast furnace slags"; Paper presented at the Int. Conf. on slags and blended cements; Mons, Belgium; Sept. 7-11, 1981.

29. Parker, T.W., and Nurse, R.W. "Investigation on granulated blast furnace slags for the manufacture of Portland-Blast furnace cement", National Building Studies, Technical Paper J.O.S.I.R., HSMO, London; 1949.

30. Schroder, F. "Slags and slag cements"; Proceedings of the 5th Int. Symposium on the chemistry of cement; 4, 149-199; Tokyo; 1968.

31. Foster, J.R. Private Communications, 1978, 179, 1980, in ref. 4.

32. Schramli, W. "The characterization of blast furnace slags by means of differential thermal analysis"; Zement-Kalk-Gips, 15(4), 140-147; 1963.

33. Miller, R.G.J., and Willis, H.A., J. Polymer Sci., 19, 485; 1956.

34. Farrow, G., and Ward, I.M. Polymer, 1, 330; 1960.

35. Hendus, H., and Schnell, G. Kunststoffe, 51, 69; 1961.

36. Dougherty, K. "Slag chemistry characterization and potential uses"; Paper presented at the slag cements symposium, Penn. State University, March 12-14; 1984.

37. Carrier, G.B. "Electron microscopic technique for determining the percent crystallinity of glass-ceramic materials"; J. Am. Ceram. Soc., 47(8), 365-367; 1974.

38. Doherty, P.E., and Leombruno, R.R. "Transmission Electron Microscopy of Glass-Ceramics"; J. Am. Ceram. Soc. 47(8), 368-370; 1974.

39. Lauf, R.J. "Microstructures of coal fly ash particles"; Bull. Am. Ceram. Soc., 61(4), 487-490; 1982.

40. Hulett, L.D., and Weinberger, A.J. "Some etching studies of the microstructure and composition of large aluminosilicate particles in fly ash from coal-burning power plants"; Env. Sci. and Techn 14(8), 965-0970; 1980.

41. Hulett, Jr.; Weinberger, A.J.; Northcutt, K.C.; and Ferguson, M. "Chemical species in fly ash from coal-burning power plants"; Science, 210, 1356-1358; 1980.

42. Terrier, P. "Research into the hydraulicity of granulated blast furnace slags"; CILAMS Information, 8(1), 1-6; 1973.

43. Kruger, J.E. "Contributions to the knowledge of the characteristics of vitreous blast furnace slag with a high magnesia content"; D.S. thesis, University of Pretoria, R.S.A., 175 pp.; 1976.

44. Diamond, S. "On the glass present in low-calcium and in high-calcium fly ashes"; Cement and Concrete Research, Vol. 13, 459-464; 1983.

45. Valenkov, N., and Poral-Koshits, E.A., Z. Krist. Vol. 95; p. 195; 1936.

TABLES

Table 1 - Annual production of glassy waste materials in Canada

Type	Quantity ($\times 10^6$ tonnes)	Ref.
Iron blast furnace slags	2.84	(3)
Steel slags	3.22	(3)
Non-ferrous slags	3.73	(3)
Fly ash	2.5	(4)
Silica fume	0.2	(5)

Table 2 - Sources and quantities of iron blast furnace slags in Canada

Source No.	Location	Quantities (tonnes/year)
F1	Sydney, Nova Scotia	172 000
F2	Sault Ste. Marie, Ontario	1 100 000
F3	Hamilton, Ontario	660 000 (220 000 pelletized)
F4	Hamilton, Ontario	907 000
	Total	2 839 000

From reference 18.

Table 3 - Sources and quantities of steel slags in Canada

Source No.	Location	Quantities (tonnes/year)
S1	Sydney, Nova Scotia	127 000
S2	Montreal, Quebec	5 400
S3	Montreal, Quebec	9 000
S4	Contrecoeur, Quebec	227 000
S5	Contrecoeur, Quebec	16 000
S6	Sault Ste. Marie, Ontario	635 000
S7	Welland, Ontario	27 000
S8	Burlington, Ontario	36 000
S9	Hamilton, Ontario	640 000
S10	Whitby, Ontario	455 000
S11	Hamilton, Ontario	500 000
S12	Hamilton, Ontario	450 000
S13	Selkirk, Manitoba	14 000
S14	Regina, Saskatchewan	65 000
S15	Edmonton, Alberta	10 000
S16	Vancouver, British Columbia	6 000
	Total	3 222 400

From reference 7.

Table 4 - Sources and quantities of copper, nickel, and lead smelting slags in Canada

Source No.	Location	Metal	Quantities (tonnes/year)
1	Noranda, Quebec	Cu	474 000
2	Noranda, Quebec	Ni	252 000
3	Murdochville, Quebec	Cu	308 000
4	Falconbridge, Ontario	Cu, Ni	600 000
5	Copper Cliff, Ontario	Cu	145 000
6	Copper Cliff, Ontario	Ni	1 451 000
7	Thompson, Manitoba	Ni	464 000
8	Flin Flon, Manitoba	Cu	-
9	Kamloops, British Columbia	Cu	-
10	Belledune, British Columbia	Pb	127 000
11	Trail, British Columbia	Pb	159 000
			3 728 000

From references 10,11.

Table 5 - Production/utilization statistics for coal ash: Major ash uses in the world (1977)*

Ash production	U.S.A.	Poland	United Kingdom	Fed.Rep. Germany	German Dem.Rep.	Canada	World
Total ash produced ($\times 10^3$ tonnes)	61 495	15 000	12 336	15 000	15 000	2 626	278 443
Total ash utilized ($\times 10^3$ tonnes)	9 079	5 512	5 070	3 413	2 485	711	31 605
% Ash production utilized	14.8	36.7	41.1	22.7	16.5	27.1	11.4
End use:		---Per cent of utilized ash---					
1. Structural fill	24.3	0.2	44.8	5.8	-	75.9	18.3
2. Portland-cement replacement	15.8	9.1	--	9.1	-	18.3	17.7
3. Addition to portland cement	4.1	1.8	0.6	--	24.2	0.3	12.9
4. Road stabilizer	4.7	38.1	--	--	1.6	--	10.1
5. Aerated concrete block	--	18.2	32.2	--	1.0	--	5.8
6. Blasting and roofing grit†	14.9	--	--	7.8	--	--	5.1
7. Asphalt mineral filler	1.3	--	--	29.3		?	3.7
8. Cement raw material	5.3	--	--	4.6	-	--	3.2
9. Lightweight aggregate*	2.88	?	6.0	--	9.1	--	2.5
10. Bricks and ceramics	--		--	6.9	3.4	--	1.8
11. All other uses**	26.9	32.7	16.4	36.6	60.6	5.2	30.1

†boiler and cyclone slag.

*bottom ash and sintered (Lytag) ash.

**agriculture, fillers, ice control, mineral extraction, mineral wool, grout, etc.

Table 6 - Techniques for glass content determination

Technique	Used for	Ref.
1. X-Ray techniques		
- QXRD Method	mineral dusts, portland cement, coal ashes, slags, glass-ceramics	17-21, 23-25
- Amorphous Intensity Method	glass-ceramics	26
- Amorphous Hump Method	pozzolans	17, 27, 28
- Amorphous-Crystalline Method	polymers	29
- Differential Intensity Method	polymers	30
2. Optical techniques		
- McMaster Individual Particle Analysis	slags	17, 24, 31
- South African Optical Procedure	slags	32
- Parker and Nurse Method	slags	33
- Rheinhausen Optical Method	slags	34
- Optical Mineralogical Composition	slags	35
3. Spectroscopic techniques		
- Automated UV Reflectance	slags	36, 37
- Reinhausen UV Method	slags	34, 37
- Infrared Method	polymers, slags, fly ashes	22, 12, 41
- NMR Method	polymers	22
4. Electron-optical-techniques	glass-ceramics, fly ashes	42,43, 44
5. Solution method	fly ashes	45, 46
6. Density method	polymers	22

Table 7 - Methods of glass content determination that are potentially applicable

QXRD Method
Amorphous Intensity Method
Amorphous Hump Method
Amorphous-Crystalline Scattering Method
Differential Intensity Method
Infrared Method
TEM Technique
Solution Technique
Density Technique

Table 8 - Composition of fly ashes and blast furnace slags

Source	SiO_2	Al_2O_3	B_2O_3	P_2O_5	SO_3	TiO_2	Cr_2O_3	MnO_2	Fe_2O_3	SrO	CaO	MgO_2	NA_2O	K_2O	ZnO	PbO	C	LOI	Total
Wabamun	58.6	21.3	0.16	0.09	0.34	0.63	<0.01	0.07	3.33	-	11.1	1.80	0.57	0.67	0.007	0.005	0.51	0.77	99.3
Sundance	53.7	23.2	0.17	0.11	0.34	0.59	<0.01	0.06	3.86	-	12.5	1.36	2.03	0.55	0.009	0.008	0.49	0.39	99.0
Forestburg	52.0	21.2	0.74	0.42	0.52	0.44	<0.01	0.05	5.08	-	10.5	1.61	4.74	1.17	0.010	0.006	0.10	0.77	98.6
Nanticoke	48.8	21.5	0.14	0.27	0.96	1.00	0.01	0.04	10.6	-	5.95	1.12	0.87	0.95	0.011	0.007	6.30	7.54	98.5
Lakeview	43.7	22.7	0.17	0.33	1.66	1.11	0.02	0.04	15.7	-	3.82	1.09	0.87	1.63	0.021	0.007	7.34	9.7	100.2
Lingan	45.5	22.5	0.04	0.13	0.97	0.85	0.02	0.09	20.1	-	1.29	1.37	0.83	3.32	0.037	0.024	2.53	3.47	99.6
Dalhousie	37.1	12.3	0.04	1.55	1.77	0.60	0.01	0.25	38.9	-	4.45	0.78	0.64	1.64	0.019	0.005	0.42	1.54	100.5
Estevan	43.2	22.1	-	0.41	0.85	0.78	<0.01	0.03	3.45	0.49	13.0	3.15	8.43	0.84	-	-	0.53	0.93	97.3
Thunder Bay	41.2	21.1	-	0.64	6.84	0.93	<0.01	0.03	3.92	0.52	12.4	3.09	6.91	0.01	-	-	0.15	2.31	98.7
Standard	38.8	6.55	-	0.02	3.30	0.30	<0.01	1.19	1.30	0.04	35.1	12.1	0.37	0.47	-	-	0.76	-0.84	100.3
Atlantic	35.1	9.34	-	0.02	2.90	0.34	<0.01	0.46	0.98	0.04	40.1	9.62	0.18	0.22	-	-	0.04	-1.84	99.4

Table 9 - Specific gravities of the source materials

Source	Pycnometry		Le Chatelier Method	
	As received	After grinding	As received	After grinding
Wabamun	2.28	2.47	2.13	1.99
Sundance	2.15	2.44	1.99	2.89
Forestburg	2.00	2.43	1.61	2.50
Nanticoke	2.32	2.59	2.16	2.50
Lakeview	2.52	2.61	3.74	2.43
Lingan	2.60	2.76	1.82	2.66
Dalhousie	3.10	3.05	2.97	3.52
Estevan	2.49	-	-	-
Thunder Bay	2.67	-	-	-
Standard Slag	3.00	-	-	-
Atlantic Slag	2.98	-	-	-

Table 10 - Densities, particle sizes, and surface areas of the source materials

Source	Average specific gravity ($g.cm^{-3}$)*	From Sedigraph Analysis Surface area ($M^2.g^{-1}$)**	Wet sieving retained on No. 325 Sieve	B.E.T. (Krypton) ($m^2.g^{-1}$)	Blaine ($m^2.g^{-1}$)
Wabamun	2.28	0.2587	42.5	2.2	0.2387
Sundance	2.15	0.3247	18.1	1.0	
Forestburg	2.00	0.5360	30.6	1.9	
Nanticoke	2.32	0.2463	39.7	3.8	
Lakeview	2.52	0.3864	21.6	4.4	
Lingan	2.60	0.3441	16.4	1.0	
Dalhousie	3.10	0.1954	17.8	0.4	0.2127
Estevan	2.49	0.5256	22.7	1.6	
Thunder Bay	2.67	0.4877	3.1	1.1	
Standard Slag	3.00	0.5362	12.6	2.5	
Atlantic Slag	2.98	0.7201	1.7	2.0	

* By Pycnometry.
** Calculated assuming spherical particle shape.

Table 11 - Comparison of concentrations of selected oxides from SEM/EDXA analysis and chemical analysis

Oxide	SEM/EDXA Range	SEM/EDXA Average (no. of locations)	Chemical analysis (bulk ash)
SiO_2	15.58-87.13	52.62 (8)	58.6
Al_2O_3	5.66-25.58	15.41 (8)	21.3
SO_3	5.11-5.38	5.19 (2)	0.34
TiO_2	2.28-11.60	6.94 (2)	0.63
FeO, Fe_2O_3	1.59-76.88 (FeO)	17.39 (5) (FeO)	3.33 (Fe_2P_3)
CaO	1.80-53.16	19.43 (7)	11.1
MgO	0.59-1.78	1.34 (3)	1.80
K_2O	4.40	4.40 (1)	0.76

Table 12 - EDXA oxide analysis of Wabamun fly ash in cross-section

Oxide	Location A	B	3	4A	4B	4C	4D
SiO_2	26.96	70.07	51.27	66.84	55.69	63.15	49.24
Al_2O_3	4.80	7.17	31.29	15.70	14.68	20.56	16.35
TiO_2	1.50	0.48	4.86	1.71	4.06	1.60	1.91
FeO	24.78	2.75	2.27	3.08	5.78	3.03	5.32
SO_3	-	-	-	-	3.04	-	-
CaO	41.56	18.57	9.17	6.12	8.53	4.80	23.87
MgO	0.40	0.34	0.33	0.31	-	-	0.68
K_2O	-	-	0.80	6.24	7.52	6.45	2.64
MnO	-	0.17	-	-	-	-	-
Cl	-	-	-	-	0.70	0.41	-

Table 13 - Results of modified McMaster individual particle analysis on Standard and Atlantic slags*

Sample I.D.	X	S_X	S_{X-1}	X(n)	S_n
Operator A					
Standard slag	87.0	13.1	13.0	84.3	2.3
(no gypsum	81.4	19.1	19.3		
plate)	84.4	17.1	17.3		
Standard slag	75.2	20.6	20.8	75.9	2.5
(gypsum	73.2	23.0	23.3		
plate)	79.2	20.8	21.0		
Operator B					
Standard slag	48.2	36.0	36.4	47.1	1.1
		47.6	37.0	37.3	
		45.6	34.1	34.5	
Atlantic slag	60.8	33.5	33.8	59.7	1.8
		57.2	37.7	38.1	
		61.0	35.6	36.0	
Operator C					
Standard slag	70.0	24.7	25.0	73.7	2.8
		76.7	18.0	18.8	
		74.3	17.1	17.2	
Atlantic slag	69.4	26.3	26.6	68.9	1.3
		67.2	25.8	26.0	
			70.2	17.7	17.9

* According to CSA Standard A363-M1983.

Table 14 - Mineralogy of Canadian fly ashes and slags

Source	Phases Detected (1,2)
Wabamun	Q, M
Sundance	Q, M, H
Forestburg	Q, M
Nanticoke	Q, M, H, Ma
Lakeview	Q, M. H, Ma
Lingan	Q, M. H, M
Dalhousie	Q, M. H, M
Thunder Bay	Q, CS, $C\bar{S}$, $N_3A\bar{S}_6$
Estevan	Q
Standard Slag	Mel
Atlantic Slag	Mer

1 Q: α-quartz, M: mullite, H: hematite, Ma: magnetite, Mel: melilite, Mer: merwinite, $C\bar{S}$: $CaSO_4$, $N_3A\bar{S}_6$: $Na_3Al(SO_4)_3$.
2 Sillimanite ($Al_2O_3.SiO_2$) has an XRD pattern almost identical to that of mullite ($3Al_2O_3.2SiO_2$). (The assignment given here was based on the relative peak intensities of the two phases.)

Table 15 - Intensity ratios for four phases and NaCl

α-quartz			Mullite			Magnetite			Hematite		
$2\theta_Q$	$2\theta_{NaCl}$	I_Q/I_{NaCl}	$2\theta_M$	$2\theta_{NaCl}$	I_{Ma}/I_{NaCl}	$2\theta_{Ma}$	$2\theta_{NaCl}$	$I_{Ma}I/_{NaCl}$	$2\theta_H$	$2\theta_{NaCl}$	I_H/I_{NaCl}
20.8	31.7	1.11	16.4	31.7	0.265	30.1	31.7	0.14	33.3	31.7	4.42
26.7	31.7	6.11	26.0	31.7	0.470	35.4	31.7	2.38	35.7	31.7	3.08
20.8	45.5	3.08	35.2	31.7	0.349	43.1	31.7	0.508	54.2	31.7	2.17
26.7	45.5	15.9	16.4	45.5	0.847	57.1	31.7	0.555	33.3	45.5	8.83
			26.0	45.5	1.68	30.1	45.5	2.00	35.7	45.5	6.17
			35.2	45.5	1.12	35.4	45.5	6.67	54.2	45.5	4.33
						43.1	45.5	1.42			
						57.1	45.5	1.56			

Table 16 - Contents of crystalline phases and glass in seven Canadian fly ashes

Fly Ash	α-quartz	Mullite	Magnetite	Hematite	LOI	Glass
Wabamun	8.7	11.5	-	-	0.8	79.8
Sundance	4.1	10.2	-	1.4	0.4	83.9
Forestburg	2.9	6.1	-	-	0.8	90.2
Nanticoke	8.3	23.5	4.4	2.1	7.5	54.2
Lakeview	6.2	19.8	5.6	3.1	9.7	55.6
Lingan	4.0	12.6	6.2	1.6	3.5	72.1
Dalhousie	3.2	3.3	17.2	4.7	1.5	70.1

Table 17 - Settling parameters

Source	Density ($g.cm^{-3}$)	Solvent	Density ($g.cm^{-3}$)	Viscosity 20°C (P)	Time* (s)
CaF_2	3.18	Ethanol	0.7893	0.0120	14 400
Mullite	3.07	Ethanol	0.7893	0.0120	15 500
Glass**	2.54	Ethanol	0.7893		

*Settling time over 20 cm.
**Composition glass: CaO, 15.63%; MgO, 2.55%; SiO_2, 65.98%; Al_2O_3, 15.84%.

Table 18 - Composition of mixtures prepared for the standard curves (in grams)

u-Quartz	Glass	CaF_2	Mullite	Glass	CaF_2	Magnetite	Glass	CaF_2	Hematite	Glass	CaF_2
2.000	-	1.000	3.000	-	.100	6.000	-	1.000	6.000	-	1.000
1.800	.200	1.000	2.700	.300	.100	5.500	.500	1.000	5.500	.500	1.000
1.600	.400	1.000	2.400	.600	.100	5.000	1.000	1.000	5.000	1.000	1.000
1.400	.600	1.000	2.100	.900	.100	4.500	1.500	1.000	4.500	1.500	1.000
1.200	.800	1.000	1.800	1.200	.100	4.000	2.000	1.000	4.500	1.500	1.000
1.000	1.000	1.000	1.500	1.500	.100	3.500	2.500	1.000	3.500	2.500	1.000
.800	1.200	1.000	1.200	1.800	.100	3.000	3.000	1.000	3.000	3.000	1.000
.600	1.400	1.000	.900	2.100	.100	2.500	3.500	1.000	2.500	3.500	1.000
.400	1.600	1.000	.600	2.400	.100	2.000	4.000	1.000	2.000	4.000	1.000
.200	1.800	1.000	.300	2.700	.100	1.500	4.500	1.000	1.500	4.500	1.000
.160	1.840	1.000	.250	2.750	.100	1.250	4.750	1.000	1.250	4.750	1.000
.120	1.880	1.000	.200	2.800	.100	1.500	5.000	1.000	1.000	5.000	1.000
.080	1.920	1.000	.150	2.850	.100	.500	5.500	1.000	.500	5.500	1.000
.040	1.960	1.000	.100	2.900	.100	.300	5.700	1.000	.300	5.700	1.000
.020	1.980	1.000	.150	2.950	.100	.100	5.900	1.000	.100	5.900	1.000

Table 19 - Peaks scanned for the standard curves

Phases	2θ	2θ-range scanned
CaF_2	28.3	27.47 - 29.13
CaF_2	47.0	46.17 - 48.83
α-Quartz	20.8	20.0 - 21.66
α-Quartz	26.6	25.8 - 27.46
α-Quartz	50.1	49.3 - 50.96
Mullite	16.4	15.57 - 17.23
Mullite	39.2	38.37 - 40.03
Mullite	60.6	59.77 - 61.43
Magnetite	30.1	29.27 - 30.93
Magnetite	43.0	42.17 - 43.83
Magnetite	62.5	61.69 - 63.35
Hematite	24.1	23.27 - 24.93
Hematite	49.4	48.57 - 50.23
Hematite	63.9	63.12 - 64.78

Table 20 - Crystalline and glass content of eight Canadian fly ashes (wt %)

Fly ash	α-quartz	Mullite	Magnetite	Hematite	LOI	Glass
Wabamun	10.9	12.2	-	-	0.8	76.1
Sundance	4.7	9.8	-	2.2	0.4	82.9
Forestburg	3.1	7.1	-	-	0.8	89.0
Nanticoke	9.1	17.3	4.8	1.6	7.5	59.7
Lakeview	5.5	25.2	3.6	2.5	9.7	53.5
Lingan	4.6	10.4	1.6	2.6	3.5	77.3
Dalhousie	12.4	2.9	3.3	3.2	1.5	77.7
Estevan	4.7	-	-	-	0.9	94.5

Table 21 - Composition of the mixtures prepared for standard curves for melilite and merwinite (in grams)

Mullite	Glass	CaF_2	$\frac{\text{Melilite}}{CaF_2}$	Merwinite	Glass	CaF_2	$\frac{\text{Merwinite}}{CaF_2}$
3.000	0.000	0.200	15.0	4.000	0.000	0.200	20.0
2.750	0.250	0.200	13.75	3.500	0.500	0.200	17.5
2.500	0.500	0.200	12.5	3.000	1.000	0.200	15.0
2.250	0.750	0.200	11.25	2.500	1.500	0.200	12.5
2.000	1.000	0.200	10.0	2.000	2.000	0.200	10.0
1.750	1.250	0.200	8.75	1.500	2.500	0.200	7.5
				1.000	3.000	0.200	5.0
1.500	1.500	0.200	7.50	0.750	3.250	0.200	3.75
1.250	1.750	0.200	6.25	0.600	3.400	0.200	3.00
1.000	2.000	0.200	5.00	0.500	3.500	0.200	2.50
0.750	2.250	0.200	3.75	0.400	3.600	0.200	2.00
0.500	2.500	0.200	2.50	0.300	3.700	0.200	1.50
0.250	2.750	0.200	2.25	0.200	3.800	0.200	1.00
				0.050	3.950	0.200	0.250

Table 22 - Peaks scanned for the standard curves for melilite and merwinite

Phases	2θ	2θ-range scanned
Melilite curve		
CaF_2	46.97	46.14 - 47.80
Melilite	31.20	30.60 - 32.26
Merwinite curve		
CaF_2	28.40	27.00 - 28.66
	55.70	55.00 - 56.66
Merwinite	31.30	30.20 - 31.86
	33.60	32.80 - 34.46

Table 23 - Crystalline and glass contents of two blast furnace slags

Sample	2θ	$I_{M,2\theta}$	2θ'	$I_{F,2\theta'}$	$\frac{I_{M,2\theta}}{I_{F,2\theta'}}$	Average $\frac{I_{M,2\theta}}{I_{F,2\theta'}}$	% M	% $\bar{M}$	% Glass
Standard (Melilite)	31.20	1592	46.97	4987	0.3192	0.3329	11.7	11.7	88.3
	31.20	1794	46.97	5378	0.3336				
	31.20	1821	46.97	5266	0.3458				
Atlantic (Merwinite)	31.30	581	28.40	996	0.583	0.448	(4.49)		
	31.30	503	28.40	1464	0.344				
	31.30	560	28.40	1343	0.417				
	31.30	581	55.70	443	1.312	1.069	(3.65)		
	31.30	503	55.70	476	1.057				
	31.30	560	55.70	668	0.838				
	33.60	2298	27.40	996	2.307	1.849	12.92	11.9	88.1
	33.60	2521	28.40	1464	1.722				
	33.60	2037	28.40	1343	1.517				
	33.60	2298	55.70	443	5.187	4.511	10.80		
	33.60	2521	55.70	476	5.296				
	33.60	2037	55.70	668	3.049				

Table 24 - Glass contents determined with the differential intensity method

	Cordierite		Wabamun
	A	B	
% Glass (Known)	20	70	-
Integral index (C_1)	0.681	0.542	0.180
Crystallinity (C_1) %	68.1	54.2	18.0
% Glass (C_1)	31.9	45.8	82.0
Correlation index (C_c)	0.795	0.278	-0.0104 (0.164)
Correlation coefficient (r)	0.722	0.772	-0.0508 (0.529)
Crystallinity (C_c) %	79.5	27.8	-1.0 (16.4)
% Glass (C_c)	20.5	72.2	101.0 (83.6)

Table 25 - Specific gravities of three fly ashes and analogues determined by pycnometry

Fly ash	Specific gravity fly ash	Specific gravity glassy analogue	Specific gravity crystalline analogue
Wabamun	2.47	2.67	2.68
Sundance	2.44	2.65	2.73
Forestburg	2.43	2.77	2.80

Table 26 - XRD $2\theta_{Imax}$ for nine fly ashes, two slags, and their glossy analogues

Source	$2\theta_{Imax}$	$2\theta_{Imax}$(glass)	CaO (wt %)I	ΣCaO + MgO+ Na_2O+K_2O (mol/100g)
Wabamun	23.2	24.5	11.1	0.259
Sundance	23.4	25.3	12.5	0.295
Forestburg	25.4	25.7	10.5	0.316
Nanticoke	23.0	24.0	5.95	0.158
Lakeview	24.0	24.2	3.82	0.126
Lingan	24.4	25.5	1.29	0.106
Dalhousie	23.0	-	4.45	0.127
Estevan	29.0	26.4	13.0	0.455
Thunder Bay	25.4	26.4	12.4	0.419
Standard Slag	30.6	29.5	35.1	0.937
Atlantic Slag	30.8	28.4	40.1	0.959

Table 27 - Glass content values (%) determined by various methods

Source material	McMaster method	QXRD method	NCXRD method	Avg. of QXRD/NCXRD	DIXRD method	Image analysis
Wabamun	NA	76.1	62.1	69.1	82.0 (C_i) 101.0 (C_C) 83.6 (C_C*)	93.4
Sundance	NA	82.9	77.4	80.2		
Forestburg	NA	89.0	82.4	85.7		
Nanticoke	NA	59.7	83.8	71.8		
Lakeview	NA	53.5	99.3	76.4		
Lingan	NA	77.3	84.4	80.8		
Dalhousie	NA	76.7	-	76.7		
Estevan	NA	94.5	70.0	82.2		
Thunder Bay	NA	-	86.9	86.9		
Standard Slag	47.1-84.3	88.3	72.4	80.4		
Atlantic Slag	59.7-68.9	88.1	42.8	65.5		

*Determined by omitting non-corresponding XRD peaks for the computation of C_C.

FIGURES

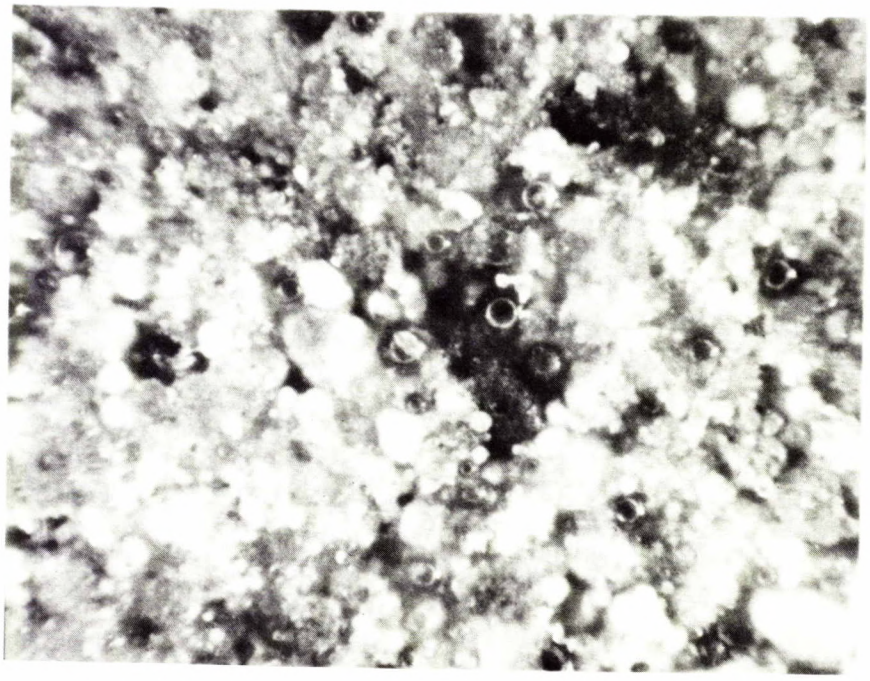

Fig. 1 - Optical micrograph of Wabamun fly ash in an Elvacite medium (magnification 137x)

A	
SiO_2	63.31
Al_2O_3	20.62
CaO	13.73
FeO	1.74

B	
SiO_2	65.68
Al_2O_3	20.92
CaO	1.80
TiO_2	11.60

C	
SiO_2	87.13
Al_2O_3	8.47
FeO	4.40

D	
SiO_2	29.77
Al_2O_3	12.62
CaO	44.53
SO_3	5.38
FeO	3.76

E	
SiO_2	27.04
Al_2O_3	9.93
CaO	53.16
SO_3	5.11
FeO	2.97

H	
SiO_2	15.58
Al_2O_3	5.66
CaO	1.89
FeO	76.88

Fig. 2(a) - SEM micrograph of Wabamun fly ash in an Elvacite medium (magnification 20 μ)

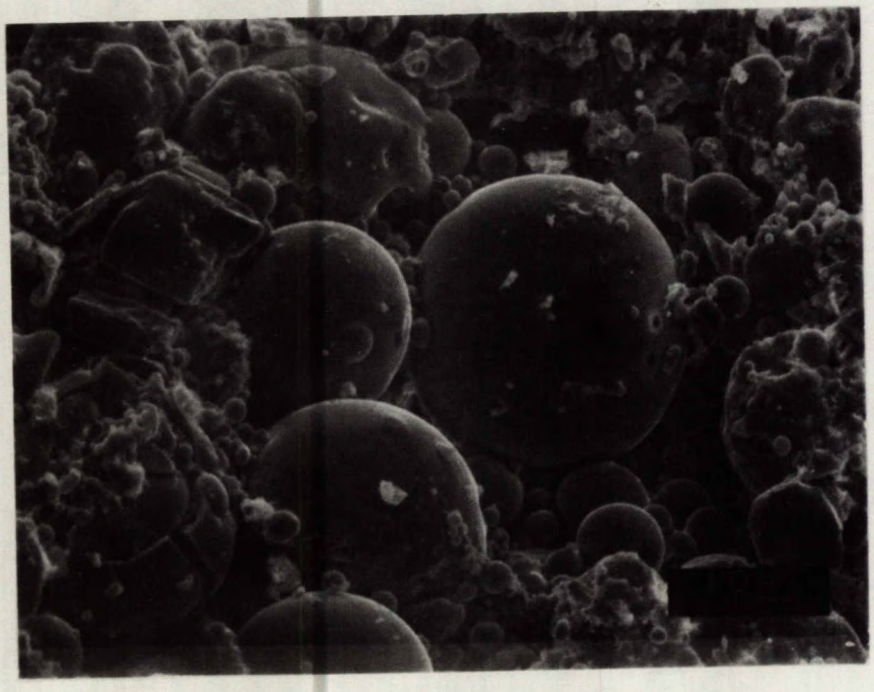

Fig. 2(b) - Detail of 2(a) (magnification 10 μ)

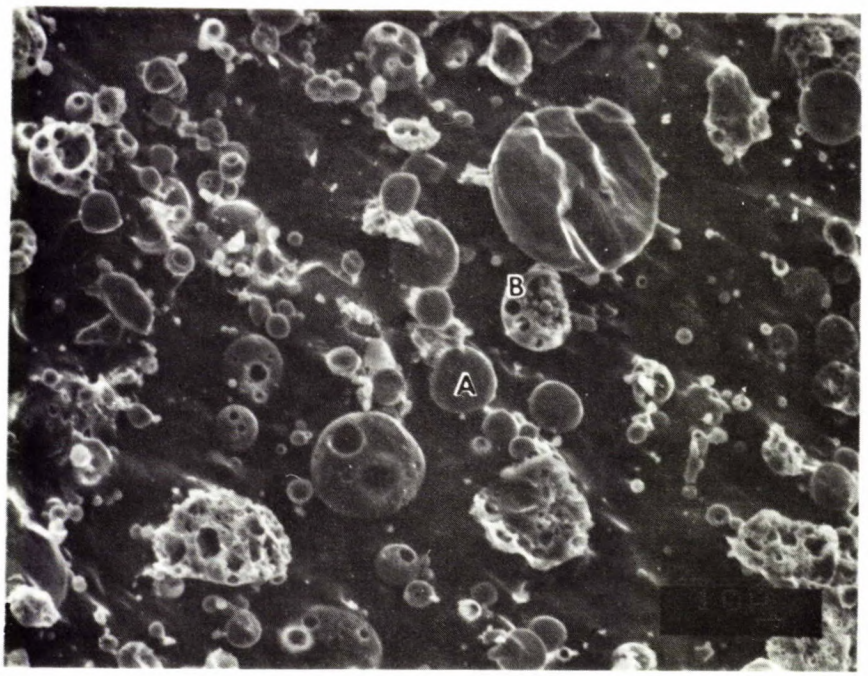

(a) Secondary Electron mode

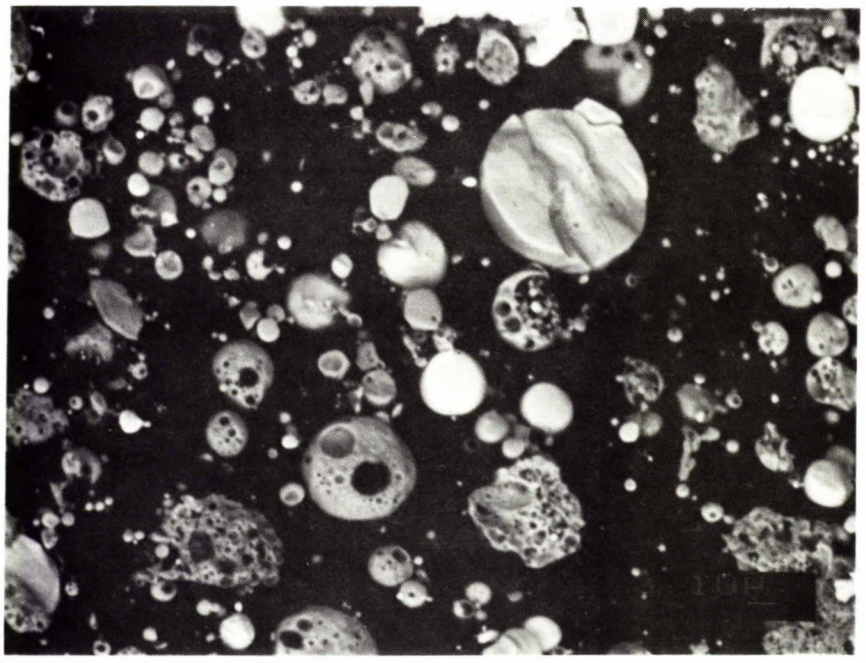

(b) Back-Scatter mode

Fig. 3 - Cross section of Wabamun fly ash after ion etching

	3
SiO_2	51.27
Al_2O_3	31.29
TiO_2	4.86
FeO	2.27
CaO	9.17

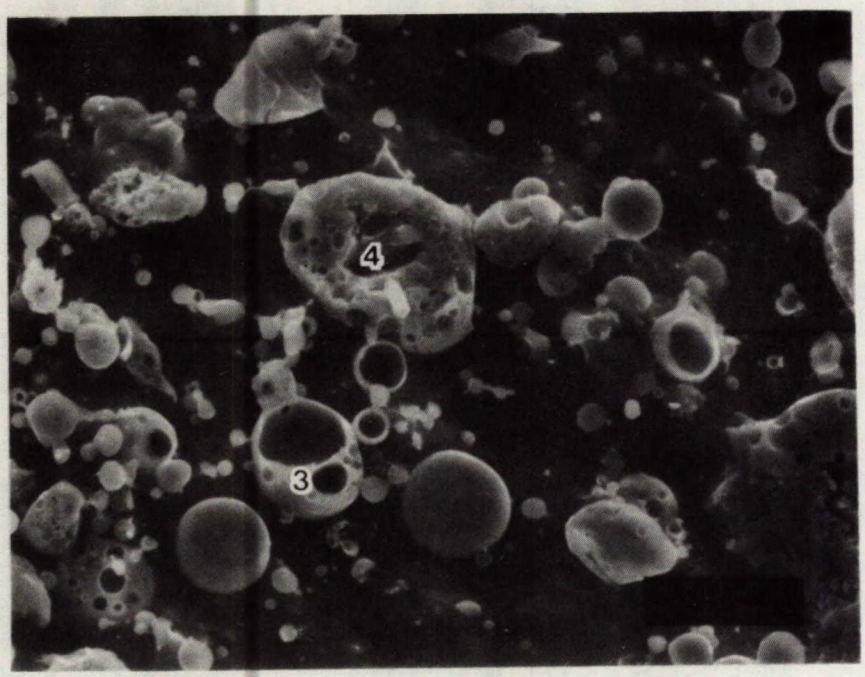

(a) Secondary Electron mode

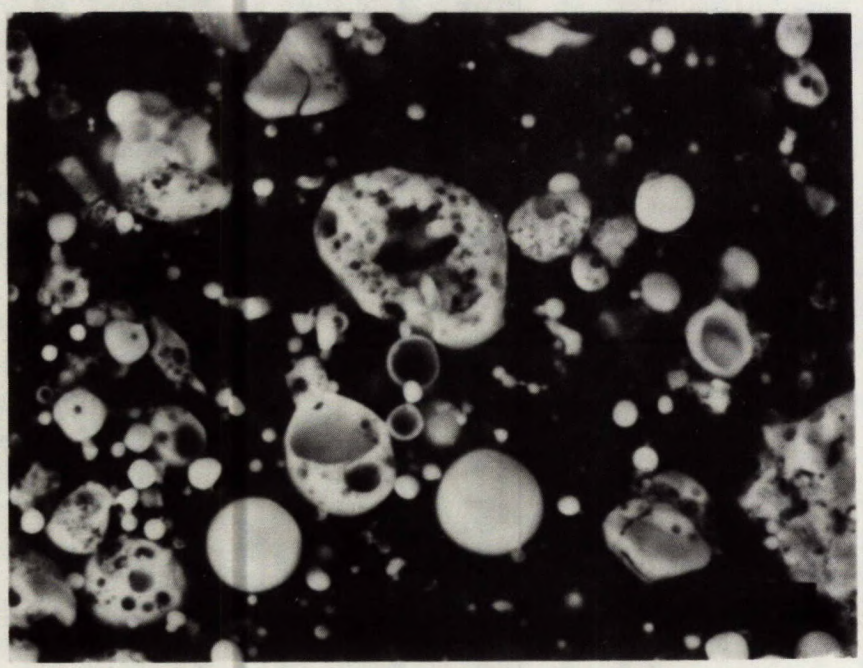

(b) Back-Scatter mode

Fig. 4 - Another view of cross section of Wabamun fly ash after ion etching

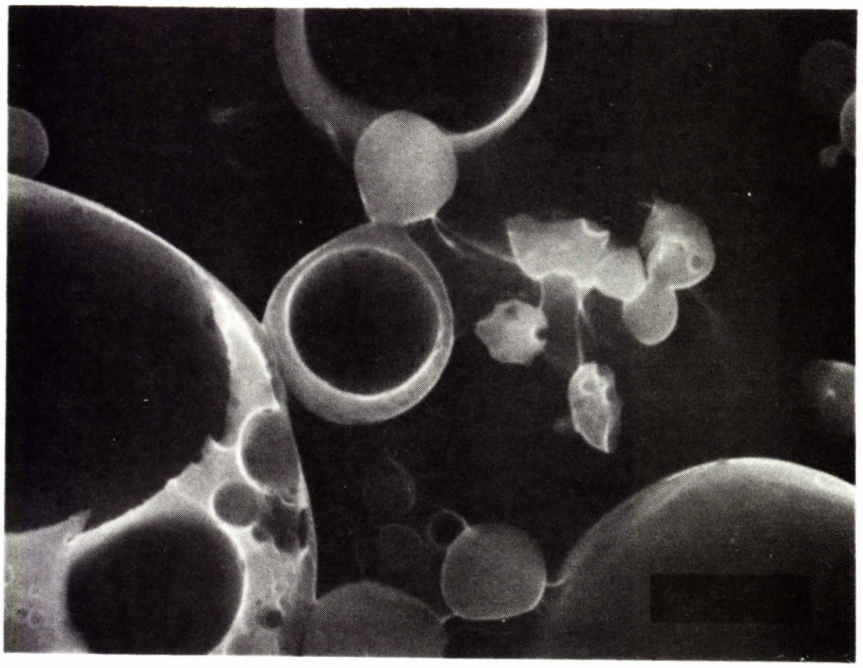

(a) Secondary Electron mode

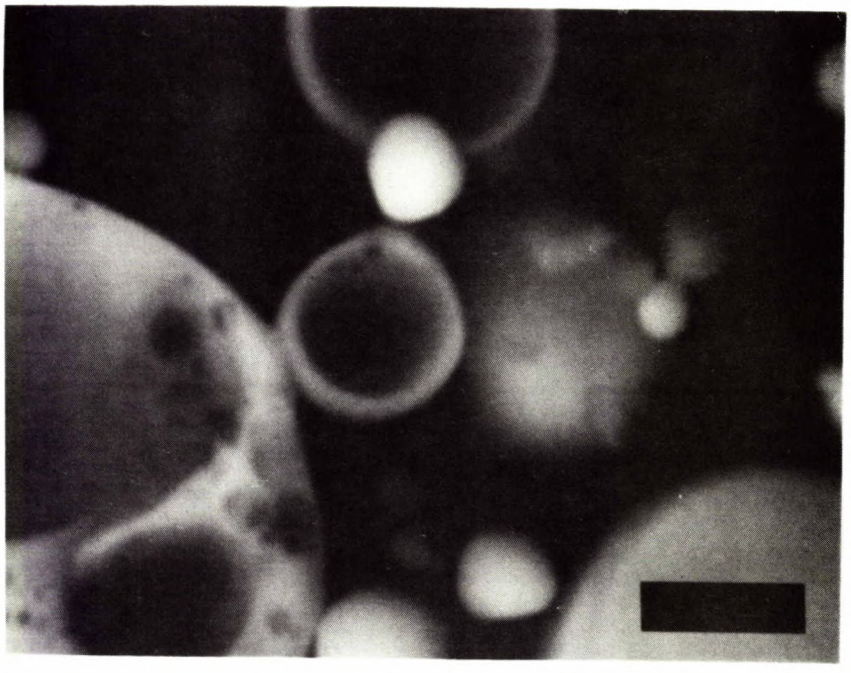

(b) Back-Scatter mode

Fig. 5 - SEM micrograph of location 3 in Fig. 4 at higher magnification

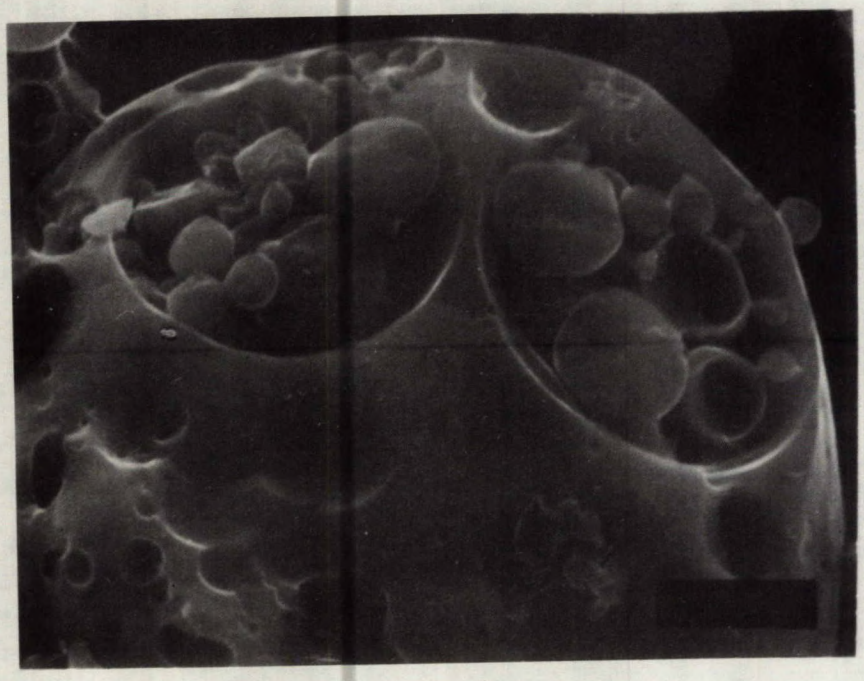

(a) Secondary Electron mode

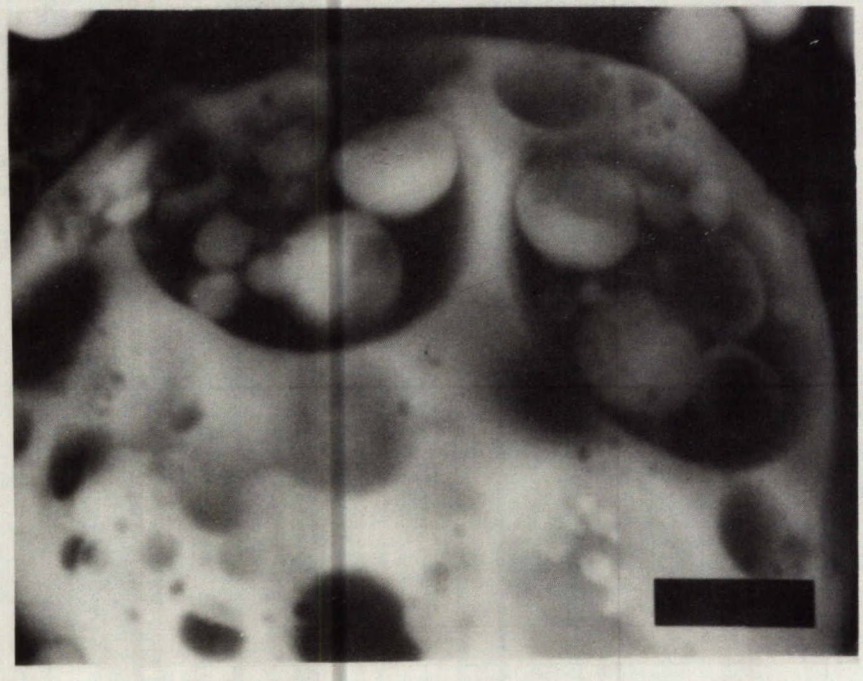

(b) Back-Scatter mode

Fig. 6 - SEM micrograph of a plerosphere

4A

SiO_2	66.84
Al_2O_3	15.70
TiO_2	1.71
FeO	3.08
CaO	6.12
K_2O	6.24

4B

SiO_2	55.69
Al_2O_3	14.68
TiO_2	4.06
FeO	5.78
SO_3	3.04
CaO	8.53
K_2O	6.24

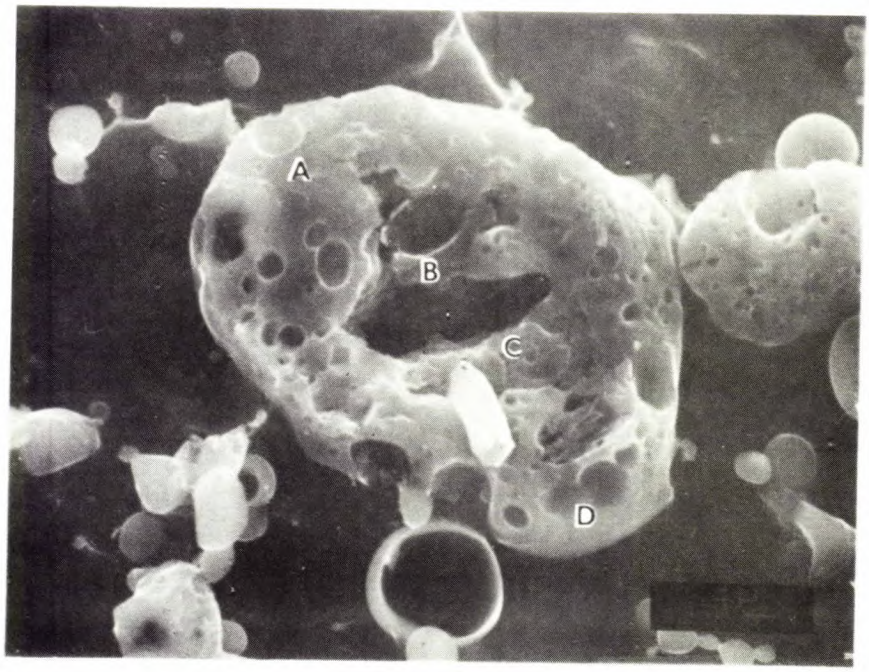

(a) Secondary Electron mode

4C

SiO_2	63.15
Al_2O_3	20.56
TiO_2	1.60
FeO	3.03
CaO	4.80
K_2O	6.45

4D

SiO_2	49.24
Al_2O_3	16.35
TiO_2	1.91
FeO	5.31
CaO	23.87
K_2O	2.64

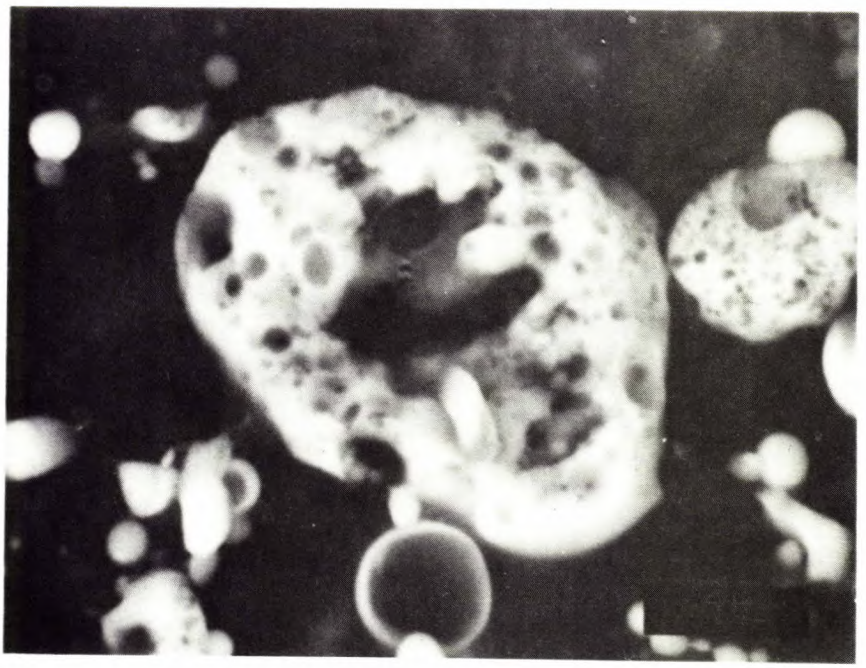

(b) Back-Scatter mode

Fig. 7 - SEM micrograph of location 4 in Fig. 4 at higher magnification

(A) 100% GLASS (B) 75% GLASS (C) 50% GLASS

(D) 25% GLASS (E) 0% GLASS

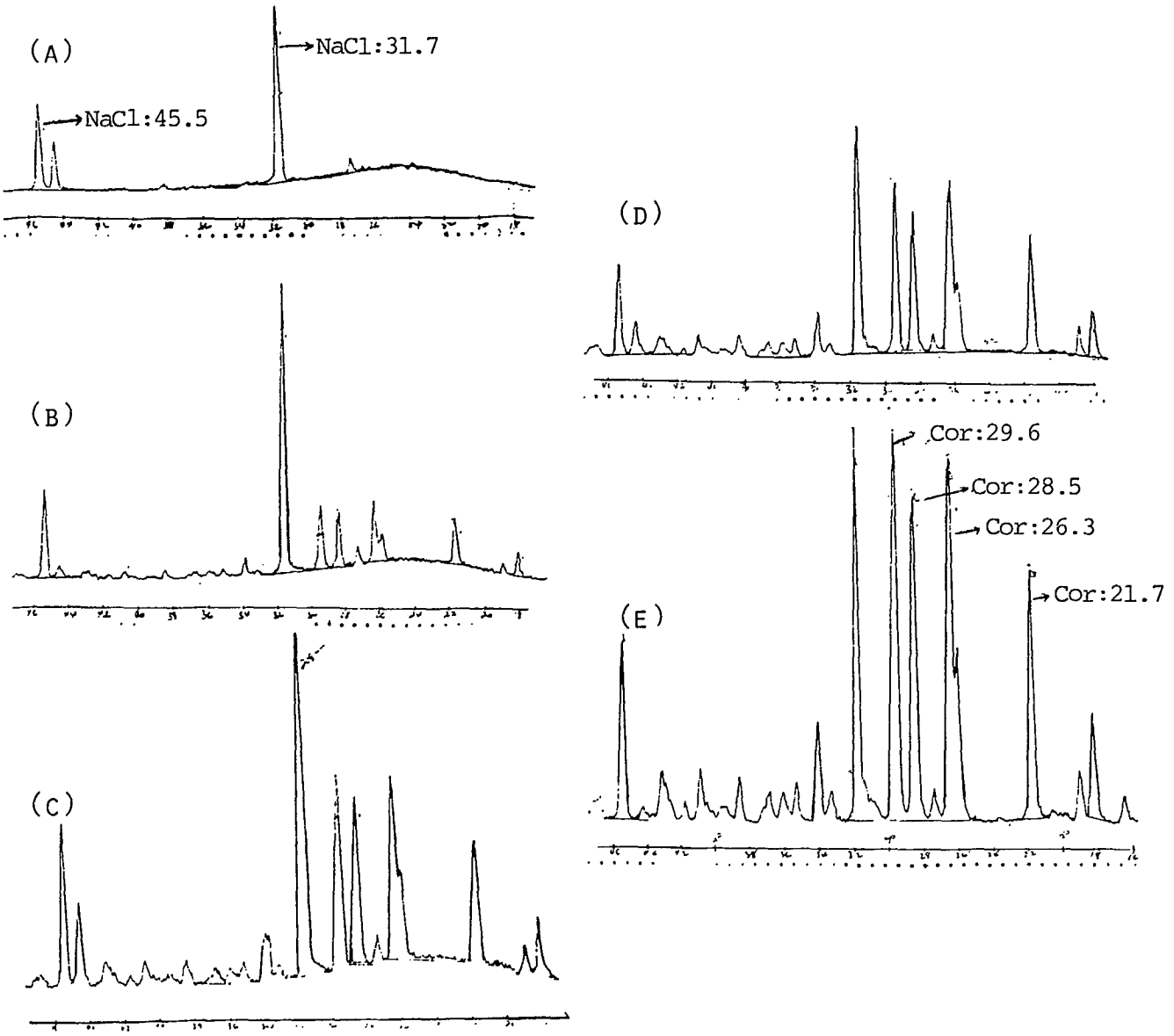

Fig. 8 - XRD patterns for Cordierite glass/α-Cordierite mixtures for glass content determination (QXRD method)

Fig. 9 - Intensity ratios for Cordierite glass/α-Cordierite mixtures versus glass content (QXRD Method)

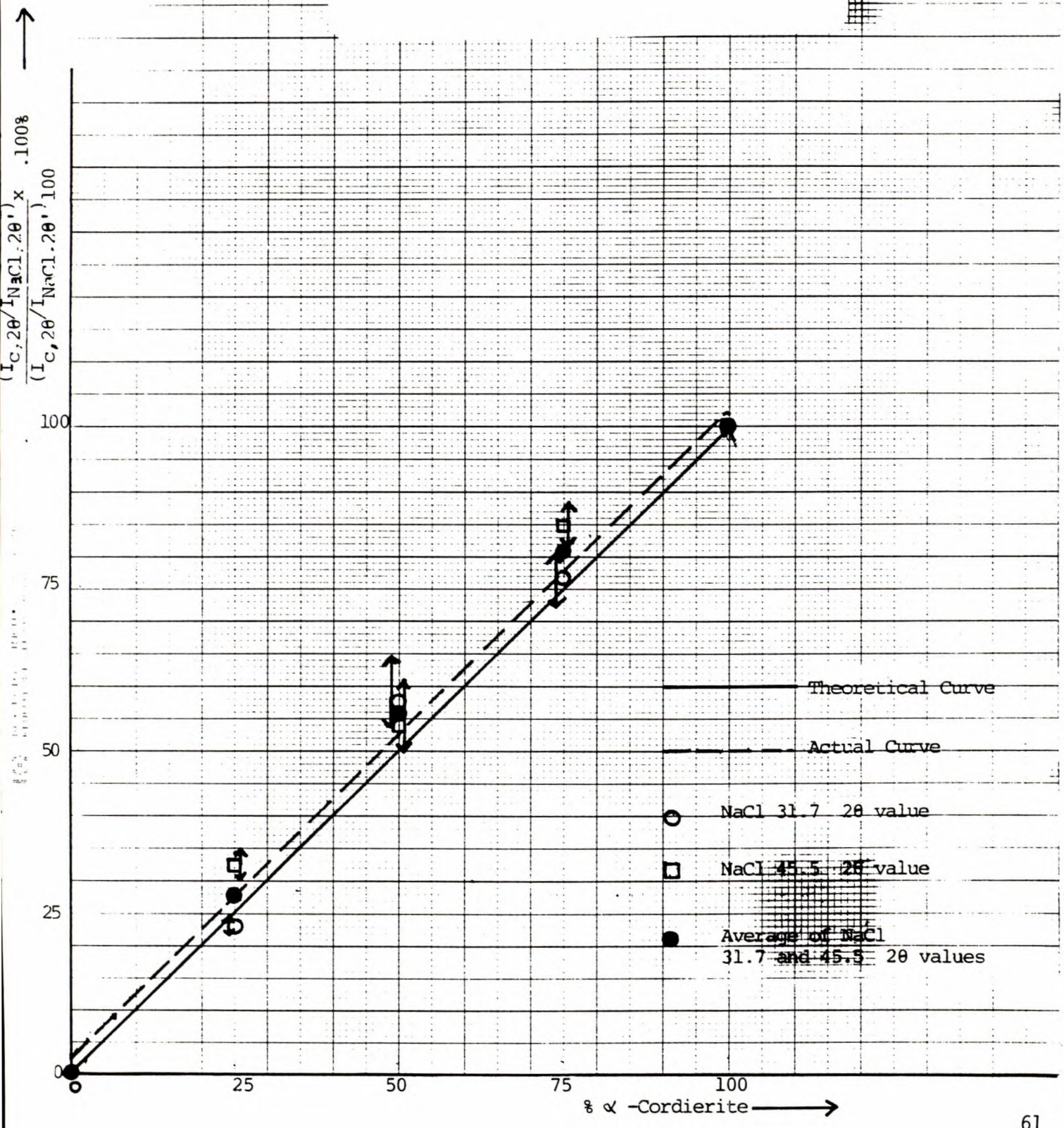

Fig. 10 - Standard curve for α-Quartz 2θ = 20.8, 2θ' = 28.3

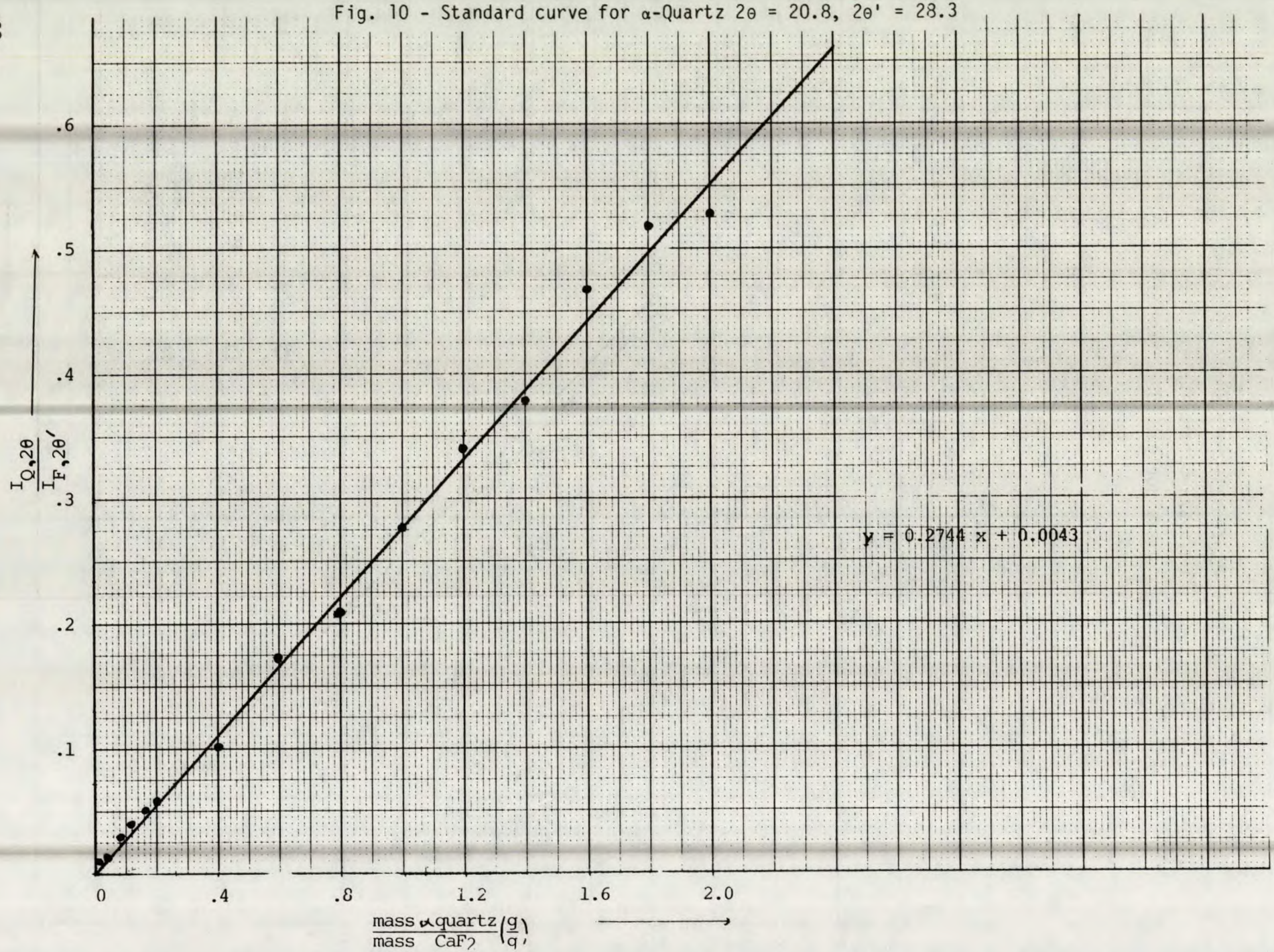

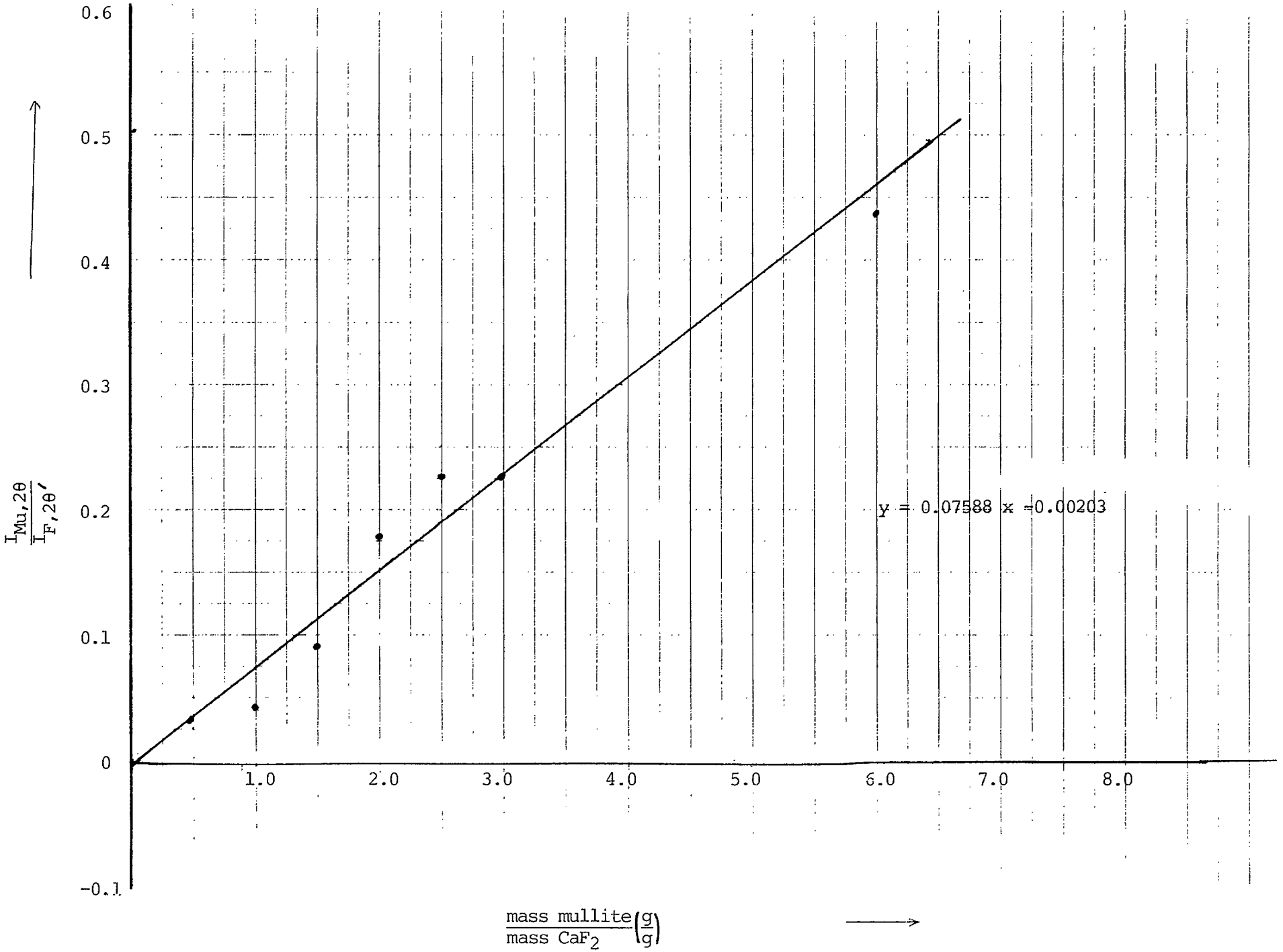

Fig. 11 - Standard curve for Mullite 2θ = 60.6, 2θ' = 28.3

Fig. 12 - Standard curve for Magnetite $2\theta = 30.1$, $2\theta' = 28.3$

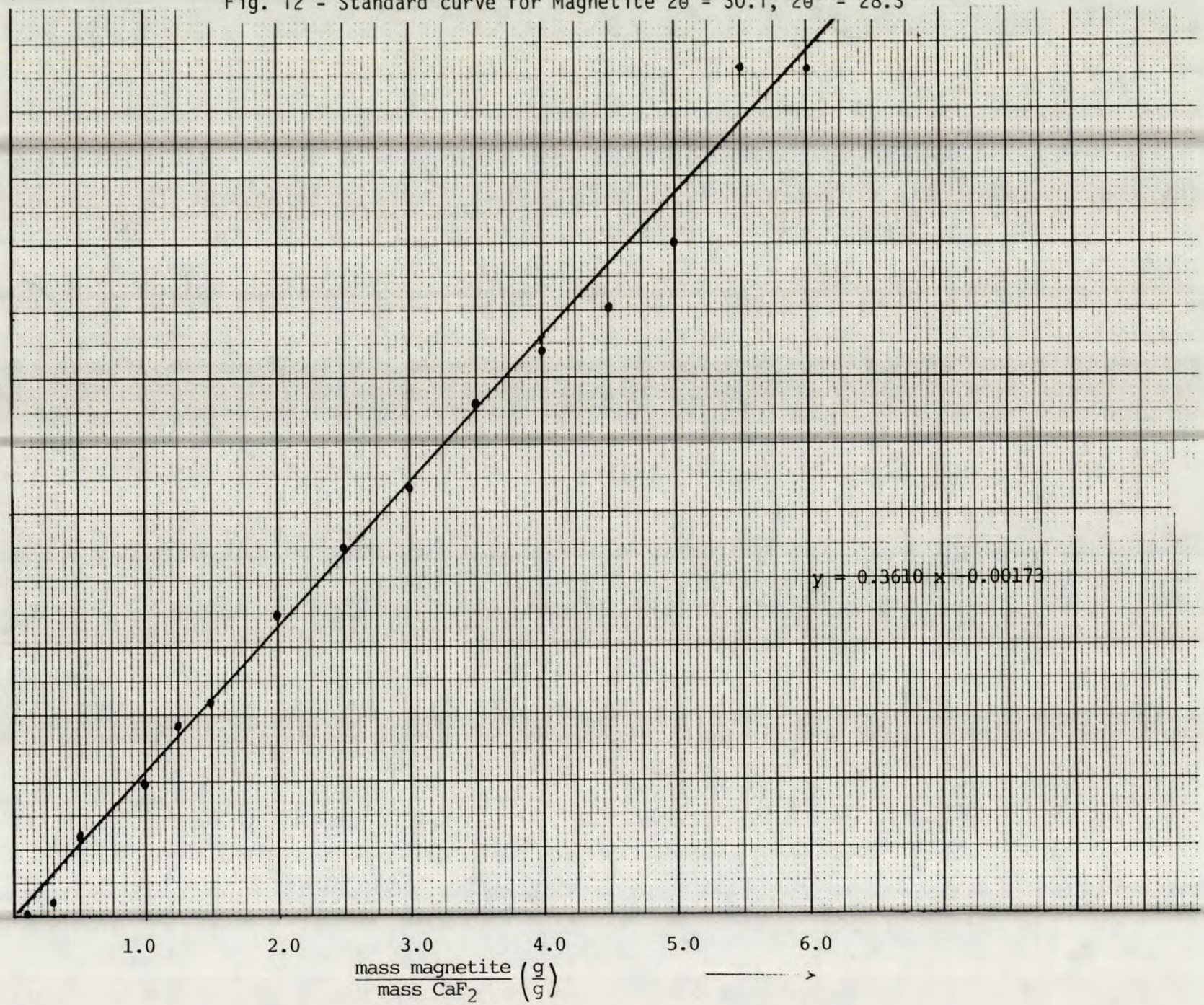

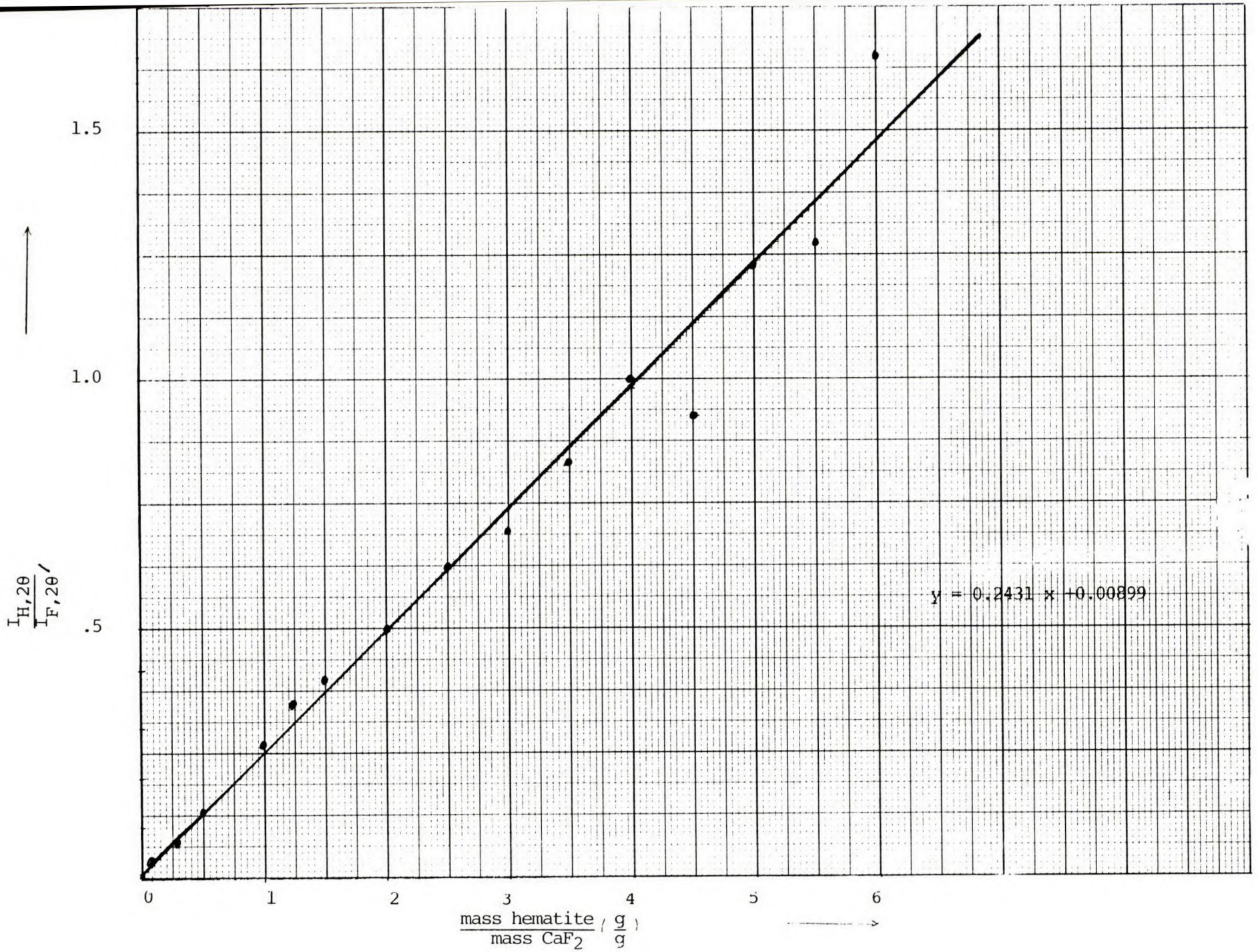

Fig. 13 - Standard curve for Hematite 2θ = 24.1, 2θ' = 28.3

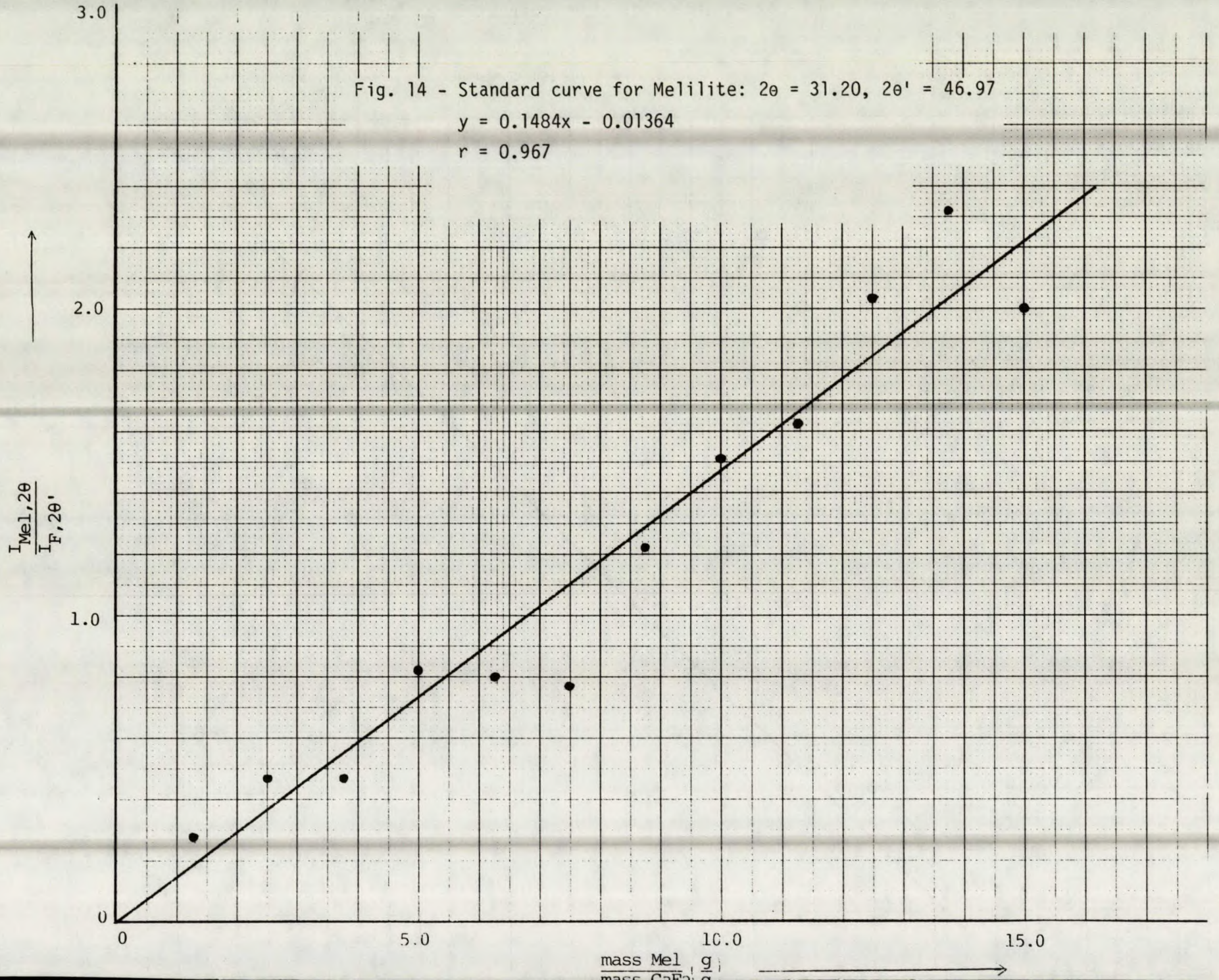

Fig. 14 - Standard curve for Melilite: $2\theta = 31.20$, $2\theta' = 46.97$

$y = 0.1484x - 0.01364$

$r = 0.967$

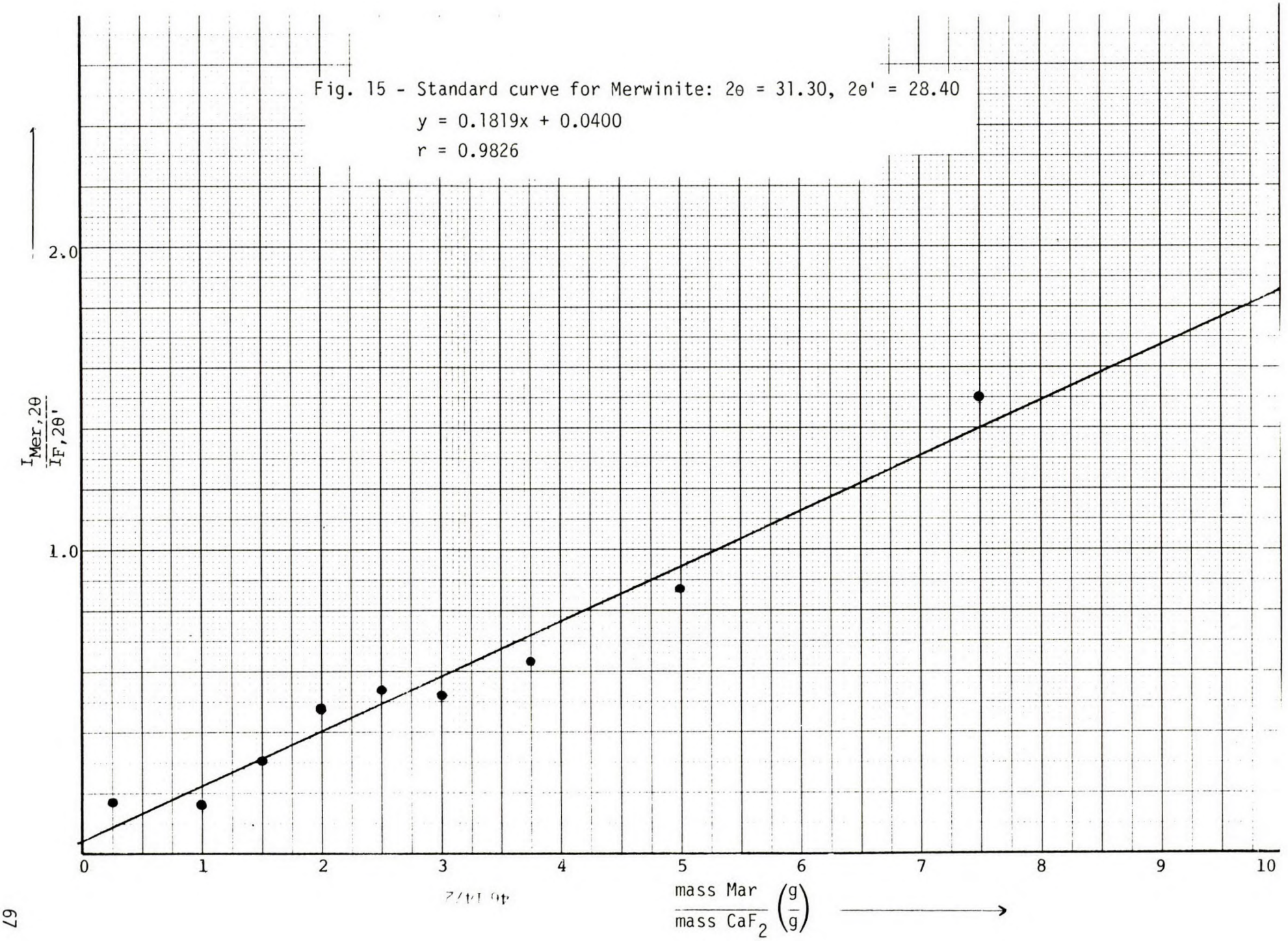
Fig. 15 - Standard curve for Merwinite: 2θ = 31.30, 2θ' = 28.40
y = 0.1819x + 0.0400
r = 0.9826
$\frac{I_{Mer,2\theta}}{I_{F,2\theta'}}$
2.0
1.0
0
1
2
3
4
5
6
7
8
9
10
mass Mar / mass CaF_2 $\left(\frac{g}{g}\right)$

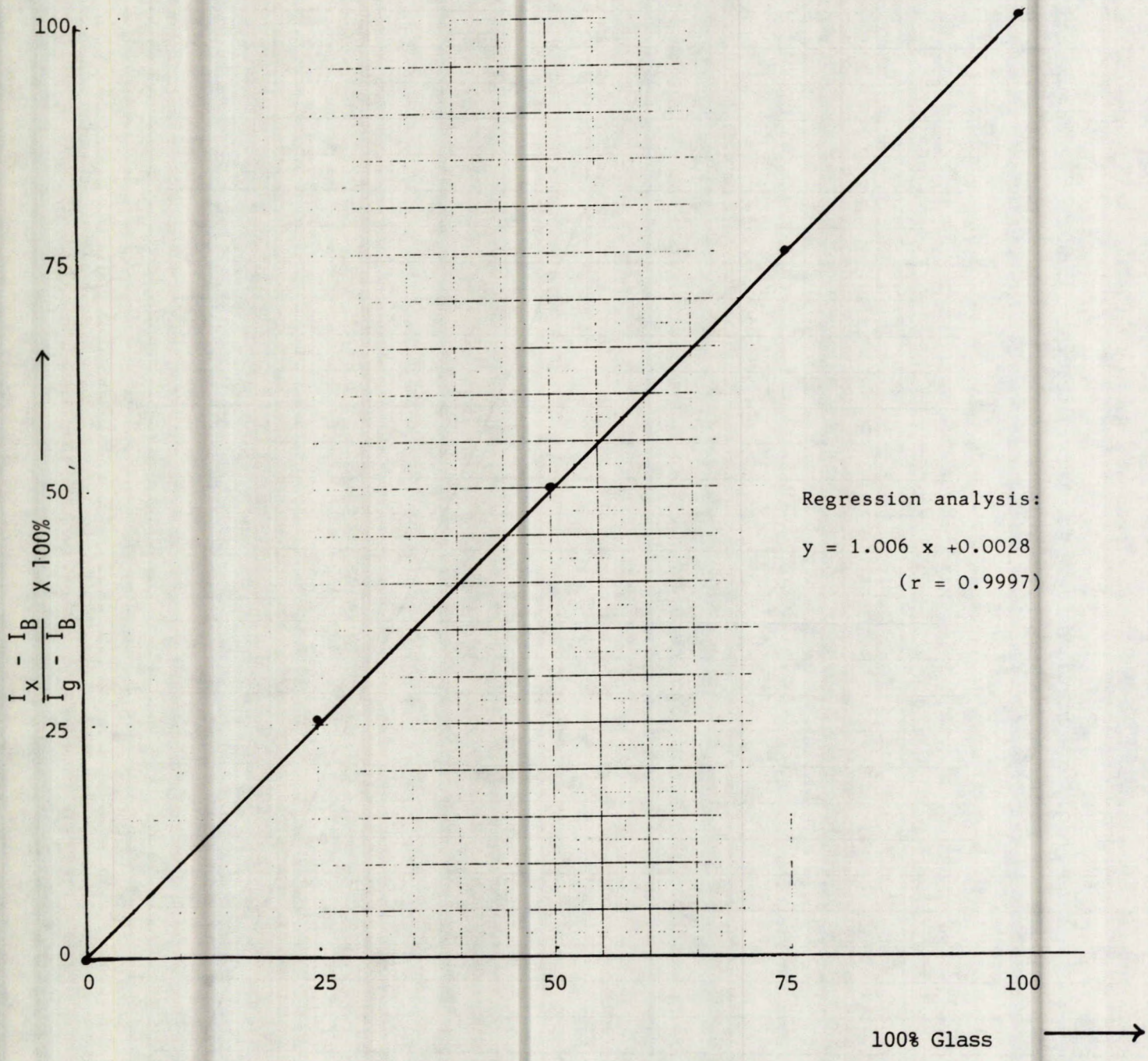

Fig. 16 - Intensity ratio of glassy halo at 24° 2θ versus glass content for Cordierite glass/α-Cordierite mixtures

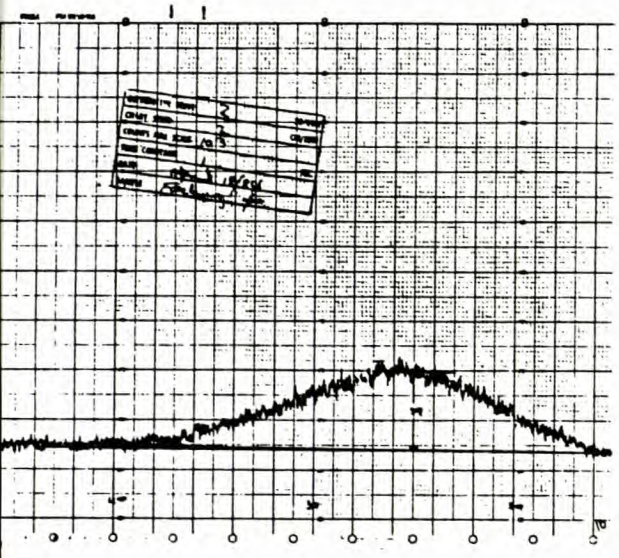

(a) 100% Glass

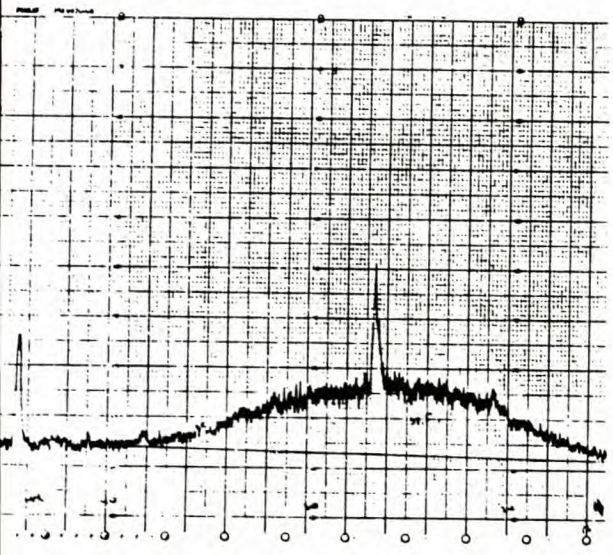

(b) Forestburg Flyash

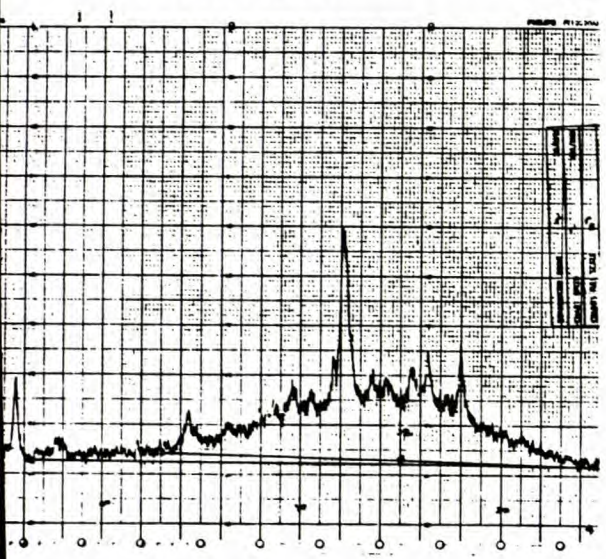

(c) 75% Glass

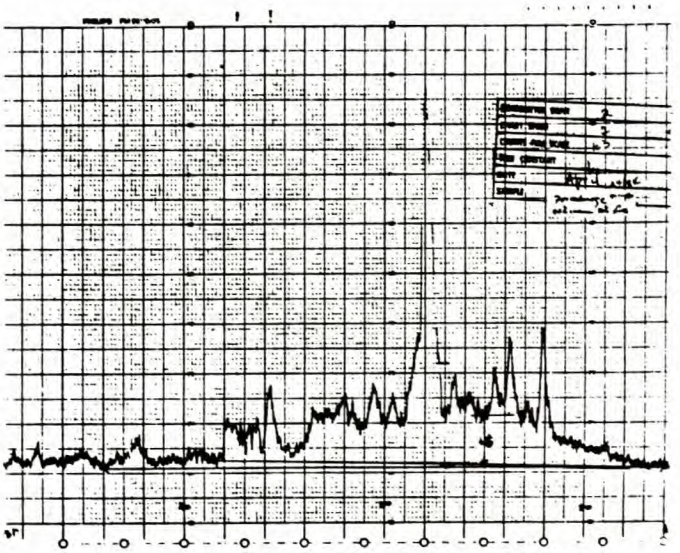

(d) 50% Glass

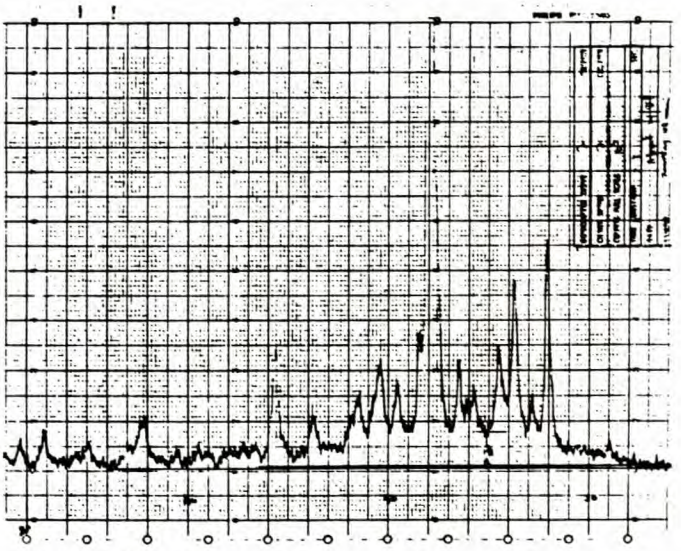

(e) 25% Glass

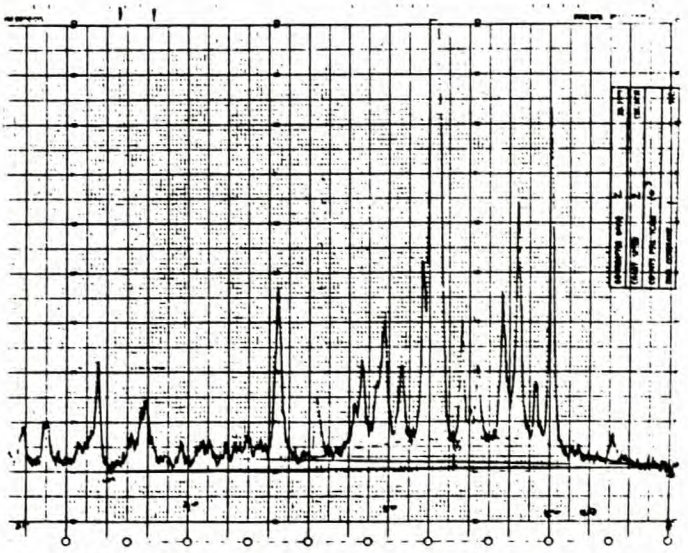

(f) 0% Glass

Fig. 17 - XRD patterns of mixtures of vitrified and redevitrified Forestburg fly ash

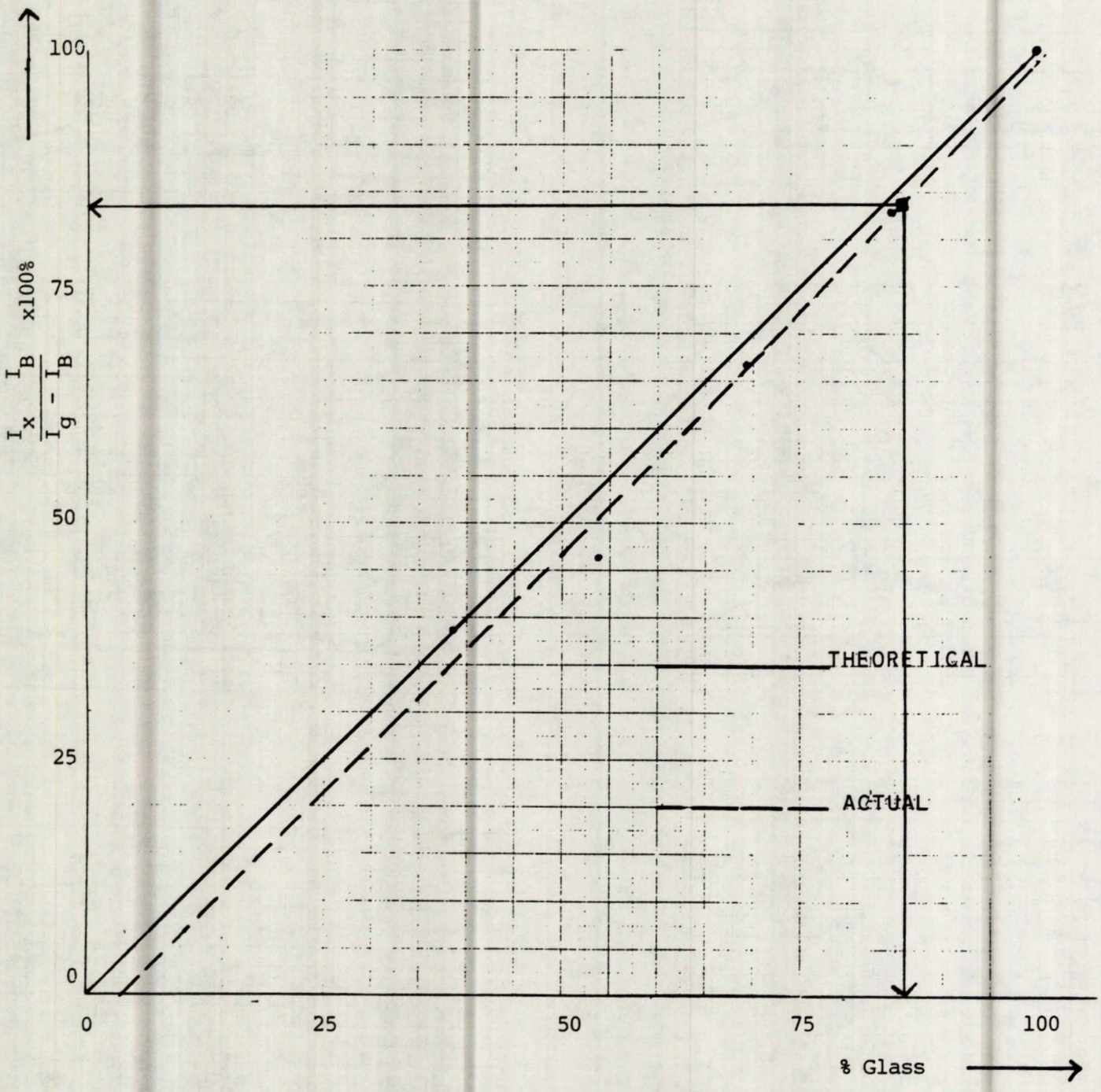

Fig. 18 - Intensity ratio of glassy halo at 25° 2θ versus glass content for Forestburg glass and redevitrified glass mixtures

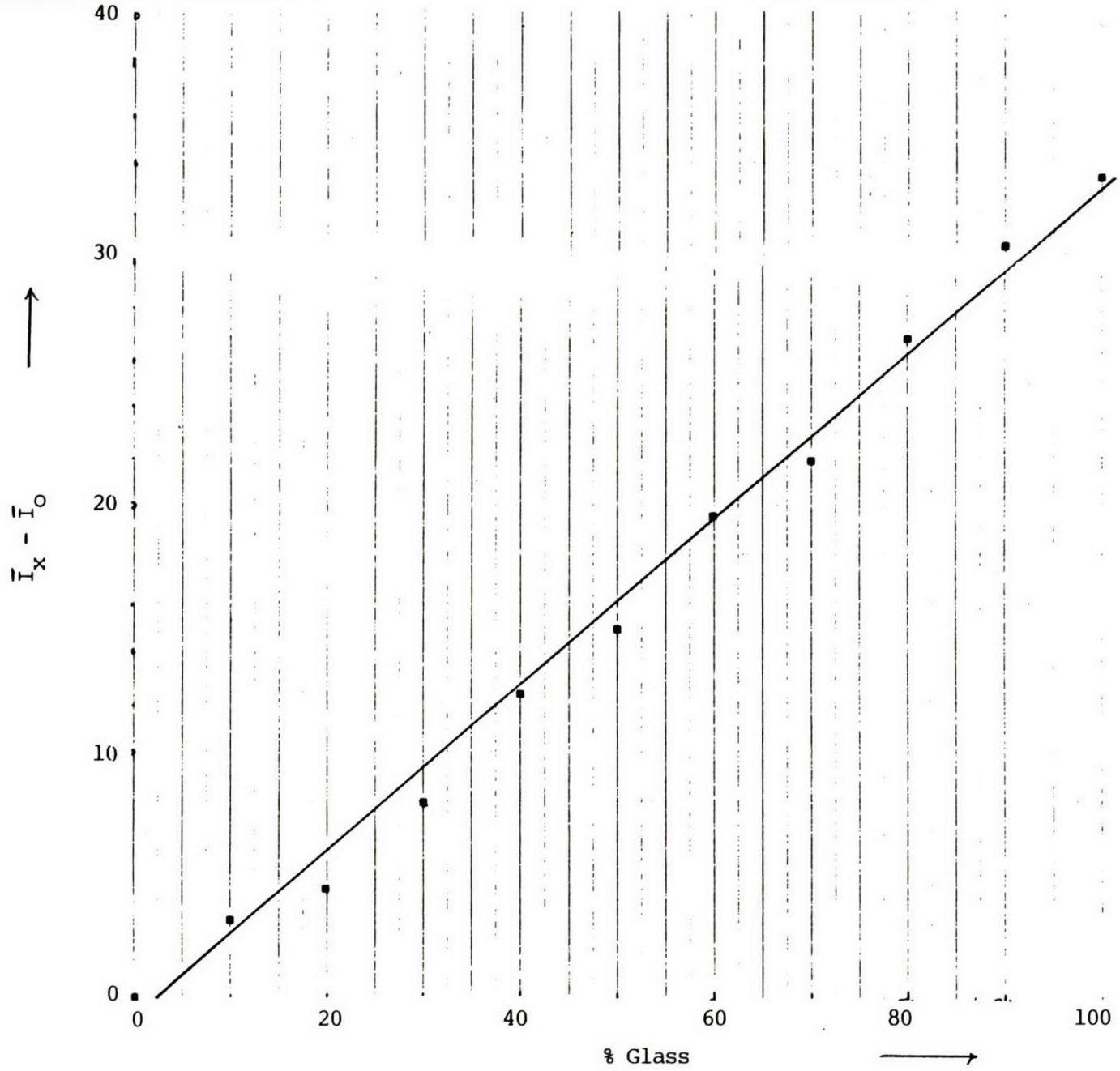

Fig. 19 - Scattering intensity $\bar{I}_x - \bar{I}_o$ at 2θ-24° versus glass content for Cordierite glass/α-Cordierite mixtures

Fig. 20 - Scattering intensity $\bar{I}_x - \bar{I}_o$ at 2θ-25° versus glass content for Wabamun fly ash

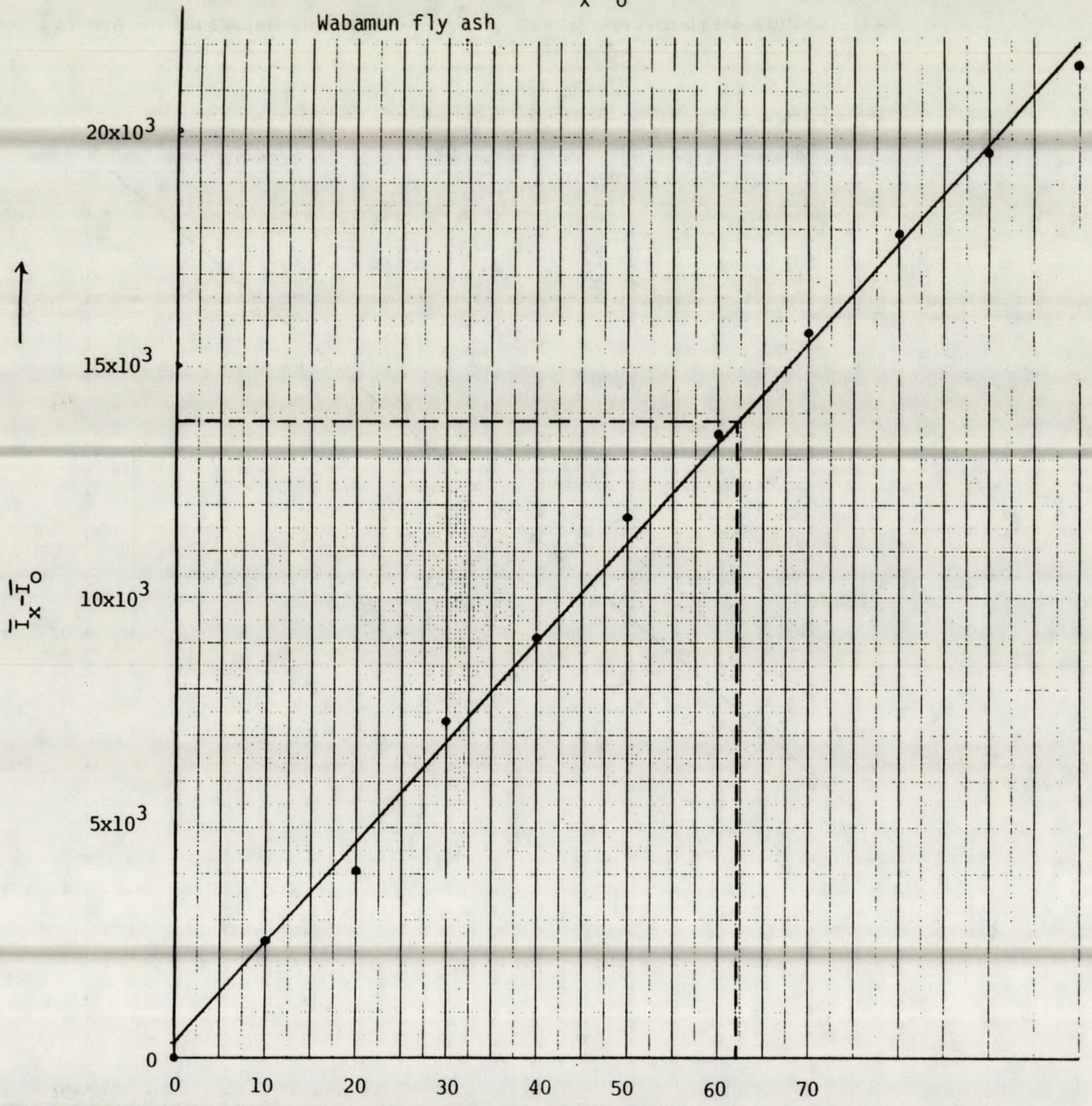

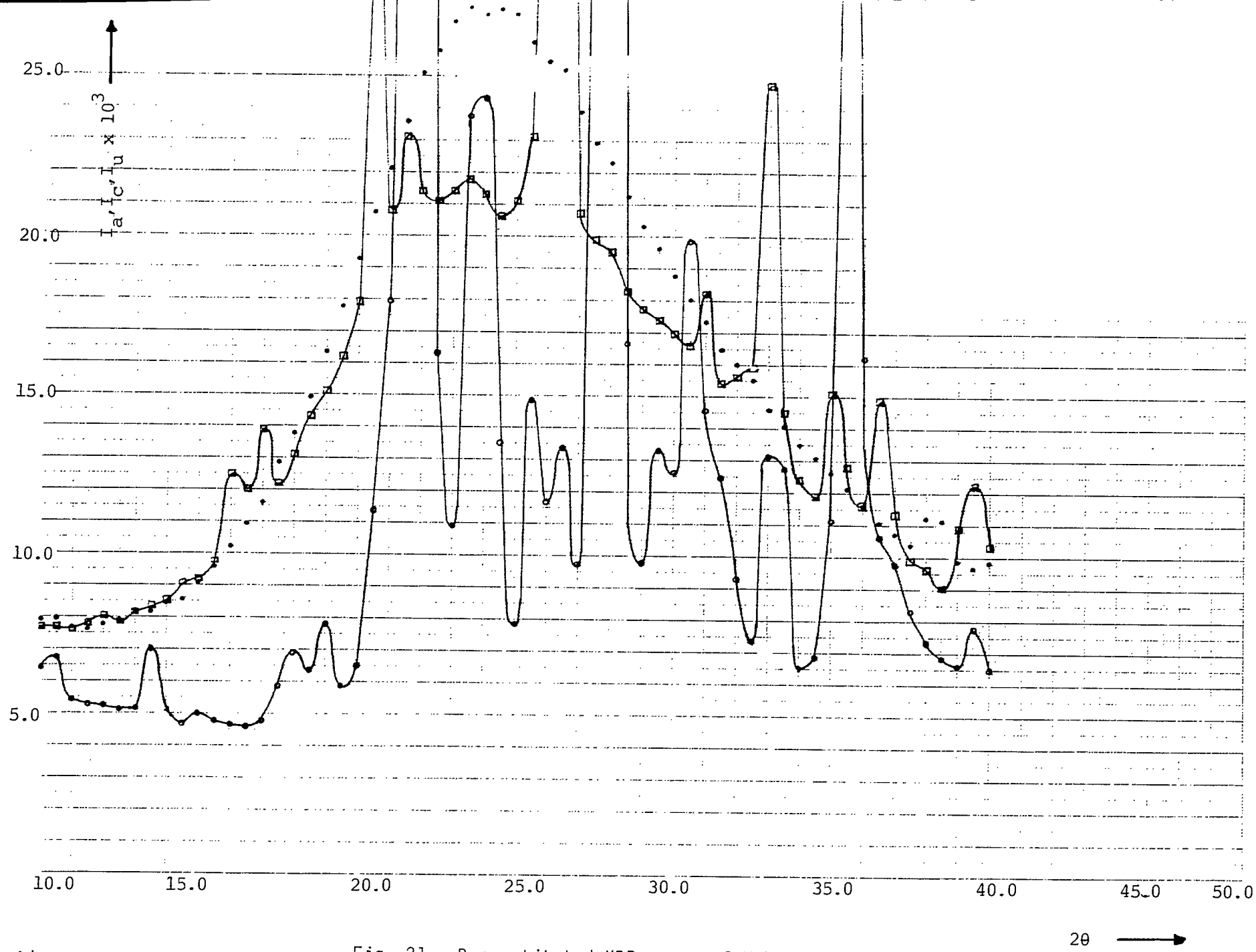

Fig. 21 - Reconstituted XRD scans of Wabamun fly ash

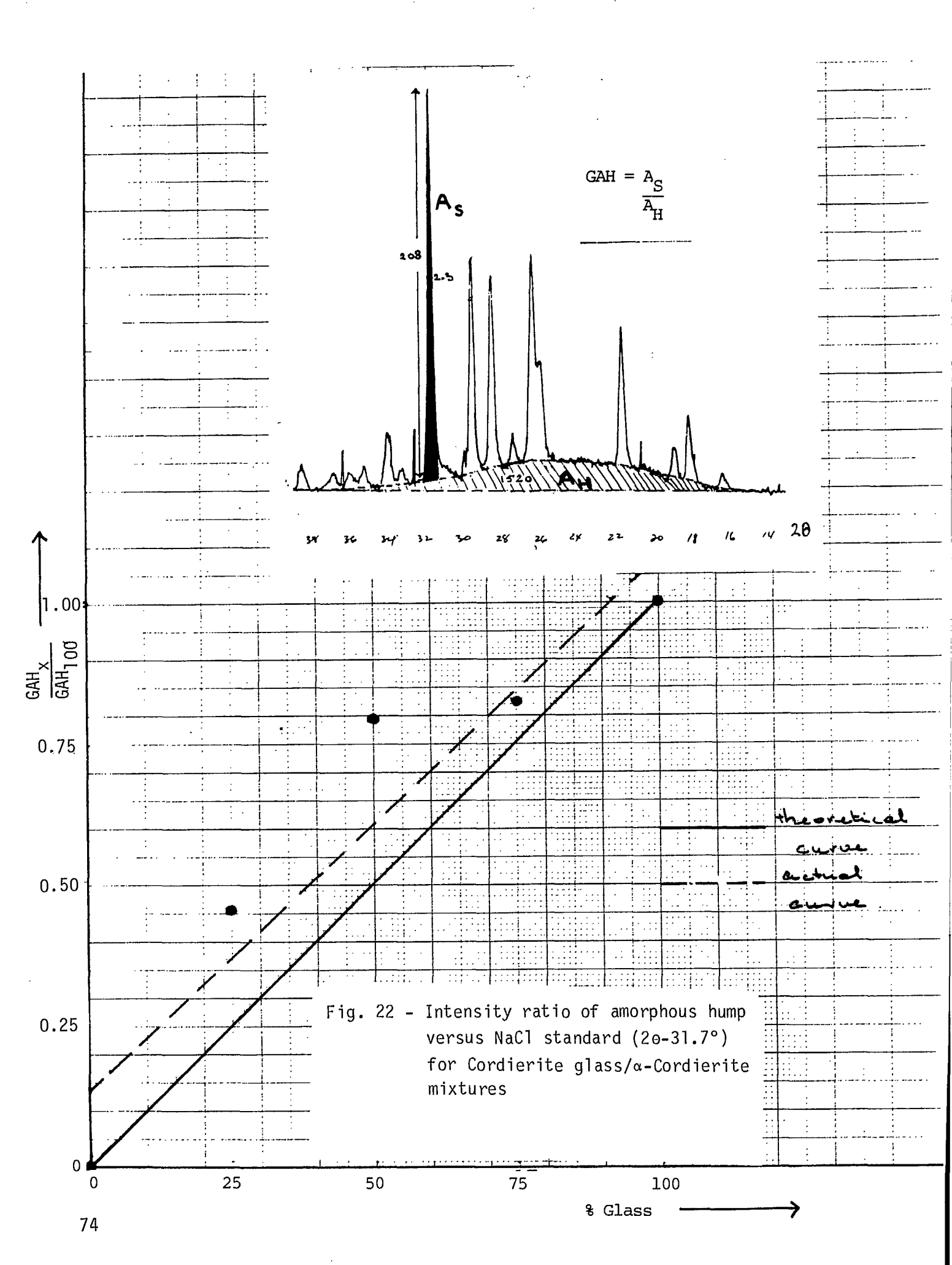

Fig. 22 - Intensity ratio of amorphous hump versus NaCl standard (2θ-31.7°) for Cordierite glass/α-Cordierite mixtures

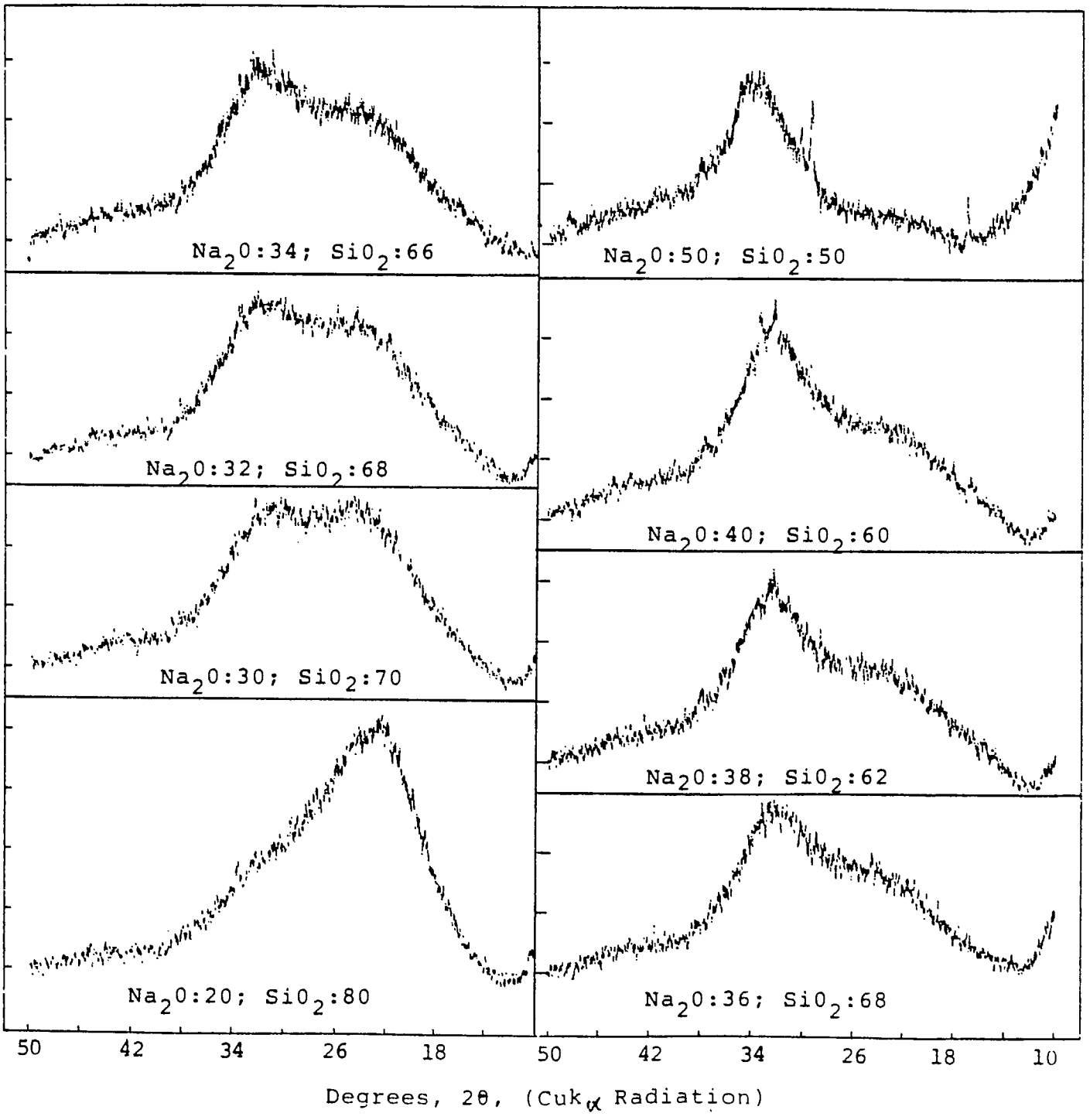

Fig. 23 - X-ray diffraction patterns of glasses in Na_2O-SiO_2 system

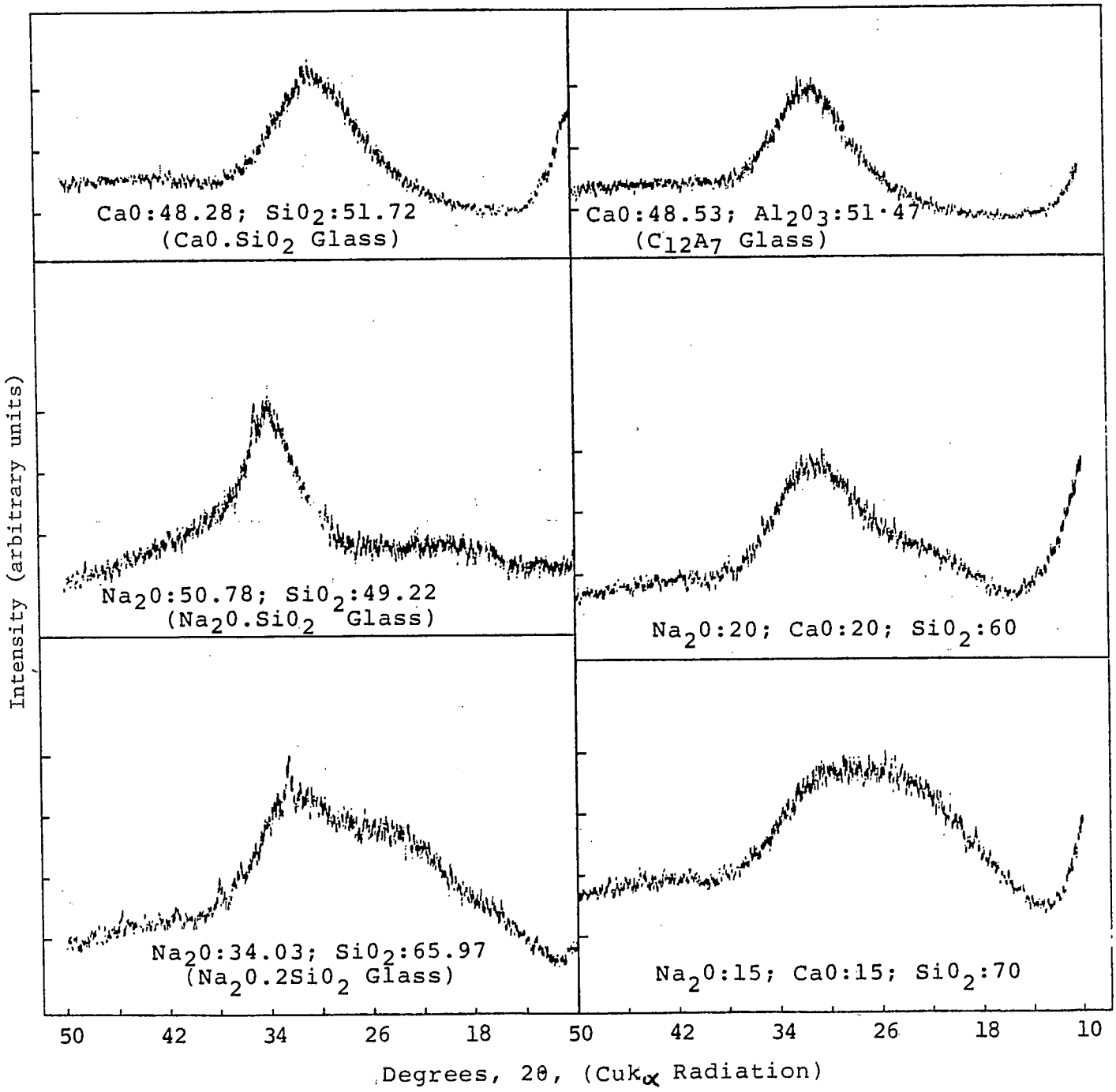

Fig. 24 - X-ray diffraction patterns of glasses in Na_2O-CaO-SiO_2 and other systems

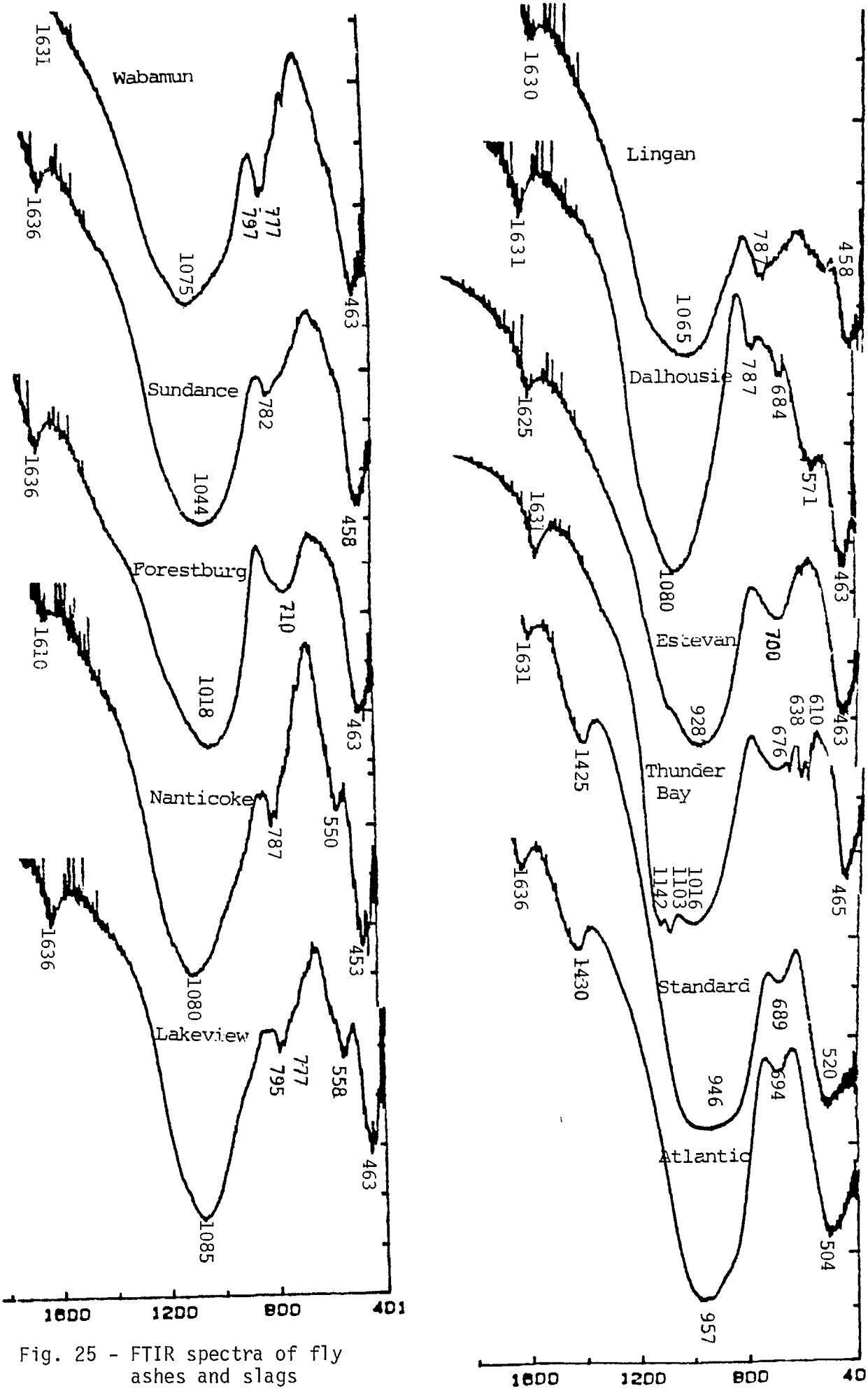

Fig. 25 - FTIR spectra of fly ashes and slags

Fig. 26 - FTIR spectrum of Sundance fly ash in the 4000-400 cm^{-1} range

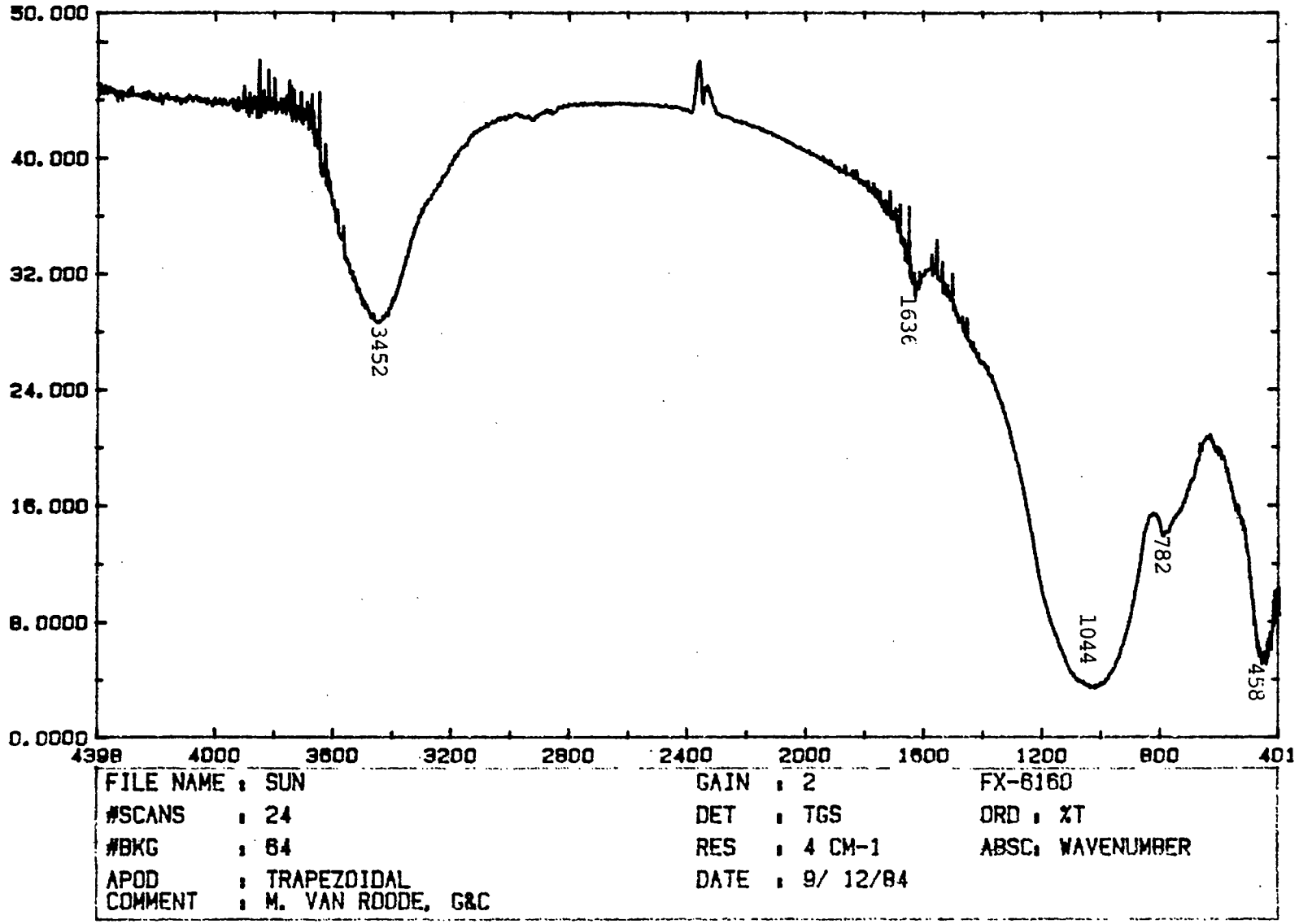

APPENDIX A

MODEL GLASSES FOR X-RAY DIFFRACTION

APPENDIX A – MODEL GLASSES FOR X-RAY DIFFRACTION

A series of synthetic glasses in the Na_2O-SiO_2, CaO-SiO_2, Na_2O-CaO-SiO_2, and CaO-Al_2O_3-SiO_2 system was prepared for an X-ray diffraction study using the following approach.

Materials

The starting materials used were Na_2CO_3 reagent grade, silica powder (240 mesh), and Al_2O_3 and $CaCO_3$ reagent grade.

Glass Preparation

The preparation of the synthetic glasses was carried out by wet mixing of the batch materials in a glass mortar. After drying at 110°C for 1 h the mixtures were melted in Pt crucibles.

Glasses in the Na_2O-SiO_2 system were prepared on a 20 g scale by melting between 1320 and 1360°C for one h and quenched on a stainless steel plate in air. The glass was crushed and remelted for an additional one h and quenched in the same manner. The glass with composition $0.5Na_2O/0.5SiO_2$ devitrified when prepared on a 20 g scale. It was, therefore, prepared on a 2 g scale and the Pt crucible containing the melt was partially quenched in water to prevent devitrification.

Glasses in the CaO-SiO_2, CaO-Al_2O_3-SiO_2, and Na_2O-CaO-SiO_2 systems were prepared on a 5 g scale. Melting was carried out at 1600°C for 15 to 30 min. The melts were quenched by partial quenching of the Pt crucibles in cold water.

X-ray Measurements

X-ray powder patterns were collected of the ground samples (-75 µm) using a diffractometer equipped with goniometer, using a nickel-filtered CuK_α radiaton at 40 kV and 30 mA.

Preparation of Melilite and Merwinite for QXRD Studies

Melilite, a solid solution of akermanite (C_2MS_2) and gehlenite (C_2AS), and merwinite (C_3MS_2) were synthesized for use in admixtures needed for the preparation of standard curves for QXRD measurements as follows:

Melilite:

A melilite composition was chosen based on 70% C_2MS_2 and 30% C_2AS. This oxide composition is:

CaO, 41.0%; MgO, 10.4%; Al_2O_3, 11.2%; and SiO_2, 37.5%.

$CaCO_3$ and $MgCO_3$ were used as sources of CaO and MgO, respectively. The batch materials were thoroughly mixed, ball-milled in ethanol for four hours and calcined overnight at 1050°C. Melting was carried out for two hours at a temperature of 1450°C.

Melting was first attempted in Pt/30% Rh crucibles but severe corrosion led to the choice of clay crucibles for further melts. A partly crystallized glass was produced upon cooling the crucibles in the kiln. The XRD pattern of the crystalline fraction showed strong peaks at d-spacings of 2.87 (2θ = 31.2) and 1.76 (2θ = 51.8) indicative of a melilite phase. The partly devitrified glass was powdered to -75 µm and heat treated overnight at 1220°C to give a fully crystalline material identified as melilite from the XRD pattern.

Merwinite:

Merwinite was prepared by mixing batch materials with composition:

CaO, 5.11%; MgO, 12.3%; SiO_2, 3.66%.

Again $CaCO_3$ and $MgCO_3$ were used as batch materials. These were ball milled for four hours in ethanol and calcined overnight at 1050°C. Melting was carried out at 1420°C for two hours in clay crucibles. A partly devitrified glass was formed as for melilite. X-ray analysis of the devitrified pieces showed the presence of merwinite. The glass was powdered to a -75 µm and heat treated at 1100°C overnight to give merwinite as determined by its XRD pattern.

Reduction of particle size:

Ball milling for four days in ethanol using a corundum medium was used to reduce the particle size of the melilite and merwinite. Powders had been prepared prior to ball milling by crushing and sieving to give a -200 mesh material. Settling experiments were used to collect fine crystallites. The fraction <6 μm was collected since there were not sufficient particles <5 μm.

Preparation of cordierite glass and α-cordierite for X-ray diffraction studies

Cordierite ($2MgO.2Al_2O_3$) was synthesized for XRD studies using the following oxide composition:

MgO	:	13.78%
Al_2O_3	:	34.86%
SiO_2	:	51.36%.

Reagent-grade magnesium carbonate, alumina, and silica flour, in the stoichiometric proportions 2:2:5 were ball-milled for 30 min in ethanol, in porcelain ball-mill jars, using a corundum medium. The dried powders were heated to 1625°C and soaked at this temperature for 10 min in a platinum crucible. The melt was cast into bars in a mould pre-heated to 600°C. The bars were annealed at 700°C.

α-Cordierite was prepared by crystallizing glass bars at 1000°C for two days. The XRD pattern of the crystalline polymorph was in good agreement with literature data.

Preparation of glassy and redevitrified analogues of fly ashes and slags

Glassy and redevitrified analogues of fly ashes and slags were prepared for glass content studies.

Table 9 gives relevant data pertaining to the 11 source materials of this study.

The fly ashes and slags were melted at the melting temperature for periods between one and two hours, followed by rapid quenching. XRD patterns of the quenched glass were measured to establish that complete vitrification had indeed occurred.

One fly ash, Dalhousie, which has a high iron oxide content, could not be fully vitrified. Two other fly ashes, Nanticoke and Lakeview, could initially not be fully vitrified either but subsequent extension of the melting time produced the fully vitreous analogue of the fly ash.

Some of the source materials of selected source materials were cast in bars and annealed at 750°C for 16 h. Specimens 2 in. long were cut from the annealed bars for measurement of the dilatometric softening point (DSP) and coefficient of thermal expansion (CTE). DSP and CTE values for selected source materials are given in Table A1.

Powders of the quenched fly ashes and slags (-45 μm) were heat-treated according to the nucleation/crystallization schedule in Table 1. XRD patterns were obtained from the heat treated powders to ensure that full devitrification had occurred. One fly ash, Lingan, showed residual glass which could not be fully redevitrified even if the crystallization stage were further extended.

Table A.1 - Nucleation/crystallization parameters*

Source	Melting temp (°C)	DSP (°C)	CTE (cm/cm/°C)	Nucleation (°C/hr)	Crystallization (°C/hr)
Wabamun	1575	776	-	810/16 h	950/16 h
Sundance	1575			810/16 h	950/16 h
Forestburg	1575			810/16 h	950/16 h
Nanticoke	1575			830/16 h	1050/4 d
Lakeview	1575			830/16 h	1050/4 d
Lingan	1575	810		870/16 h	950/48 h
Dalhousie	1550				
Estevan	1575			810/16 h	950/16 h
Thunder Bay	1575	773	6.5×10^{-6}	830/16 h	930/16 h
Standard Slag	1575	777	7.3×10^{-6}	830/16 h	950/16 h
Atlantic Slag	1575			810/16 h	950/16 h

* DSP: dilatometric softening point; CTE: coefficient of thermal expansion